SYNTHESIS-ENABLED UNDERSTANDING OF THE MECHANISM OF ACTION OF AMPHOTERICIN B AND THE DEVELOPMENT OF INCREASED THERAPEUTIC DERIVATIVES

BY

MATTHEW M. ENDO

THESIS

Submitted in partial fulfillment of the requirements
for the degree of Master of Science in Chemistry
in the Graduate College of the
University of Illinois at Urbana-Champaign, 2016

Urbana, Illinois

Advisor:

Professor Martin D. Burke

ABSTRACT

The polyene macrolide amphotericin B (AmB) remains a critically vital antifungal as the last line of defense against a wide range of life-threatening fungal pathogen. Despite its clinical usage for over half a century, AmB has evaded the development of clinically relevant microbial resistance. AmB has been shown to form ion channels similar to that of their protein counterparts, which has led to the proposal that AmB kills yeast cells via membrane permeabilization. The capacity for ion channel formation and cytotoxicity of AmB are thought to be dependent upon membranous sterol, but the role of sterols in this mechanism and whether membrane permeabilizaton and biological activity are even linked has remained unclear. Thus, the complete understanding of the mechanism of action of AmB would enable the development of new antifungals with an improved therapeutic index, as well as guide the pursuit of new antimicrobials that evade resistance.

To elucidate the operative mechanism, we pursued a systematic functional group deletion strategy where derivatives of AmB are synthesized lacking a single protic functional group to understand its role in AmB's activity. The C35 hydroxyl group of AmB has been proposed to be critical for ion channel formation and so we accessed the derivative lacking the C35 hydroxyl via an iterative cross-coupling (ICC) strategy. The resulting derivative maintained the capacity to bind membranous ergosterol, but could no longer cause membrane permeabilization. Despite the lack of channel activity, this derivative still demonstrated potent fungicidal activity. Deletion of the mycosamine sugar yielded a derivative that could no longer bind ergosterol and was completely inactive against yeast. Collectively, these results led us to conclude that the primary mechanism by which AmB kills yeast is the binding of the ergosterol and that channel formation is a complementary mechanism that marginally increases AmB's potency. This finding suggests that toxicity to humans is likely due to the binding of the major mammalian sterol: cholesterol.

Given the importance of the mycosamine appendage on the binding of sterol, we pursued an atomistic understanding of this interaction. The axial C2' hydroxyl group of AmB has been proposed to be critical in binding both sterols. Surprisingly, derivatives lacking or epimerizing the C2' hydroxyl maintained the capacity to bind ergosterol but could no longer bind cholesterol. Consistent with sterol binding being the operative mechanism for toxicity, both derivatives exhibited potent antifungal activity but no toxicity in human cells and mice. However, synthetic access to both derivatives limited their further pursuit. We hypothesized that the sterol selectivity

resulted from a ligand-selective allosteric modification and proposed that a similar effect could be achieved by derivatization of the accessible C41 carboxylate. Similar to the C2' modified analogues, the new AmB ureas also demonstrated a preferential binding for ergosterol over cholesterol. This corresponded with their potent activity against a wide range of fungal pathogens as well as their substantial decrease in toxicity to human cells and mice. Despite their decreased toxicity, the AmB ureas maintained the ability to evade resistance similar to that of the parent compound.

To my grandfather Richard Young who continues to watch over me

current members of Alex, Anna, and Sam, it was incredible how different the bay changed with changing people, but it was great place to work as it was filled with great thoughts and great fun.

I was also fortunate to collaborate with a number of people outside of the Burke group as well. Thank you David Andes and Karen Marchillo at the University of Wisconsin, Madison for evaluating our compounds in the murine model of candidiasis. Lastly, I would like to thank Susan Lindquist, Ben Vincent, and Luke Whitesell for their work in evaluating our compounds in their ability to evade resistance.

There are a number of friends outside of the Burke group, I must thank as well. First of all, my incredible friend Tommy Osberger. We came into grad school together and I was able to gain so much from you in chemistry and in life. You and Thy are some of my closest friends and I'm thankful for you guys being able to put up with me. Scott Sisco and Seiko Fujii, you guys were great friends and it was fun getting to hang out with you guys whenever Seiko allowed you to hang out. To the Speed Marvels softball team, that include Tony Grillo, Noah Bindman, Pat Knerr, Josh Kaitz, and Justin, being with you guys every Wednesday evening was a blast. Even though we weren't the best, those evenings were often the highlight of my week.

My family needs all the credit for my development as a person. My parents, Glenn and Roberta Endo, worked so hard to provide me with the opportunities in life that I've had that led to me being here in Illinois. My grandparents, Richard and Frances Young, raised me to be the person I am today and your lessons continue to serve me to better myself each and every day. My sister, Melanie Shigemasa, has and will always be there looking out for me and knowing that has allowed me take many risks that have shaped my life. Finally, I must thank the person that will travel the roads of life together with me: Qi Chen. My graduate career has been incredibly tough for both of us, but your continuous strength and love has kept me going through all these years. Thank you so much for your patience and support as we can finally start our wondrous life together away from these confining walls.

TABLE OF CONTENTS

LIST OF ABBREVIATIONS

Ac   acetate

AmB   amphotericin B

AmBAU   amphotericin B aminoethylurea

AmBCU   amphotericin B carboxylethylurea
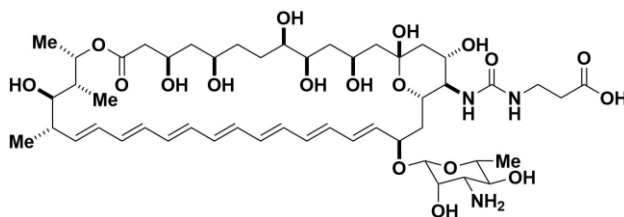
AmBMU   amphotericin B methyl urea
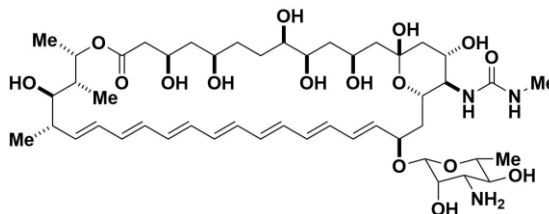
AmdeB   amphoteronolide B
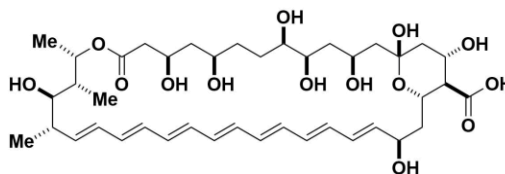
AmE   amphotericin B methyl ester
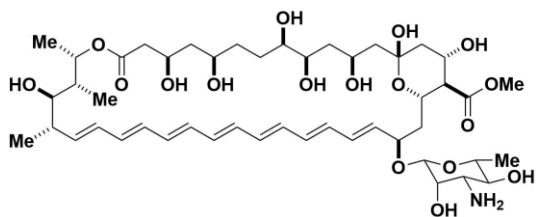
BLM   black lipid membrane

C2'deOAmB   C2'-deoxy amphotericin B
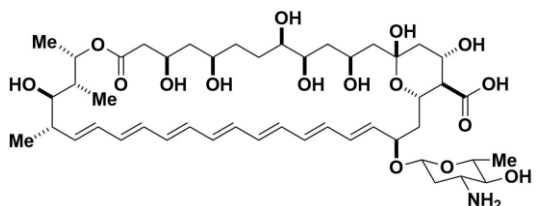
C2'epiAmB   C2'-epi amphotericin B
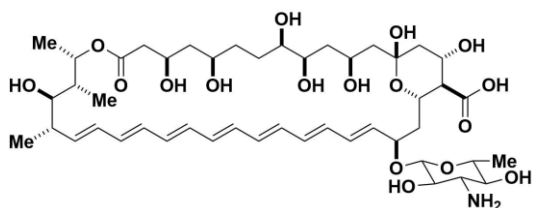
C35deOAmB   C35-deoxy amphotericin B
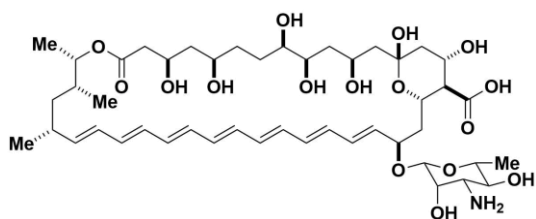
CD   circular dichromism

CSA   (±)-10-camphorsulfonic acid
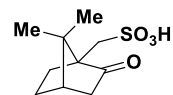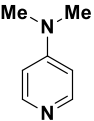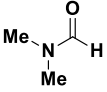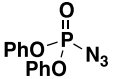
DCM   dichloromethane
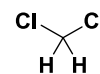
DIAD   diisopropyl azodicarboxylate
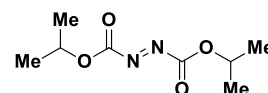
DMAP 4-(dimethylamino)-pyridine

DMF dimethyl formamide

DMSO dimethyl sulfoxide

DPPA diphenyl phosphoryl azide

HPLC high performance liquid chromatography

hTERT1 human telomerase reverse transcriptase 1

ICC iterative cross-coupling

ITC isothermal titration calorimetry

IP intraperitoneal

IV intravenous

LUV large unilamellar vesicle

MeAmB C41-methyl amphotericin B
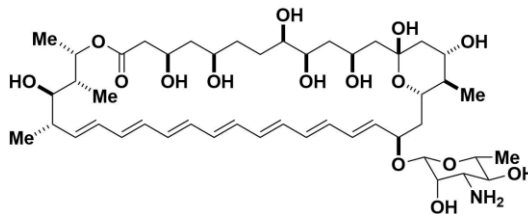
MeAmdeB   C41-methyl amphoteronolide B
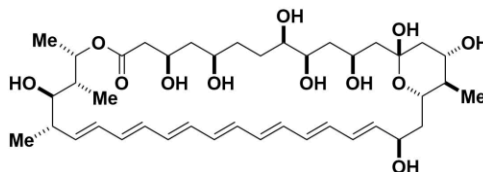
MHC   minimum hemolytic concentration

MIC   minimum inhibitory concentration

MIDA   *N*-methyliminodiacetic acid
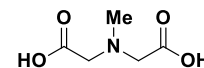
MNBA   2-methyl-6-nitrobenzoic anhydride
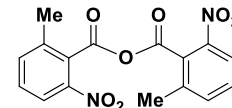
MTC   minimum toxic concentration

NAcAmB   *N*-acetyl amphotericin B
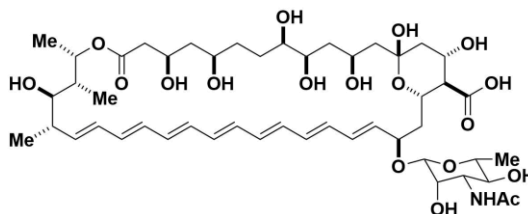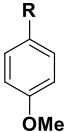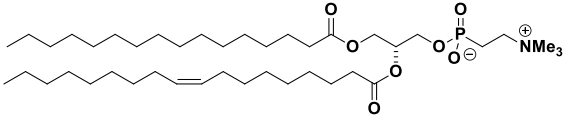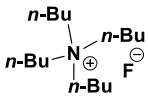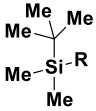
NMR   nuclear magnetic resonance

NOE   nuclear Overhauser effect

Ph₃P   triphenylphosphine
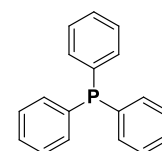
PMP	*p*-methoxyphenyl	
POPC	1-palmitoyl-2-oleoyl-*sn*-glycero-3-phosphocholine	
pyr	pyridine	
RPTEC	renal proximal tubule epithelial cell	
SPR	surface plasmon resonance	
SSNMR	solid-state nuclear magnetic resonance	
TBAF	tetra-*n*-butylammonium fluoride	
TBS	*t*-butyldimethylsilyl	
TEM	transmission electron microscopy	
Tf	trifluoromethane sulfonate	
THF	tetrahydrofuran	
TLC	thin layer chromatography	

TMSE	2-(trimethylsilyl)ethyl	
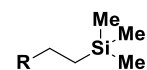
UV   ultraviolet

X-Phos   2-dicyclohexylphophino-2',4',6'-triisopropylbiphenyl
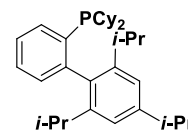
CHAPTER 1

CURRENT UNDERSTANDING OF THE MECHANISM OF
ACTION OF AMPHOTERICIN B

Portions of this chapter were adapted from Endo, M. M.; Cioffi, A. G.; Burke, M. D. *Syn. Lett.* **2016**, *27*, 337-354.

1-1 AMPHOTERICIN B: THE HIGHLY TOXIC ARCHETYPE FOR RESISTANCE-EVASIVE ANTIMICROBIALS

Invasive fungal infections represent a major health crisis as they are responsible for more than 1.5 million deaths each year, a figure exceeding that of either malaria or tuberculosis.[1] Fungal pathogens account for approximately 10% of all hospital acquired infections with the *Candida* species being the fourth most common microbial systemic infection.[2] Furthermore, invasive fungal infections may actually be substantially underreported due to the difficulties of diagnosis from the high occurrence rate of false negatives in conventional blood cultures.[3] Thus, the development of a safe and effective antifungal therapy stands to have a significant impact on human global health.

In 1953, William Gold and his colleagues isolated the natural product amphotericin B (AmB, **1.1**) from the soil bacterium *Streptomyces nodosus* on the banks of the Orinoco River region of Argentina.[4-7] Prior to this discovery, the prognosis for patients with systemic fungal infections was extremely grim as mortality rates were near 100%.[8] However, AmB, as a new potent and broad-spectrum antifungal dramatically changed the outlook for patients undergoing treatment for invasive fungal infections[9,10] and has remained the last line of defense against a wide range of fungal pathogens.[11]
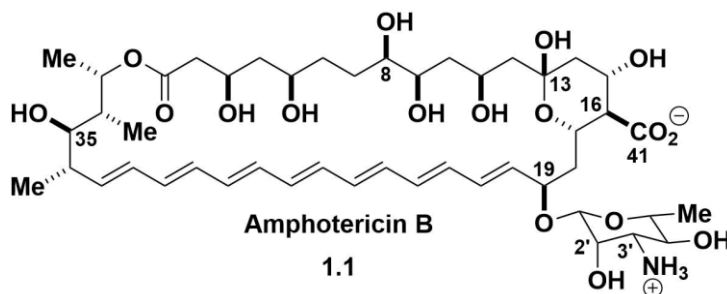
Figure 1.1: Chemical structure of amphotericin B (AmB).

Despite its clinical usage for over half a century, there have been very few reports of the emergence of clinically relevant resistance to AmB, which is in stark contrast to the history of all other clinically significant antimicrobials.[11] This may potentially be due to the unselective nature of AmB. Generally, less selective pharmacological action is associated with reduced vulnerability to resistance as well as increased toxicity.[12,13] AmB is exceptionally toxic to human cells, especially kidney cells,[14] which limits the dose and/or duration of treatment with AmB. Thus, the development of less toxic derivatives of AmB would have an incredible impact on human health. However, this would require understanding how AmB kills both yeast and human cells. Despite extensive studies for over half a century, the mechanism by which AmB is toxic to both cell types remains unclear.

1-2 ION CHANNEL HYPOTHESIS

One of the earliest studies to attempt to elucidate the mechanism of action for AmB came from Kinsky in 1961 where he found that AmB caused a decrease in the dry weight of the mycelial mats of *Neurospora crassa* along with the presence of cytoplasmic constituents in the growth medium.[15,16] This led Kinsky to conclude that the mechanism of AmB was due to the alteration of permeability in the cell's membrane. There were three potential mechanisms to how AmB was permeabilizing membranes: gross membrane disruption, ionophoric transport, or discrete ion channel formation (Figure 1.2A). Andreoli and coworkers utilized planar lipid bilayer assay to observe that the electrical resistance had decreased while the physical integrity of the membrane was maintained in the presence of AmB.[17] Based on these results, gross membrane disruption is a highly unlikely mechanism. To distinguish between the other two mechanisms, Finklestein and coworkers compared the electrophysiological properties of AmB with the known ionophore valinomycin.[18] Valinomycin-mediated conductance increased linearly with concentration, while AmB-mediated conductance increased proportionally to a large power of concentration. Furthermore, the conductance due to valinomycin addition increased with increasing temperature, while AmB-promoted conductance decreased with increasing temperature. These observed differences are inconsistent with AmB behaving as an ionophore. However, it was not until 1976 that the direct observation of the discrete AmB single ion channels was made by Ermishkin and coworkers with the planar lipid bilayer technique.[19] These single ion channels displayed gating

and ion selectivity properties that are typically attributed to protein ion channels. These remarkable characteristics have led to AmB becoming the archetype for ion channel-forming small molecules.

From 1973-1974, Andreoli,[20,21] Finkelstein and Holz,[22] and de Kruijff and Demel[23] proposed the barrel-stave model of the AmB ion channel (Figure 1.2B). In this model, eight AmB molecules self-assemble to form the transmembrane pore. The hydrophobic polyene is oriented outward to interact with the lipid membrane while the hydrophilic polyol lines the inside of the channel enabling ion conductance. The barrel-stave model was further advanced by Ermiskin and coworkers based on a series of electrophysiology studies using AmB derivatives that were modified at the C41 carboxylate and/or C3' ammonium.[24] Modification of either charged functional group significantly diminished the lifetime of the open channel, which led to the proposal that the positive and negative charges of AmB were critical in stabilizing the supermolecular channel structure via intermolecular salt-bridges between the C41 carboxylate of one AmB and the C3' ammonium on a neighboring AmB (Figure 1.2B and 1.2C). Molecular dynamics (MD) studies further supported the hypothesis of this critical intermolecular salt-bridge.[25-27]
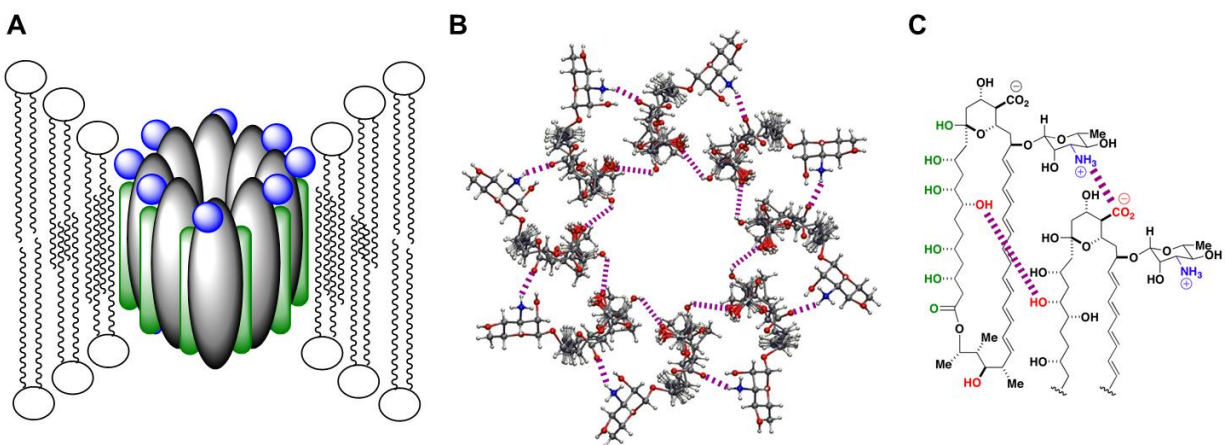
Figure 1.2: The classical ion channel model for AmB's activity. (A) Representation of the ion channel in a lipid bilayer membrane. (B) Bird's eye view of the computational model for the putative AmB ion channel. (C) Proposed polar interactions that stabilize the ion channel supermolecular structure.

To study this putative intermolecular salt-bridge, Murata and coworkers synthesized AmB dimers that linked the C41 carboxylate of one AmB molecule with the C3' ammonium of another with linkages of varying lengths (Figure 1.3).[28] These dimers displayed little to no biological activity. However, the dimer with the longest linker **1.4** was able to permeabilize membranes similar to AmB in a solution phase NMR-based assay.[29] This led to the reasoning that either the

intermolecular salt bridge is not present in the ion channel or that a certain distance/flexibility is required for this interaction for activity. It is important to note that AmB dimers were also synthesized that contained intermolecular linkages between the C41 carboxylate[30] or C3' ammonium.[31] Like the C41-C3' AmB dimer,[28] the membrane permeabilization activity of these conjugates also had linkage length-dependence. However, antifungal activity was not reported. This calls into question the importance of the proposed AmB ion channel to the observed antimycotic properties. Furthermore, these covalently modified derivatives contain an inherent steric interference, which makes proper evaluation of the potential intermolecular salt bridge difficult to assess.
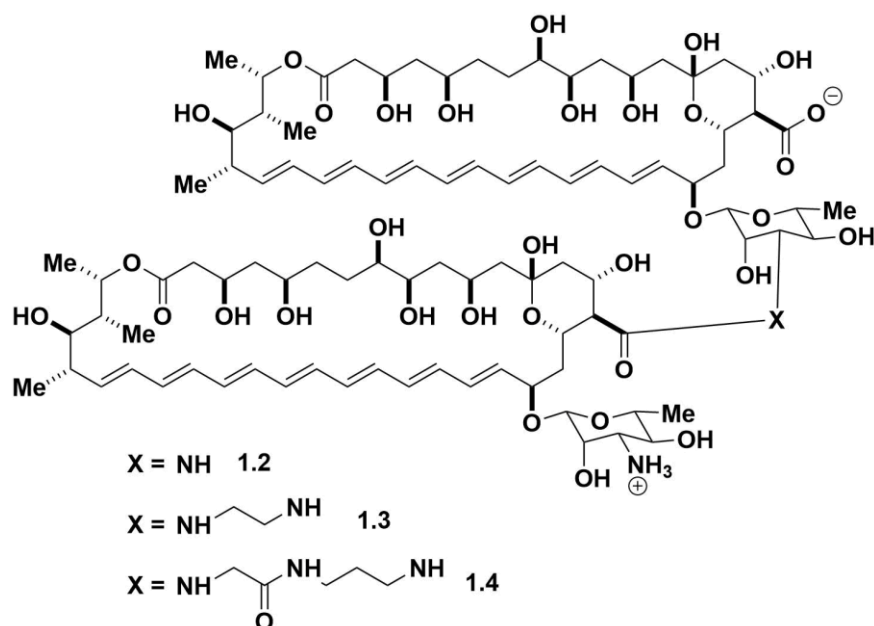
Figure 1.3: Chemical structures of covalently linked dimers of AmB.

In addition to the salt bridge, molecular dynamics experiments predicted further stabilization of the ion channel from the hydrogen bond network between the C8 hydroxyl of one molecule of AmB with the C9 hydroxyl of a neighboring AmB molecule.[26] Interestingly, the C8 hydroxyl is installed as a post-polyketide synthase (PKS) modification via a cytochrome P450 monooxygease encoded by the *amphL* gene. Inactivation of the *amphL* gene led to the biosynthesis of C8-deoxyamphotericin B (C8deOAmB, **1.5**).[32] This derivative maintained potent antifungal activity (~fourfold decrease in activity relative to AmB) demonstrating that either the C8 hydroxyl is not necessary in stabilizing the ion channel or that perhaps the ion channel is not required for antifungal activity.
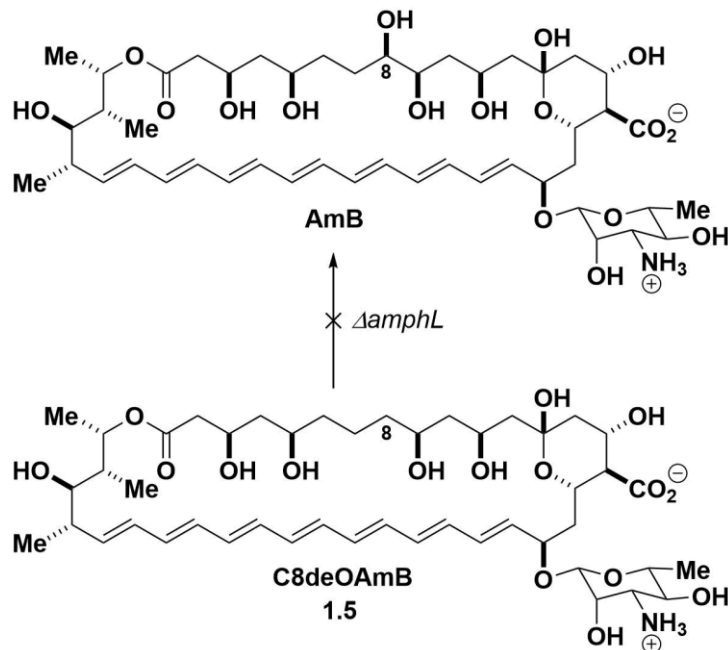
Figure 1.4: Biosynthetic access to C8deOAmB by inactivation of the post-PKS enzyme responsible for the oxidation at C8. C8deOAmB maintained antifungal activity against yeast albeit slightly decreased in potency.

The previous studies focused on trying to understand the roles of key functional groups of AmB, however early studies with AmB suggested that AmB's mechanism of action was related to sterols present in the target organism. Kinsky and coworkers observed that AmB was selectively toxic to sterol-containing cells, such as *N. crassa* protoplasts and rat erythrocytes, while the bacteria *Bacillus megaterium* was completely resistant.[33,34] However, due to the complication of the cell wall for *B. megaterium* may prevent AmB from accessing the cellular membrane, Feingold utilized the unique model organism *Acholeplasma laidlawii* which does not biosynthesize sterols but will incorporate sterols found in its growth media into its cellular membrane.[35] *A. laidlawii* grown with cholesterol-containing media were killed rapidly by AmB, while *A. laidlawii* grown in sterol-free media were completely resistant to AmB.

The dependence on sterols for AmB's potent antimicrobial activity along with sterols' ability to modulate global membrane properties[36-38] led to the idea that AmB's selective activity toward organisms containing sterols is due to the sterols altering the physical properties of the membrane enabling ion channel formation. This hypothesis was first proposed by Feingold and coworkers based on the surprising result that sterols embedded in certain lipid membranes *attenuated* the activity of AmB.[39,40] This report used a glucose release assay in which liposomes comprised of various lipids contained glucose and upon addition of AmB, the release of glucose

5

from the liposomes was quantified. When treating liposomes comprised of egg lecithin with AmB, the expected increase in glucose release was observed upon increasing amounts of embedded cholesterol **1.7**. Strikingly, liposomes made from the saturated lipids dipalmitoyl lecithin or distearoyl lecithin saw the opposite trend where increasing amounts of embedded cholesterol resulted in decreasing the observed glucose release.
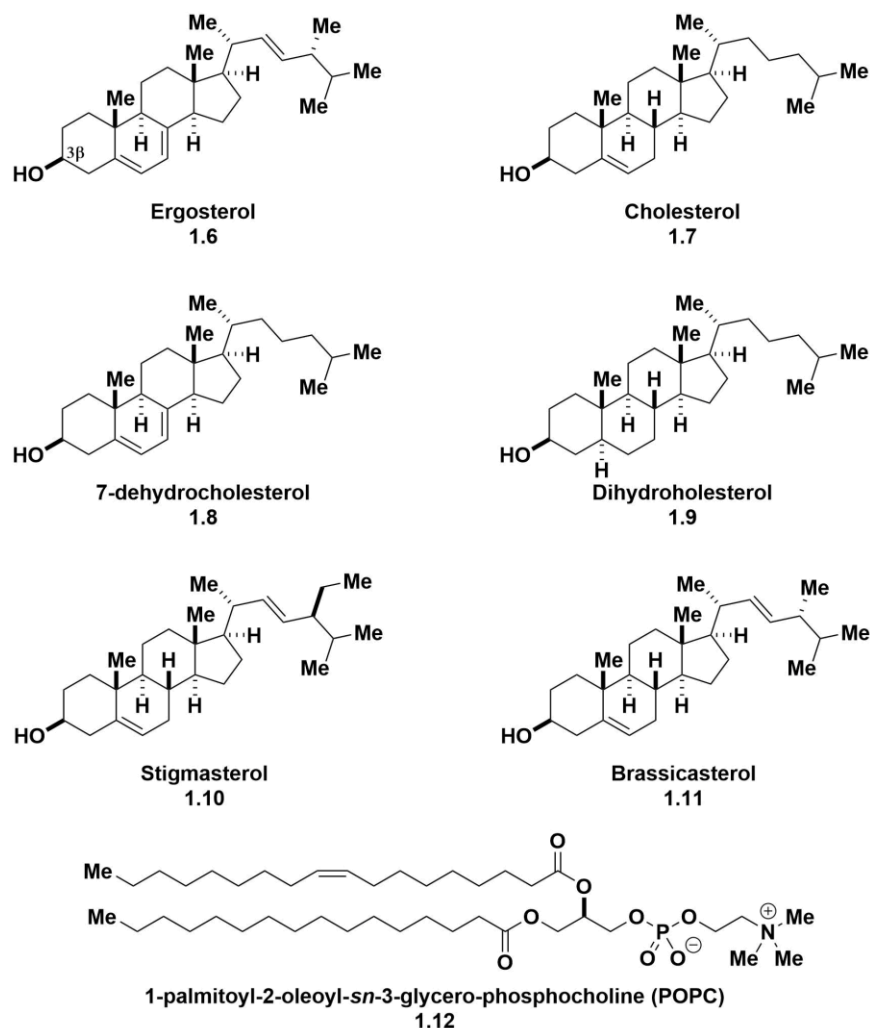
Figure 1.5: Chemical structures of lipids used to study the effects of various sterols had on the activity of AmB.

Recent liposome studies have also observed similar trends in specific biophysical systems. Murata and coworkers utilized a ^{31}P-NMR method to measure AmB-mediated potassium flux in liposomes comprised of egg yolk PC or 1-palmitoyl-2-oleoyl-*sn*-3-glycero-phosphocholine (POPC, **1.12**) lipids.[41] When AmB was pre-embedded in the liposomes, increasing amounts of cholesterol decreased the amount of potassium flux consistent with trend observed by Feingold.[39,40] However, when AmB was externally added to the liposomes, potassium flux

6

increased with increasing amounts of cholesterol until a maximum of about 20% cholesterol in the liposomes. Additional cholesterol after that point began inhibiting potassium flux. Carreira and coworkers also probed the effects of sterols on POPC liposome vesicles of varying sterol concentrations via AmB-mediated potassium efflux.[42] With ergosterol **1.6** and cholesterol liposomes, maximum potassium efflux was observed at 5% sterol content and increasing amounts of either sterol resulted in decreased efflux. Interestingly, maximum potassium efflux for liposomes with 7-dehydrocholesterol **1.8** or dihydrocholesterol **1.9** were observed at 13% sterol content. These results lend support to an indirect sterol-mediated alteration of the membrane to promote ion channel formation.

Evidence of AmB ion channel activity in certain sterol-free systems has also been utilized toward this hypothesis. Hartsel and coworkers utilized a fluorescence-based assay to measure AmB-induced potassium leakage from sterol-free egg PC small unilamellar vesicles (SUVs).[43] They reported that at ratios of 1:1000 of AmB to lipid that potassium leakage was observed. However, SUVs are poor models for studying membrane phenomena as their small size results in a higher radius of curvature, which in turn causes them to be more susceptible to permeabilization.[44] Furthermore, due to egg PC being derived from natural sources it may contain small amounts of cholesterol. Towards these criticisms, AmB's promotion of potassium leakage was studied in sterol-free egg PC large unilamellar vesicles (LUVs)[45] and POPC LUVs.[46] Interestingly, AmB-mediated permeabilization in these sterol-free vesicles was *not* observed under isoosmotic conditions. The requirement for stressed membranes (either via larger radii of curvature or osmotically) to enable membrane permeabilization does question the validity of AmB ion channels in sterol-free systems. Ortega-Blake and coworkers utilized patch clamp techniques with membranes comprised of asolectin,[47] DMPC,[47] egg lecithin,[48] and isolated *E. coli* membrane extracts.[48] The AmB ion channels observed in sterol-free membranes had similar electrophysiological properties to the AmB ion channels in the corresponding sterol-containing membranes. However, as the authors noted, supraphysiological concentrations of AmB were used to form ion channel in these sterol-deficient membranes. Nevertheless, the observation of ion channel activity in these sterol-free membranes have been employed to support the notion that sterols are not directly interacting with AmB but facilitating AmB ion channel formation by modulating the membrane. However, as already stated, there are a number of limitation to these studies as they have been applied to only model membranes and not a more physiologically

7

relevant system. Consequently, the ion channel model dictates improving the therapeutic index of AmB would require selective ion channel formation in fungal cells over human cells. This would be a very challenging problem to solve. Furthermore, it would mean that the toxicity of AmB and its channel forming capabilities are intrinsically linked and inseparable.

1-3 DIRECT STEROL BINDING HYPOTHESIS

Just three years after the discovery of AmB, Gottlieb and coworkers discovered that an extract from carrots protected the mold *Penicillium oxalicum* from the toxicity of AmB.[49] The active protective agent in the carrot extract was discovered to be a mixture of sterols, which were isolated and found to interfere with AmB's antifungal activity. This interesting protective effect would eventually lead to an alternative model based on AmB's observed sterol-dependence. Rather than sterols facilitating the insertion of AmB into membrane, Kotler-Brajtburg, et al. proposed that AmB directly binds membrane sterols and consequently forms ion channels.[50] Specifically, the C41 carboxylate,[51,52] C3' ammonium,[27,51-53] or C2' alcohol[54-59] have all been predicted to mediate this interaction. Based on this model, the selective toxicity for yeast over human cells stems from AmB's greater affinity for ergosterol (the main fungal sterol) over cholesterol (the main mammalian sterol). Early work in support of this model arose from changes in the ultraviolet-visible (UV/Vis), circular dichromism (CD), and infrared (IR) spectra of AmB with membranes containing sterols.[60-66] Conversely, it has been argued that the sterol-dependent changes in UV/Vis and CD are due to the aggregation of AmB and not a direct binding between AmB and sterols.[67] Towards this understanding, solid-state NMR (SSNMR) with AmB and ergosterol has been utilized to study their interaction.[68,69] However, in order to gain a real understanding of this binding, it is necessary to obtain a complete atomistic understanding of each individual interaction between these two small molecules.

Chemical modifications to AmB have been done to probe these precise interactions in the binding between AmB and sterols. Specifically, acylation of the C3' ammonium and esterification of the C41 carboxylate yielding *N*-acylamphotericin B (NAcAmB, **1.13**) and amphotericin B methyl ester (AmE, **1.14**), respectively were studied to probe the roles of the C41 carboxylate and C3' ammonium in this binding (Figure. 1.6).[51,52] Liposomes were loaded with one of the sterols in Figure 1.5 and treated with AmB, NAcAmB, or AmE. AmB caused permeabilization in liposomes with all the sterols tested. In stark contrast, NAcAmB had substantially reduced activity compared

to AmB, which suggested that the C3' ammonium hydrogen bonds with the 3β hydroxyl (Figure 1.5) of the sterols to promote the AmB/sterol interaction consistent with one of the proposed models.[27,51-53] However, these results are complicated due to the difficulty of discerning between the loss in hydrogen bonding capability with the increased steric hindrance in these covalently-modified derivatives. Interestingly, AmE selectively caused permeabilization in liposomes containing either ergosterol or brassicasterol, which have identical hydrophobic tails. This selective activity of AmE led to the proposal that the binding between AmB and sterols is stabilized by a network of hydrogen bonds with a minor contribution of stabilization between the polyene of AmB with the hydrophobic steroidal core. However, loss of the free carboxylate, as in the case of AmE, results in a disruption of the hydrogen bond network leading to the van der Waals contact between the polyene and steroidal core playing a major role in this binding interaction. However, like NAcAmB, this proposal is complicated by the inability to separate the decrease in hydrogen bonding capability with the added steric hindrance of the alkyl esters.
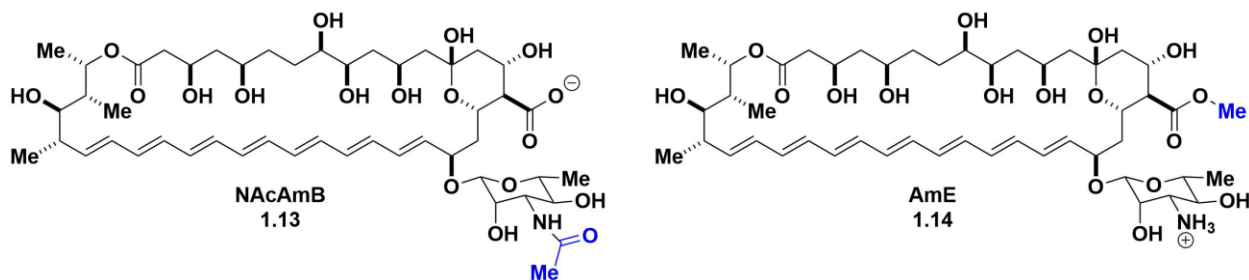
Figure 1.6: Chemical structures of two AmB derivatives: NAcAmB and AmE.
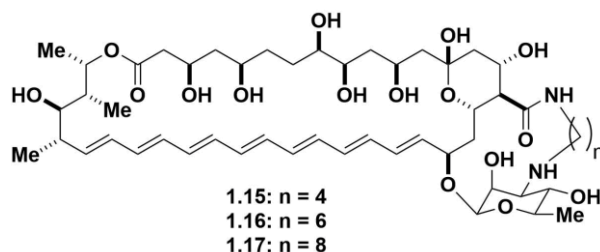
Figure 1.7: Chemical structures of tethered derivatives of AmB.

The most prominent computational models propose that the axial C2' hydroxyl forms a hydrogen bond to the 3β hydroxyl of sterols.[54-59] In order to probe this model, AmB derivatives that were conformationally restrained by a covalent intramolecular tether positioned the C2' hydroxyl in the hypothesized conformation to bind to the 3β hydroxyl of the sterols were synthesized. Derivatives **1.16** and **1.17** saw increases in ability to permeabilize ergosterol containing liposomes leading to the suggestion that the C2' hydroxyl is critical in this small

9

molecule-small molecule interaction. However, these derivatives saw substantially reduced biological activity, once again demonstrating the limitations of covalent modifications in studying this unique interaction. Further complicating these models were computational models that suggested that the C2' hydroxyl was critical in only binding ergosterol but not cholesterol.[58] The first chemical modifications to the C2' hydroxyl were synthesized as their C41 methyl esters (Figure 1.8).[59] Interestingly, the derivative in which the C2' hydroxyl is epimerized **1.18**, maintained similar antifungal activity and liposome permeabilization to its parent compound. However, epimerization and methyl etherification of the C2' hydroxyl **1.19** resulted in substantially reduced antifungal activity. Collectively, these studies utilizing covalently modified derivatives have contributed to the understanding of the interaction between AmB and sterols. However, the lack of specific sterol binding data in addition to the complication of steric hindrance with covalent modifications causes interpretation of these results to be highly complex.
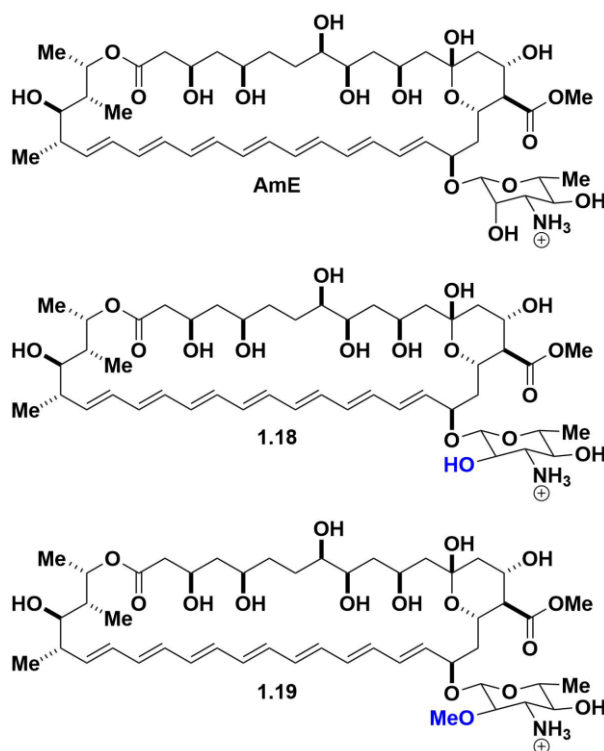
Figure 1.8: Chemical structures of AmB derivatives modified at the C2' position.

Modifications to the sterols have also been performed to probe this small molecule-small molecule interaction. Enantiomeric cholesterol (ent-cholesterol) was synthesized[70] and utilized in planar lipid bilayer studies to differentiate between the indirect promotion of permeabilization with AmB model and a direct binding with AmB model. Cholesterol and ent-cholesterol membranes

were shown to have similar global membrane properties, so the observed significant differences in AmB channel properties between the two membrane systems led to the conclusion that AmB directly binds to cholesterol.[71]
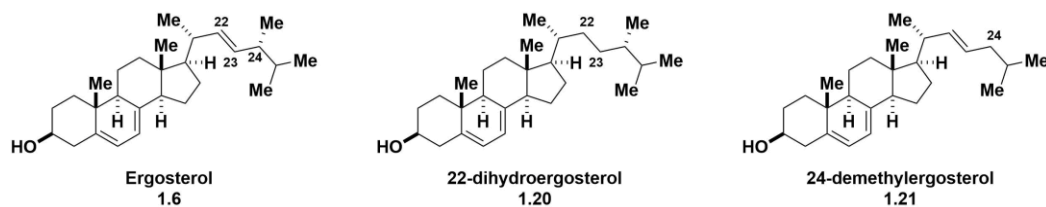
Figure 1.9: Chemical structures of ergosterol derivatives to probe modifications to the side chain.
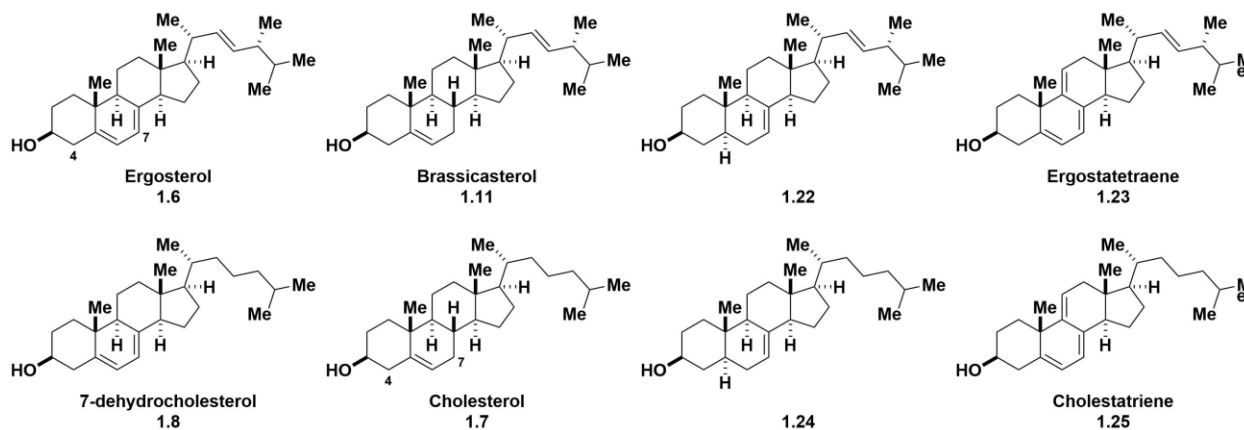
Figure 1.10: Chemical structures of sterol derivatives to probe modifications to sterol core.

Recently, modifications to the sterol side chain[72] (Figure 1.9) and steroid core[73] (Figure 1.10) were evaluated for their impact on the interaction with AmB via surface plasmon resonance (SPR), membrane permeabilization, and SSNMR. On the sterol side chain, the C22-C23 double bond and the C24 methyl group of ergosterol were both found to have major roles in its interaction with AmB as removal of either group (**1.20** and **1.21**) resulted in dramatic decreases in binding affinity and membrane permeabilization. Furthermore, the sites of unsaturation in the B ring of the sterols have a large influence in the binding interaction. Saturation of the C7-C8 double bond yielded sterols (**1.7** and **1.11**) with significantly decreased binding compared to its unsaturated counterparts. DFT calculations provided further evidence to the importance of the C7-C8 unsaturation as the sterol derivatives lacking this double bond have an axial C7 proton that sterically hinders the interaction with AmB (Figure 1.11). Collectively, these results have helped understand two of the major sites on ergosterol that allow for its strong affinity with AmB over other sterols: its unsaturated sterol side chain and the lack of an axial C7 proton. While these studies have begun to thoroughly probe the functional groups of the sterols that play major roles

11

in their interaction with AmB, to understand at an atomistic level, a different approach is required that is unhindered by covalent modifications.
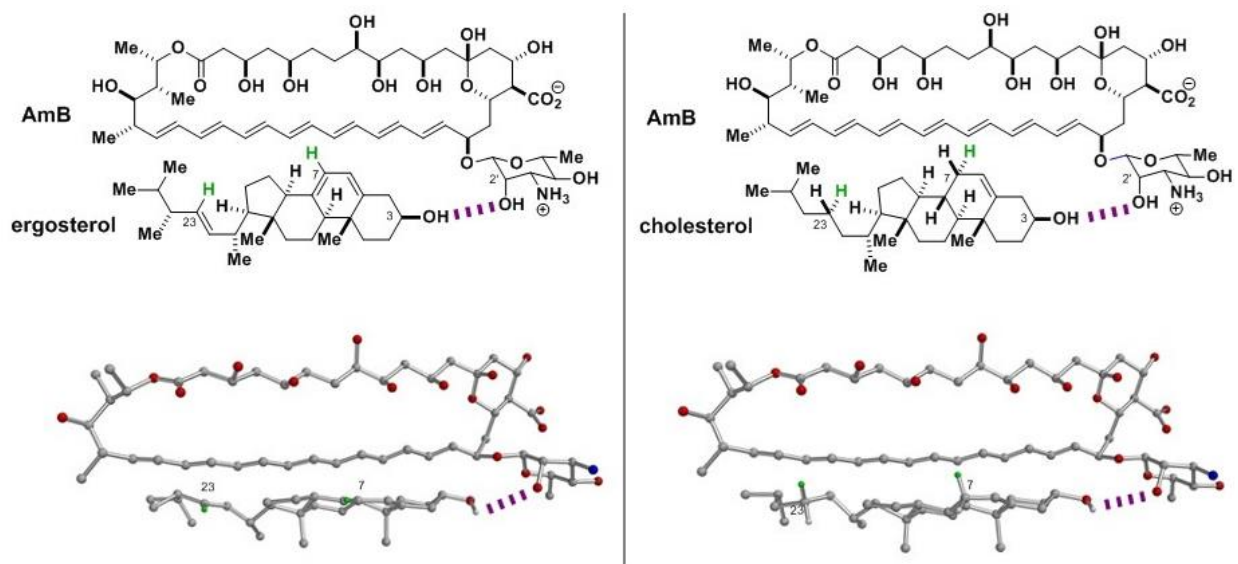
Figure 1.11: Representative chemical structures and 3D models of AmB's association with ergosterol and cholesterol based on DFT calculations. The axial C7 proton of cholesterol sterically hinders with the polyene of AmB, which may account for the selectivity for ergosterol over cholesterol.

1-4 FUNCTIONAL GROUP DELETION STRATEGY TO UNDERSTAND THE ATOMISTIC UNDERPINNINGS OF AmB

Definitive experiments to understand the mechanistic underpinnings of AmB have been challenging. As stated previously, changes in biological and biophysical properties due to covalent modification of AmB are complicated by the difficulty of discerning between the loss of a functional group moiety or the addition of steric bulk. Due to these complications, the Burke group has pursued a different strategy to probe the roles of each protic functional group by systematic deletions. This is analogous to alanine scanning[74] in peptides and proteins to identify the critical residues and the functions they serve.

The C41 carboxylate and functional groups on the C19 mycosamine have been hypothesized to play major roles in AmB's activity. In the pursuit of understanding the roles of both functional groups, Palacios, et al. synthesized derivatives lacking the C41 carboxylate (MeAmB, **1.26**), C19 mycosamine (AmdeB, **1.27**), or both (MeAmdeB, **1.28**) via degradative synthesis.[75] The ground state conformations of the macrolide were determined to not have changed for all three derivatives via Monte Carlo methods constrained by NOESY and phase-sensitive COSY NMR,[76] which allows for interpretation of any changes in activity from the natural product

12

to be based on simply the functional group deletion as opposed to substantial structural changes. Interestingly, MeAmB lacking the C41 carboxylate maintained equipotent antifungal activity as the natural product. This is in stark contrast to the prediction that this polar functional group was necessary in the biological activity of AmB. Even more interesting, the two derivatives lacking the mycosamine sugar were completely devoid of antifungal activity demonstrating that the appendage was critical for the antimycotic properties of AmB (Figure 1.12).
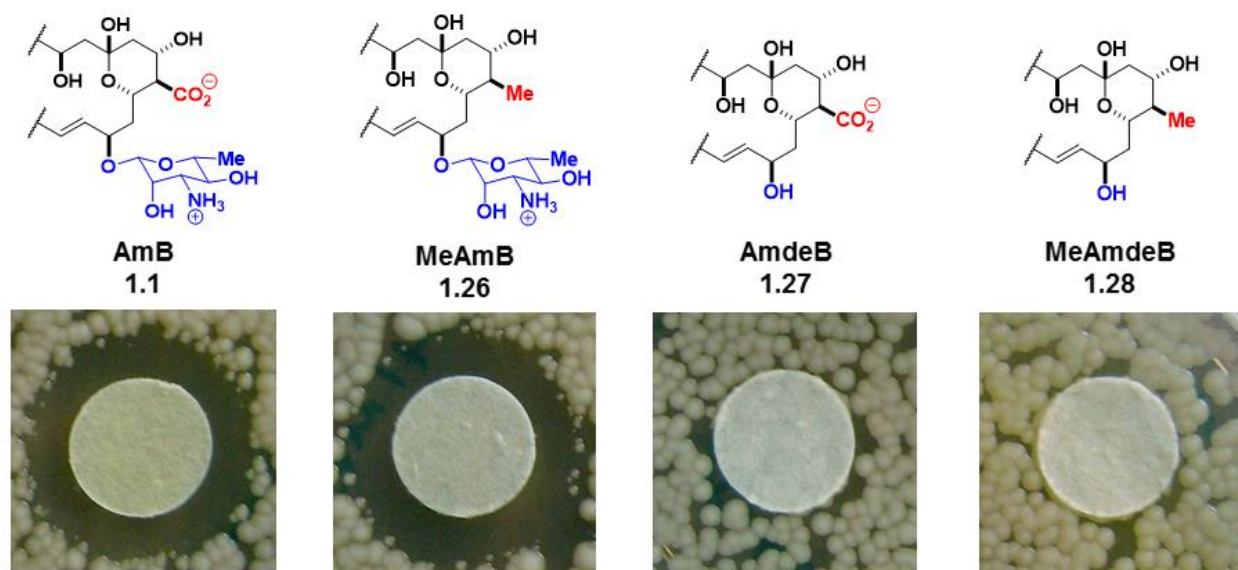
Figure 1.12: Chemical structures of AmB derivatives with functional group deletions at the C41 carboxylate, C19 mycosamine, or both. Antifungal activity is visualized by the disk diffusion assay where a zone of inhibition can be seen with the active compounds AmB and MeAmB. Figure was adapted from reference 75.

To further probe this mycosamine-dependent mechanism of action, Palacios, et al. studied the biophysical consequences for the deletion of the mycosamine.[77] AmdeB and MeAmdeB were found to lose the ability to form ion channels in planar lipid bilayer studies[19,24] and could no longer bind ergosterol via isothermal titration calorimetry (ITC).[78] Conversely, the biologically active MeAmB, like AmB, still maintained the capacity to bind ergosterol and form ion channels. Based on these findings, two possible mechanisms of action could explain AmB's antifungal activity: either sterol-dependent ion channel formation (Figure 1.13A) or the binding of ergosterol alone would be enough to kill yeast (Figure 1.13B). However, to differentiate between these two mechanisms would require the general access to any desired derivative of AmB to systematically probe modifications to AmB and their biological and biophysical consequences. Current AmB derivative syntheses involve either covalent modifications or selective degradation, but they are limited by the functionalities present in the parent compound. Thus, a general and modular

13

synthesis platform would be highly enabling toward unfettered access of any desired AmB analogue.
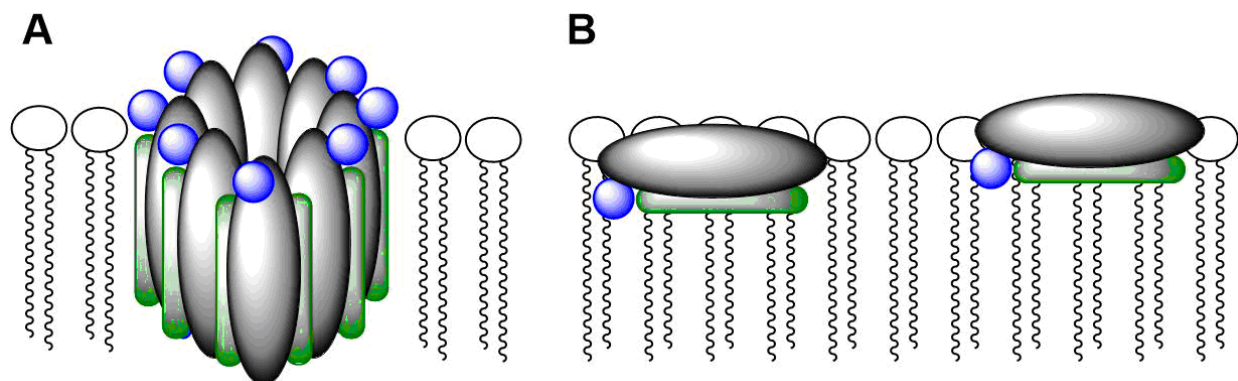
Figure 1.13: Two mechanisms by which AmB can kill yeast: (A) sterol-dependent ion channel formation or (B) the binding of sterol alone is sufficient to kill yeast.

1-5 ITERATIVE CROSS-COUPLING (ICC) AS A GENERAL STRATEGY TOWARD THE SYNTHESIS OF SMALL MOLECULES

Towards creating a general strategy for the synthesis of complex small molecules, a synthesis platform based on iterative cross-coupling (ICC) has been developed.[79] In this platform, small molecules are constructed by the continual application of the Suzuki-Miyaura reaction with bifunctional haloboronic acid building blocks enabled by the attenuation of the reactivity of the boronic acid with the *N*-methyliminodiacetic acid (MIDA) ligand (Figure 1.14). This platform is analogous to the iterative synthesis of peptides from amino acid building blocks enabled by the amine protecting group, fluorenylmethoxycarbonyl (Fmoc).[80]
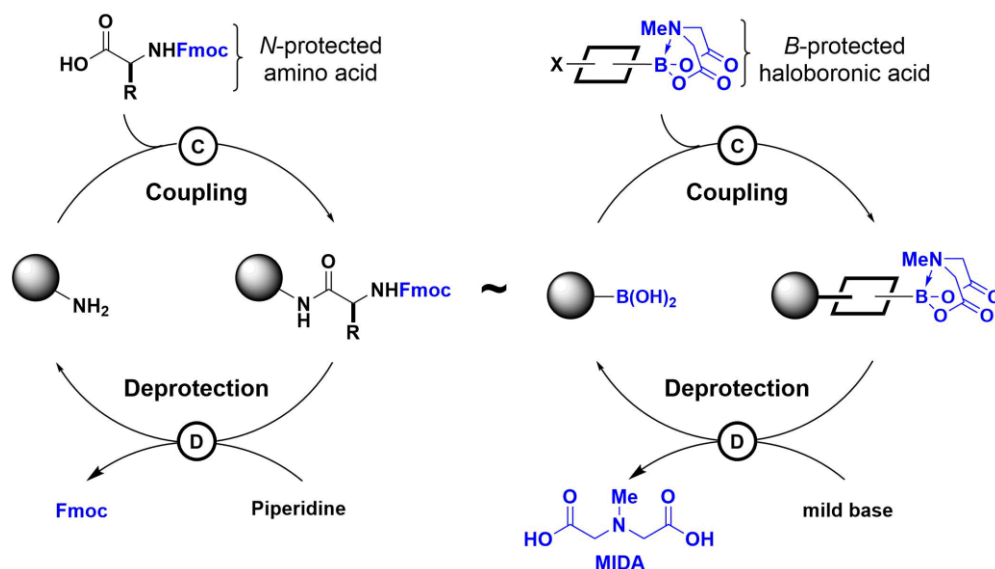
Figure 1.14: Iterative cross-coupling (ICC) where small molecules are constructed from *N*-methyliminodiacetic acid (MIDA) boronate building blocks analogous to peptide synthesis with protected amino acids. Figure adapted from Endo, M. M.; Cioffi, A. G.; Burke, M. D. *Syn. Lett.* 2016, *27*, 337-354.

Just as iterative peptide coupling has enabled the synthesis of a wide range of peptides, ICC has been utilized toward the synthesis of a number of natural products including ratahine,[79,81] retinal,[81,82] parinaric acid,[81,82] crocacin C,[81,83] peridinin,[84] synechoxanthin,[85] asnipyrone B,[86] physarigin A,[86] neurosporaxanthin β-D-glucopyranoside,[86] citreofuran,[81] oblongolide,[81] and the polyene cores of AmB[82] and vacidin A.[87] In fact, ICC has had a transformative impact on polyene synthesis as the polyene cores of over 75% of all polyene natural products can be synthesized from just 12 bifunctional MIDA boronate building blocks.[86] Furthermore, these MIDA boronates are generally free-flowing, air- and temperature-stable, crystalline solids that have an unusual binary affinity for silica gel, which has enabled the ICC platform to now be automated.[81] This general strategy could enable access to any desired AmB derivative by simply changing a single building block in this modular platform.

1-6 SUMMARY

For over sixty years, AmB has remained as the last line of defense against a wide range of invasive fungal infections. Despite its continuous usage and the extensive studies outlined above, the mechanism of which AmB kills cells remains unclear. A significant contributor to this lack of clarity has been the deficiency of definitive experiments to understand the atomistic underpinnings of this complex small molecule. Covalent modifications are the most common strategy in the derivatization of AmB. However, interpreting the findings from these derivatives are complicated

15

by the difficulty to discern whether changes in activity are due to functional group changes or increases in sterics. Recent studies using functional group-deficient derivatives have found that the C19 mycosamine is essential for the biological activity of AmB. However, further work is necessary to explore this mycosamine-dependent mechanism of action. The following chapters describe the studies taken to understand the mechanism of toxicity to both yeast and human cells and how that understanding has enabled the development of less toxic AmB derivatives.

1-7 REFERENCES

1. Brown, G. D.; et al. *Sci. Transl. Med.* **2012**, *4*, 165rv13.
2. Wisplinghoff, H.; et al. *Clin. Infect. Dis.* **2004**, *39*, 309-317.
3. Kami, M.; et al. *Br. J. Haematol.* **2002**, *117*, 40-46.
4. Gold, W.; Stout, H. A.; Pagano, J. F.; Donovick, R. *Antibiot. Annu.* **1955**, *3*, 579-586.
5. Vandeputte, J.; Wachtel, J. L.; Stiller, E. T. *Antibiot. Annu.* **1955**, *3*, 587-592.
6. Sternberg, T. H.; Wright, E. T.; Oura, M. *Antibiot. Annu.* **1955**, *3*, 566-573
7. Steinberg, B. A.; Jambor, W. P.; Suydom, L. O. *Antibiot. Annu.* **1955**, *3*, 574-578.
8. Akaike, N.; Harata, N. *Jpn. J. Physiol.* **1994**, *44*, 433-473.
9. Halde, C.; Newcomer, V. D.; Wright, E. T.; Sternberg, T. H. *J. Invest. Dermatol.* **1957**, *28*, 217-232.
10. Procknow, J. J.; Loosli, C. G. *Arch. Intern. Med.* **1958**, *101*, 765-802
11. Ellis, D. *J. Antimicrob. Chemother.* **2002**, *49*, 7-10.
12. Li, J.; et al. *Lancet Infect. Dis.* **2006**, *6*, 589-601.
13. Cortes, J. E.; et al. *N. Engl. J. Med.* **2013**, *369*, 1783-1796.
14. Rogers, T. R. *Int. J. Antimicrob. Ag.* **2006**, *27S*, S7-S11.
15. Kinsky, S. C. *Biochem. Biophys. Res. Commun.* **1961**, *5*, 353-357.
16. Kinsky, S. C. *J. Bacteriol.* **1961**, *2*, 889-897.
17. Andreoli, T. E.; Monahan, M. *J. Gen. Physiol.* **1968**, *52*, 300-325.
18. Cass, A.; Finkelstein, A.; Krespi, V. *J. Gen. Physiol.* **1970**, *56*, 100-124.
19. Ermishkin, L. N.; Kasumov, Kh. M.; Potzeluyev, V. M. *Nature*, **1976**, *262*, 698-699.
20. Andreoli, T. E. *Kidney Int.* **1973**, *4*, 337-345.
21. Andreoli, T. E. *Ann. N.Y. Acad. Sci.* **1974**, *235*, 448-468.

22. Finkelstein, A.; Holz, R. In *Membranes. Lipid Bilayers and Antibiotics*, Eiseman, G. Ed.; Marcel Dekker, Inc.: New York, 1973; vol. 2, 377-408.

23. de Kruijff, B.; Demel, R. A. *Biochim. Biophys. Acta* **1974**, *339*, 57-70.

24. Kasumov, Kh. M.; Borisova, M. P.; Ermishkin, L. N.; Potseluyev, V. M.; Silbershtein, A. Ya. *Biochim. Biophys. Acta* **1979**, *551*, 229-237.

25. Khutorsky, V. E. *Biochim. Biophys. Acta* **1992**, *1108*, 123-127.

26. Baginski, M.; Resat, H.; MacCammon, J. A. *Mol. Pharmacol.* **1997**, *52*, 560-570.

27. Baginski, M.; Resat, H.; Borowski, E. *Biochim. Biophys. Acta* **2002**, *1567*, 63-78.

28. Umegawa, Y.; Matsumori, N.; Oishi, T.; Murata, M. *Tetrahedron Lett.* **2007**, *48*, 3393-3396.

29. Hervè, M.; Cybulska, B.; Gary-Bobo, C. M. *Eur. Biophys. J.* **1985**, *12*, 121-128.

30. Yamaji, N.; Matsumori, N.; Matsuoka, S.; Oishi, T.; Murata, M. *Org. Lett.* **2002**, *4*, 2087-2089.

31. Matsumori, N.; Yamaji, N.; Matsuoka, S.; Oishi, T.; Murata, M. *J. Am. Chem. Soc.* **2002**, *124*, 4180-4181.

32. Byrne, B.; Carmody, M.; Gibson, E.; Rawlings, B.; Caffrey, P. *Chem. Biol.* **2003**, *10*, 1215-1224.

33. Kinsky, S. C.; Avruch, J.; Permutt, M.; Rogers, H. B.; Schonder, A. A. *Biochem. Biophys. Res. Commun.* **1962**, *9*, 503-507.

34. Kinsky, S. C. *Proc. Natl. Acad. Sci. USA* **1962**, *48*, 1049-1056.

35. Feingold, D. S.; *Biochem. Biophys. Res. Commun.* **1965**, *19*, 261-267.

36. Urbina, J. A.; et al. *Biochim. Biophys. Acta* **1995**, *1238*, 163-176.

37. Henriksen, J. *Biophys. J.* **2006**, *90*, 1639-1649.

38. Hsueh, Y.; et al. *Biophys. J.* **2007**, *92*, 1606-1615.

39. HsuChen, C.- C.; Feingold, D. S. *Biochem. Biophys. Res. Commun.* **1973**, *51*, 972-978.

40. HsuChen, C.- C.; Feingold, D. S. *Antimicrob. Agents Chemother.* **1973**, *4*, 309-315.

41. Matsuoka, S.; Murata, M. *Biochim. Biophys. Acta* **2002**, *1564*, 429-434.

42. Zumbuehl, A.; Stano, P.; Heer, D.; Walde, P.; Carreira, E. M. *Org. Lett.* **2004**, *6*, 3683-3686.

43. Whyte, B. S.; Peterson, R. P.; Hartsel, S. C. *Biochem. Biophys. Res. Commun.* **1989**, *164*, 609-614.

44. Milhaud, J.; Hartmann, M. A.; Bolard, J. *Biochimie*, **1989**, *71*, 49-56.

45. Wolf, B. D.; Hartsel, S. C. *Biochim. Biophys. Acta* **1995**, *1238*, 156-162.

46. Ruckwardt, T.; Scott, A.; Scott, J.; Mikulecky, P.; Hartsel, S. C. *Biochim. Biophys. Acta* **1998**, *1372*, 283-288.

47. Cortero, B.; Rebolledo-Antúnez, S.; Ortega-Blake, I. *Biochim. Biophys. Acta* **1998**, *1375*, 43-51.

48. Venegas, B.; González-Damian, J.; Celis, H. Ortega-Blake, I. *Biophys. J.* **2003**, *85*, 2323-2332.

49. Gottlieb, D.; Carter, H. E.; Sloneker, J. H.; Amman, A. *Science*, **1958**, *128*, 361.

50. Kotler-Brajtburg, J.; Price, H. D.; Medoff, G.; Schlessinger, D.; Kobayashi, G. S. *Antimicrob. Agents Chemother.* **1974**, *5*, 377-382.

51. Gary-Bobo, C. M. *Biochimie* **1989**, *71*, 37-47.

52. Hervè, M.; Debouzy, J. C.; Borowski, E.; Cybulska, B.; Gary-Bobo, C. M. *Biochim. Biophys. Acta* **1989**, *980*, 261-272.

53. Chèron, M.; et al. *Biochem. Pharmacol.* **1988**, *37*, 827-836.

54. Baran, M.; Mazerski, J. *Biophys. Chem.* **2002**, *95*, 125-133.

55. Matsumori, N.; Sawada, Y.; Murata, M. *J. Am. Chem. Soc.* **2005**, *127*, 10667-10675.

56. Neumann, A.; Czub, J.; Baginski, M. *J. Phys. Chem. B* **2009**, *113*, 15875-15885.

57. Czub, J.; Neumann, A.; Borowski, D.; Baginski, M. *Biophys. Chem.* **2009**, *141*, 105-116.

58. Neumann, A.; Baginski, M.; Czub, J. *J. Am. Chem. Soc.* **2010**, *132*, 18266-18272.

59. Croatt, M. P.; Carreira, E. M. *Org. Lett.* **2011**, *13*, 1390-1393.

60. Norman, A. W.; Demel, R. A.; de Kruijff, B.; Guerts van Kessel, W. S. M.; van Deenan, L. L. M. *Biochim. Biophys. Acta* **1972**, *290*, 1-14.

61. Bolard, J.; Seigneuret, M.; Boudet, G. *Biochim. Biophys. Acta* **1980**, *599*, 280-293.

62. Gruda, I.; Nadeau, P.; Brajtburg, J.; Medoff, G. *Biochim. Biophys. Acta* **1980**, *602*, 260-270.

63. Vertut-Croquin, A.; Bolard, J.; Chabbert, M.; Gary-Bobo, C. *Biochemistry* **1983**, *22*, 2939-2944.

64. Gruda, I.; Bolard, J. *Biochem. Cell. Biol.* **1987**, *65*, 234-238.

65. Mazerski, J.; Bolard, J. Borowski, E. *Biochim. Biophys. Acta* **1995**, *1236*, 170-176.

66. Fujii, G.; Chang, J.- E.; Coley, T.; Steere, B. *Biochemistry*, **1997**, *36*, 4949-4968.

67. Ernst, C.; Grange, J. *Biopolymers* **1981**, *20*, 1575-1588.

68. Matsumori, N.; et al. *J. Am. Chem. Soc.* **2009**, *131*, 11855-11860.

69. Anderson, T. M.; et al. *Nat. Chem. Biol.* **2014**, *10*, 400-406.

70. Rychnovsky, S. D.; Mickus, D. E. *J. Org. Chem.* **1992**, *57*, 2732-2736.

71. Mickus, D. E.; Levitt, D. G. Rychnovsky, S. D. *J. Am. Chem. Soc.* **1992**, *114*, 359-360.

72. Nakagawa, Y.; et al. *Biochemistry*, **2014**, *53*, 3088-3094.

73. Nakagawa, Y.; et al. *Biochemistry*, **2015**, *54*, 303-312.

74. Morrison, K. L.; Weiss, G. A. *Curr. Opin. Chem. Biol.* **2001**, *5*, 302-307.

75. Palacios, D. S.; Anderson, T. M.; Burke, M. D. *J. Am. Chem. Soc.* **2007**, *129*, 13804-13805.

76. Delaglio, F.; Zhengrong, W.; Bax, A. *J. Magn. Reson.* **2001**, *149*, 276-281.

77. Palacios, D. S.; Dailey, I.; Siebert, D. M.; Wilcock, B. C.; Burke, M. D. *J. Am. Chem. Soc.* **2007**, *129*, 13804-13805.

78. te Welscher, Y. M.; et al. *J. Biol. Chem.* **2008**, *283*, 6393-6401.

79. Gillis, E. P.; Burke, M. D. *J. Am. Chem. Soc.* **2007**, *129*, 6716-6717.

80. Merrifield, R. B. *Science* **1965**, *150*, 178-185.

81. Li, J.; et al. *Science*, **2015**, *347*, 1221-1226.

82. Lee, S. J.; Gray, K. C.; Paek, J. S.; Burke, M. D. *J. Am. Chem. Soc.* **2008**, *130*, 466-468.

83. Gillis, E. P.; Burke, M. D. *J. Am. Chem. Soc.* **2008**, *130*, 14084-14085.

84. Woerly, E. M.; Cherney, A. H.; Davis, E. K.; Burke, M. D. *J. Am. Chem. Soc.* **2010**, *132*, 6941-6943.

85. Fujii, S.; Chang, S. Y.; Burke, M. D. *Angew. Chem. Int. Ed.* **2011**, *50*, 7862-7864.

86. Woerly, E. M.; Roy, J. Burke, M. D. *Nat. Chem.* **2014**, *6*, 484-491.

87. Lee, S. J.; Anderson, T. M.; Burke, M. D. *Angew. Chem. Int. Ed.* **2010**, *49*, 8860-8863.

CHAPTER 2

ERGOSTEROL BINDING IS THE PRIMARY MECHANISM OF ACTION OF AMPHOTERICIN B

Despite over half a century of study, the primary mechanism of action for AmB has remained unclear. We hypothesized that ergosterol binding was the primary mechanism of AmB and similarly all mycosamine-containing polyene macrolides. To test this hypothesis, we synthesized a derivative of AmB, C35deOAmB, via an iterative cross-coupling (ICC)-based strategy. C35deOAmB retained the ability to bind ergosterol, but lacked the capacity to permeabilize membranes. This derivative was similar to natamycin, another mycosamine-containing polyene macrolide, which also binds ergosterol but does not cause membrane permeabilization. Both C35deOAmB and natamycin have potent antifungal activities that were only six-fold and four-fold less than AmB, respectively. Furthermore, removal of the mycosamine appendage from either AmB or natamycin completely abolished the ergosterol binding capacities and antifungal activities of both polyene macrolides. These results are consistent with the hypothesis that mycosamine-mediated ergosterol binding is the primary mechanism of action for mycosamine-containing polyene macrolides, and that the ion channel ability of AmB may act as a complementary mechanism that could marginally increase the potency of this natural product.

C35deOAmB was prepared in collaboration with Dr. Kaitlyn Gray, Dr. Daniel Palacios, Dr. Ian Dailey, Dr. Brice Uno, Dr. Brandon Wilcock, and Prof. Martin Burke. Natamycin aglycone was synthesized by Dr. Kaitlyn Gray. ITC experiments were performed in collaboration with Dr. Ian Dailey. Liposome and yeast efflux experiments were performed in collaboration with Dr. Daniel Palacios. MIC experiments were performed in collaboration with Dr. Daniel Palacios and Dr. Kaitlyn Gray. Killing kinetics studies were performed by Dr. Kaitlyn Gray. Ergosterol quantification were performed in collaboration with Dr. Daniel Palacios. Portions of this chapter were adapted from Gray, K. C.; Palacios, D. S.; Dailey, I.; Endo, M. M.; Uno, B. E.; Wilcock, B. C.; Burke, M. D. *Proc. Natl. Acad. Sci. U.S.A.* **2012**, *109*, 2234-2239.

2-1 BACKGROUND

As discussed in Chapter 1, despite over half a century of extensive studies, the mechanism by which AmB kills yeast remained unclear. However, the recent finding that the deletion of the mycosamine appendage resulted in complete abolishment of ergosterol binding capacity, the ability to form ion channels, and antifungal activity led us to hypothesize two possible models for AmB's toxicity to yeast.[1,2] The first model was the long-standing ion channel model where AmB binds to ergosterol and subsequently self-assembles into a transmembrane channel, resulting in membrane permeabilization and eventually cell death (Figure 1.1A).[3-8] In an alternative model, the binding of ergosterol is sufficient for the killing of yeast (Figure 1.1B) and that the ion channel capacity only further increases AmB's potency.

Several recent reports found that ergosterol plays a number of critical roles in yeast physiology. These include endocytosis,[9] pheromone signaling,[10] and membrane compartmentalization.[11] Inhibition of yeast ergosterol biosynthesis by fluconazole also inhibits membrane fusion during mating.[10] Interestingly, a similar phenomenon occurs when treated with the polyene macrolide nystatin.[10] Ergosterol is also essential for proper vacuole fusion,[12] which can be inhibited by natamycin (Figure 2.1C),[13] another polyene macrolide that has been shown to bind ergosterol but not form ion channels.[14] Furthermore, natamycin also inhibits a number of membrane transport proteins[15] that are highly dependent on ergosterol.[16]

Though incredibly rare, polyene macrolide-resistant yeast strains generally contain modified sterol content.[17,18] Additionally, structural modification and/or decreased ergosterol expression via mutations in the ergosterol biosynthesis pathway dramatically reduces the pathogenicity of these yeast strains.[19] This may explain the inability for yeast to develop AmB resistance in the clinic.[20] Collectively, these lines of evidence led us to hypothesize that AmB and all other mycosamine-containing polyene macrolides primarily kill yeast by binding membranous ergosterol and that capacity to cause membrane permeabilization for certain members only marginally increase their potency.

2-2 DESIGN OF PROBES TO TEST ERGOSTEROL BINDING AS THE PRIMARY MECHANISM OF AmB

In order to test the hypothesis that sterol binding is the primary mechanism of action of AmB, we required a derivative of AmB that retains the ability to still bind ergosterol, but lacks the

capacity to form ion channels. However, the structures of the AmB/ergosterol complex and the multimeric AmB-based ion channel have remained unknown, which makes the rational design of such a derivative very challenging. Fortunately, our group's previous studies with AmB had shown that mycosamine appendage was critical in AmB ability to bind ergosterol,[1,2] so it clear that this appendage should remain intact. Alternatively, computer modeling predicted two leading models for the AmB ion channel in which both required the C35 hydroxyl group in stabilizing this supermolecular ion channel (Figure 1.1A).[21] In the single barrel model, the AmB aggregate spans a dimpled membrane and the C35 hydroxyl groups form hydrogen bonds with the polar phospholipid head groups.[21] In the double barrel model, two single barrel units, that each spans half the length of the lipid bilayer, dimerize through hydrogen bonds between C35 hydroxyl groups of AmB molecules in the opposing membrane leaflets.[21] In both cases, the C35 hydroxyl group is predicted to play a critical role in AmB's ability to form ion channels and thus would be an attractive target towards disrupting AmB's ion channel forming capacity.
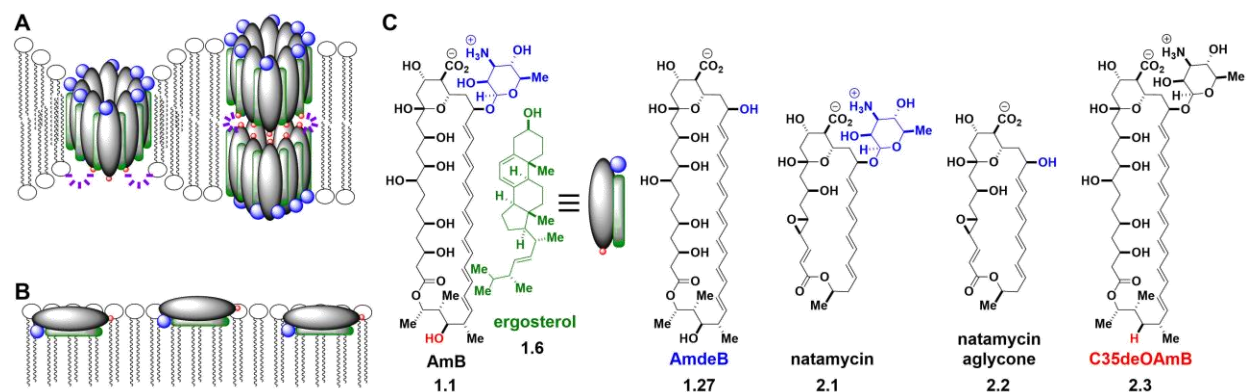
Figure 2.1: Mechanisms models and chemical structures of the mechanistic probes. A.) Representation of the single- and double-barrel ion channel models. B.) Representation of the ergosterol binding model. C.) Chemical structures of the natural products AmB, natamycin, and their derivatives to probe the dual mechanism hypothesis.

The C35 hydroxyl group has been investigated by Carreira and coworkers by synthesizing a doubly-modified derivative of AmB lacking the C35 hydroxyl and where the C41 carboxylate was protected as a methyl ester.[22,23] This derivative demonstrated a weak potassium efflux from liposomes at a concentration of 10 μM and no efflux at a concentration of 1 μM, lending support that the C35 hydroxyl plays a major role in ion channel ability. Furthermore, the authors reported a 26-fold loss in antifungal activity relative to AmB methyl ester (AmE) against *C. albicans*. However, there was no report of sterol binding for either compound. Based on the liposomal potassium efflux assay and antifungal activity, Carreira and coworkers concluded that C35

hydroxyl was critical in ion channel formation, which was necessary for the fungicidal activity of AmB.[23]

We hypothesized that the weak efflux observed by Carreira and coworkers at elevated concentrations was likely an artifact due to the increased sensitivity of liposomes to permeabilization compared to live yeast cells and/or the unique biophysical properties of net positively-charged AmB derivatives such as the C41 methyl ester derivatives.[20] In order to test this hypothesis, I performed liposomal potassium efflux assays with AmdeB, which does not bind sterol, has no antifungal activity, and does not permeabilize *S. cerevisiae* even at elevated concentrations of 30 μM (Figure 2.2A). While the derivative does not permeabilize yeast cells, it does cause potassium efflux in POPC LUVs at 10 and 30 μM (Figure 2.2B), thus demonstrating the increased sensitivity of liposomes relative to yeast cells. Additionally, I performed liposomal potassium efflux assays with AmE (net positive) compared to AmB (net neutral). Consistent with ergosterol being required for AmB ion channel formation, no substantial potassium efflux is observed when sterol-free POPC LUVs are treated with AmB even at the elevated concentration of 30 μM (Figure 2.3). However, AmE causes significant efflux in sterol-free POPC LUVs at concentrations of 10 and 30 μM (Figure 2.3), thus demonstrating the unique biophysical properties of net positive AmB derivatives. Thus, toward the goal of retaining sterol binding, abolishing the capacity to permeabilize membranes, and enabling the direct comparison in biophysical and biological properties with the natural product, we targeted C35deOAmB (Figure 2.1C), which retains the C19 mycosamine, lacks the C35 hydroxyl group, and retains the anionic C41 carboxylate.
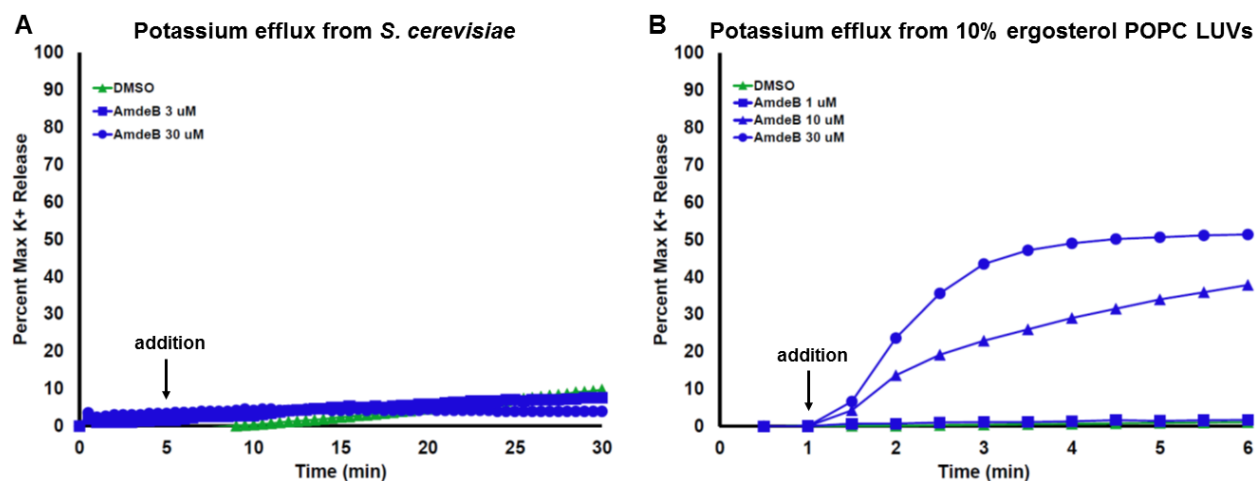
Figure 2.2: Potassium efflux upon treatment with AmdeB in (A) *S. cerevisiae* and (B) POPC LUVs.
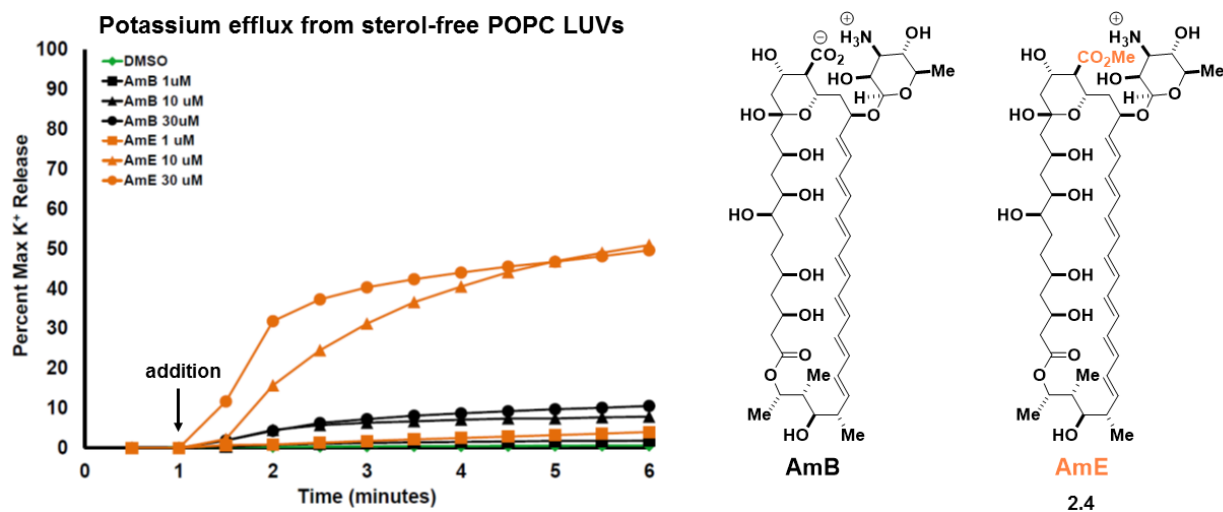
Figure 2.3: Potassium efflux upon treatment with AmB (net neutral) or AmE (net positive) in sterol-deficient POPC LUVs.

To further investigate the generality of mycosamine-dependent sterol binding in polyene macrolide natural products, we also targeted the synthesis of natamycin aglycone (Figure 2.1C). The methyl ester of this compound had been previously synthesized by Masamune and coworkers through degradative synthesis of the natural product.[24] Based on that report and our group's synthesis of AmdeB, Dr. Kaitlyn Gray completed the synthesis of natamycin aglycone to test the hypothesis that mycosamine sugar was critical in the binding of polyene macrolides with ergosterol.[20]

2-3 SYNTHESIS OF C35deOAmB

Synthesis of polyene macrolides are very challenging due to their sensitivity to light, oxygen, and many organic reagents. To overcome these challenges, we utilized an ICC-based[25] semisynthetic strategy with building blocks **2.5**, **2.6**, and **2.7** that were linked together via iterative Suzuki-Miyaura cross-couplings enabled by the *N*-methyliminodiacetic acid (MIDA) ligand (Figure 2.4). Further details on ICC can be found in Chapter 1. Based on pioneering studies by Nicolaou,[26-28] Rychnovsky,[29] and Murata,[30] the synthesis of building block **2.5** was developed by Dr. Kaitlyn Gray (Scheme 2.1).[20] Large amounts of building block **2.5** were synthesized in collaboration with Dr. Daniel Palacios, Dr. Ian Dailey, Dr. Brice Uno, and Dr. Brandon Wilcock. Beginning from the natural product, global protection of all of the protic functional groups was performed to reach protected intermediate **2.6**. The polyene was then excised via ozonolysis, and the resulting bisaldehyde was converted to the bisvinyl iodide via Takai olefination. Finally,

cleavage of the western half of the bisvinyl iodide followed by cross-coupling with bisborylated **2.7** yielded our first building block **2.5**.
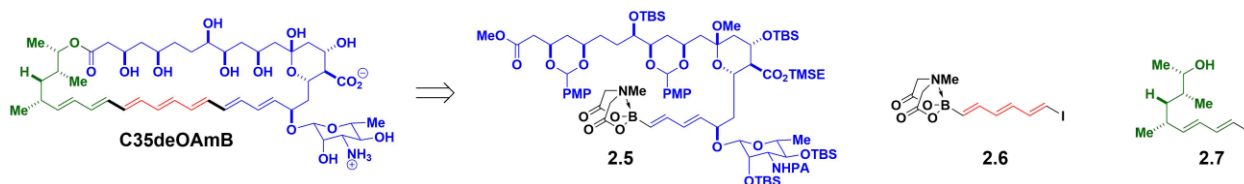
Figure 2.4: Retrosynthesis of C35deOAmB from its three building blocks.
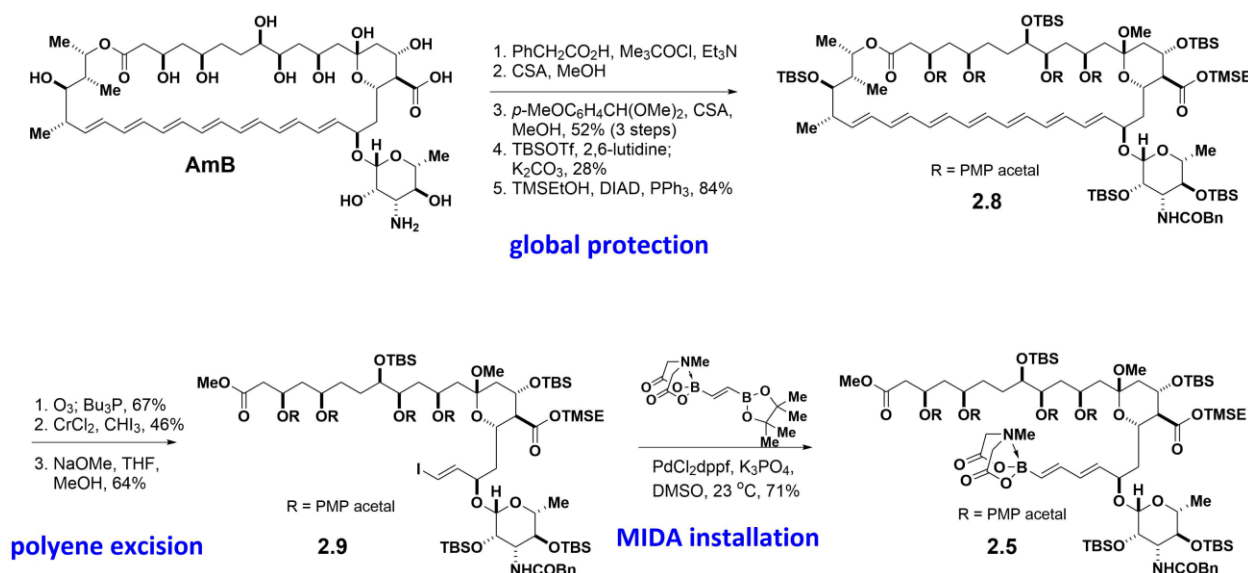
Scheme 2.1: Synthesis of building block **2.5**.

The synthesis of building block **2.6**, was previously developed in our group by Dr. Suk Joong Lee utilizing the triethylgermanium group as a masking group for halides that could be utilized in ICC.[31] Due to the need for several grams of building block **2.6**, large amounts of building block **2.6**, were synthesized by Dr. Ian Dailey, Dr. Kaitlyn Gray, and Dr. Brice Uno.[20] The synthesis of building block **2.7**, was developed and prepared by Dr. Kaitlyn Gray.[20]

With all three building blocks in hand, the macrolide skeleton of C35deOAmB was assembled by Dr. Kaitlyn Gray and Dr. Ian Dailey (Scheme 2.2).[20] Building block **2.5** was converted to the pinacol boronic ester, followed by cross-coupling with building block **2.6** yielding pentaene **2.10**. *In situ* deprotection of the MIDA boronate and cross-coupling with building block **2.7**, followed by saponification and macrolactonization resulted in **2.11**. Global deprotection were developed and performed by Dr. Kaitlyn Gray and Dr. Daniel Palacios enabling access to C35deOAmB.[20]
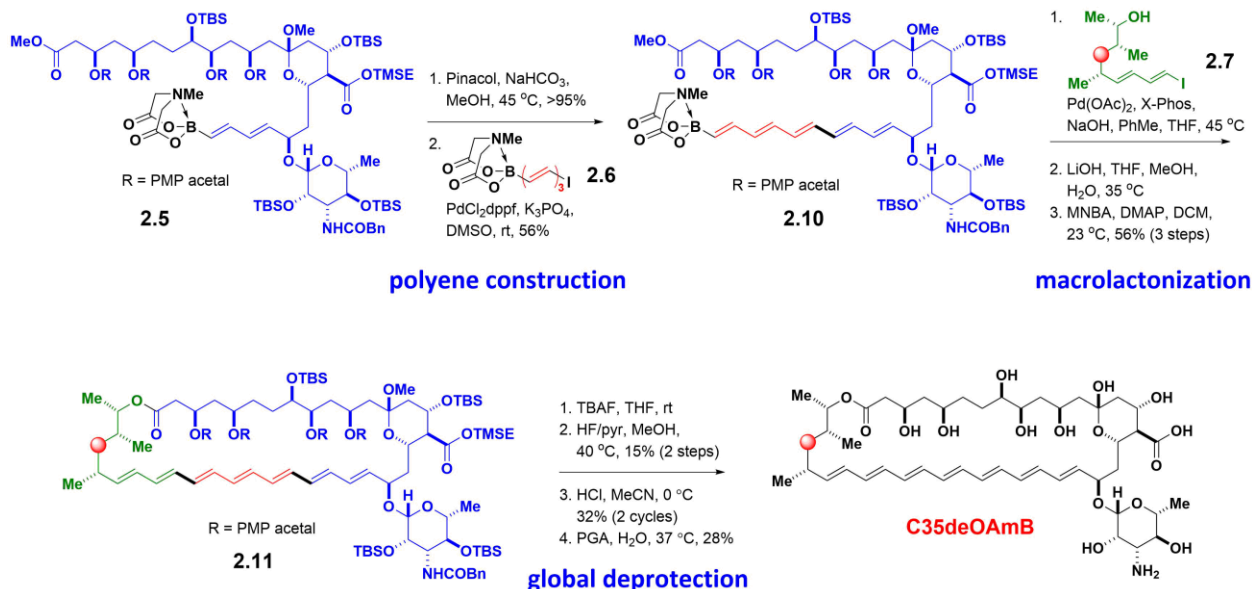
Scheme 2.2: Synthesis of C35deOAmB via ICC.

2-4 ERGOSTEROL BINDING VIA ISOTHERMAL TITRATION CALORIMETRY

With the desired probes in hand, we first set out to determine the capacity of our compounds to bind membrane-embedded ergosterol. In order to study the non-covalent binding of our probes and ergosterol, we utilized the valuable technique of isothermal titration calorimetry (ITC). ITC is a useful technique for studying the non-covalent interaction between two chemical species without having to modify either binding partner and can potentially determine all of the thermodynamic parameters of the system in a single experiment.

The ITC instrument consists of a sample cell and a reference cell within an adiabatic chamber. The sample cells and reference cells are maintained at a constant temperature by applying heat to each cell. The instrument measures the difference in heat that is being applied to each of the cells. The sample cell is filled with one of the binding partners, in our case, a solution of AmB or its derivatives in an aqueous buffer, while the reference cell is filled with aqueous buffer only. The syringe contains the other binding partner, which in our case was a suspension of large unilamellar vesicles in aqueous buffer, either sterol-containing or sterol-deficient. Using the computer software to control the syringe, the suspension is injected into the sample cell in controlled amounts. If there is a heat change upon injection, the heat applied to the sample will change and the difference in heat applied is measured over time. Integration of this heat difference over time results in the enthalpy (ΔH) of this titration system. The titration exotherms can be fitted

to a binding model, by which the binding constant (K) and stoichiometry (n) can be determined. From these parameters, the remaining thermodynamic parameters, free energy (ΔG) and entropy (ΔS), can also be determined.

Our group[2] as well as the te Welscher group[14] have previously utilized ITC to study polyene macrolides binding to membrane-embedded sterols. However, due to significant synthetic overhead to generate C35deOAmB, we needed to minimize the amount of compound used in the ITC experiment without compromising the sensitivity of the experiment. Our group had originally used a MicroCal calorimeter with a sample cell volume of 1.45 mL, but actually required 2.2 mL of sample solution for sample loading.[2] The concentration used in these experiments was 150 µM, and so a single ITC experiment required almost 300 µg of material. In collaboration with Dr. Ian Dailey, we sought to miniaturize the ITC assay using a NanoITC calorimetry that had a sample cell volume of just 190 µL, which required 300 µL of sample solution.[20] We were able to reduce our required sample amount by almost tenfold (~40 µg), enabling the completion of this study.
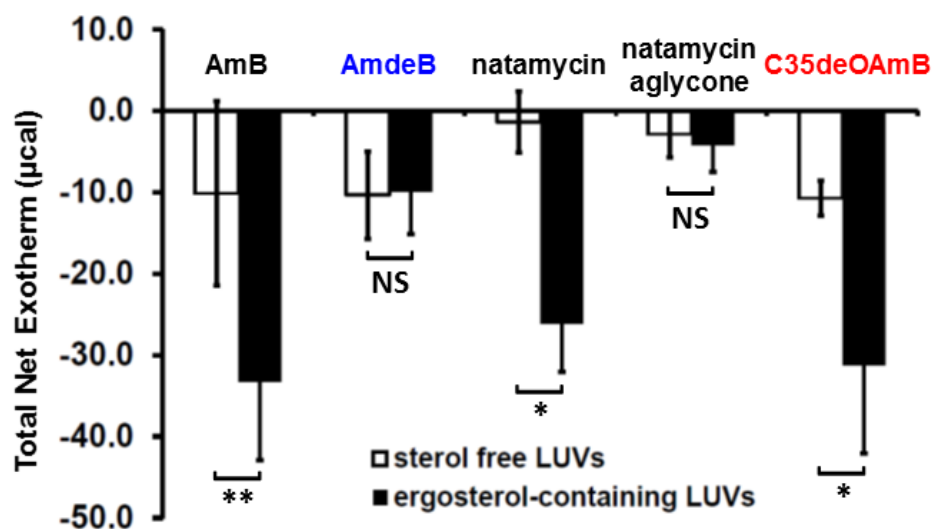
Figure 2.5: Isothermal titration calorimetry with all five probes titrated with 10% ergosterol-containing or sterol-free LUVs. * $P \leq$ 0.05, ** $P \leq 0.01$, and NS = not significant.

To validate our new ITC conditions, we first titrated AmB with either sterol-free or 10% ergosterol-containing POPC LUVs (Figure 2.5). Consistent with our previous results,[2] a substantial increase in net exotherm was observed when titrating with ergosterol-containing LUVs compared to sterol-deficient LUVs, indicating a direct binding interaction between AmB and ergosterol. We performed the same set of experiments with AmdeB and observed no change in exotherm when titrating with ergosterol-containing LUVs compared to sterol-free LUVs, again consistent with previous results that the mycosamine appendage is required for AmB to bind

ergosterol.[2] With our validated miniaturized ITC assay, we performed the same series of experiments with natamycin and its aglycone. Consistent with literature precedent,[14] we observed a significant increase in exotherm when titrating with 10% ergosterol-containing POPC LUVs relative to sterol-free POPC LUVs, demonstrating that natamycin binds ergosterol. However, natamycin aglycone showed no difference in exotherm between the two LUV systems, demonstrating for the first time that the mycosamine sugar was critical for natamycin to bind ergosterol. This provided further evidence for the hypothesis that the mycosamine appendage was a universal sterol binding element in polyene macrolides. Most importantly, we titrated C35deOAmB with our two LUVs system and observed an increase in exotherm identical to that of AmB, indicating that C35deOAmB retains its capacity to bind ergosterol.

2-5 MEMBRANE PERMEABILIZATION

Having determined the capacities for our probes to bind ergosterol, we next investigated their abilities to permeabilize membranes. In collaboration with Dr. Daniel Palacios, we developed a potassium ion efflux assay to test our probes' capacities to permeabilize lipid and yeast membranes. In this assay, we would take a suspension of the same 10% ergosterol-containing POPC LUVs from our ITC studies or *S. cerevisiae* cells in a potassium-free buffer and add our small molecule probes. The extracellular potassium concentration would be measured with a commercially available valinomycin-based potassium-selective ion probe.

Our group had previously used an electromagnetic-shielded potassium-selective ion probe to detect extracellular efflux of potassium.[2] However, the bulkiness of this shielded potassium ion probe required 15 mL of a 30 μM solution of our small molecule probes in this assay, which would be ~400 μg per experiment. Due to the synthetic overhead of our C35deOAmB probe, we once again sought to minimize the assay with a smaller unshielded potassium-selective probe. With this smaller probe, we were able to minimize the volume to 3 mL of a 30 μM solution for a five-fold (~80 μg) reduction. However, this unshielded potassium ion probe was subject to electromagnetic interference and so the assay set-up was placed in a Faraday cage to minimize undesired interference.
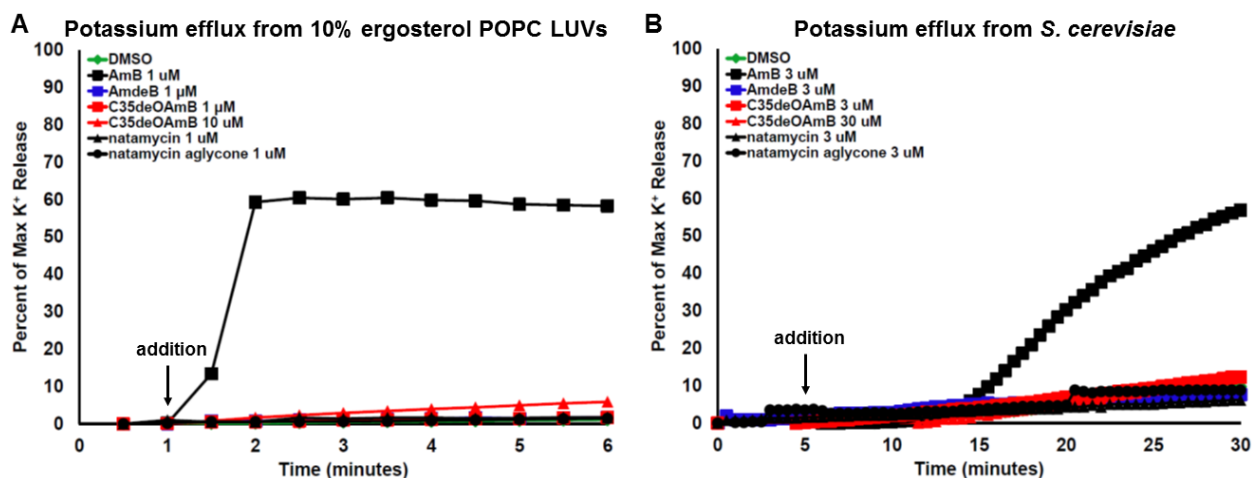
Figure 2.6: Potassium efflux in (A) 10% ergosterol-containing POPC LUVs and (B) live *S. cerevisiae* upon treatment with all five probes.

With our miniaturized potassium efflux assay, we first tested our molecular probes' capacities to permeabilize the lipid membranes of the same 10% ergosterol-containing POPC LUVs that we used in ITC experiments (Figure 2.6A). Exposure of the LUVs to AmB at a concentration of 1 μM produced a rapid efflux of potassium ions. In contrast, administration of AmdeB, natamycin, and natamycin aglycone showed no potassium efflux, demonstrating that these compounds do not permeabilize membranes. Importantly, C35deOAmB was devoid of permeabilizing activity, even at the relatively high concentration of 10 μM. We then examined the ability of our probes to permeabilize live *S. cerevisiae* cells (Figure 2.6B). AmB, at 3 μM, produced a rapid and robust efflux of potassium ions from the yeast cells, whereas AmdeB, natamycin, and natamycin aglycone did not, lacking the capacity to cause membrane permeabilization. Most importantly, C35deOAmB also was devoid of membrane permeabilization, even at the high concentration of 30 μM. Collectively, these results demonstrate that C35deOAmB retains the ability to bind ergosterol, but lacks the capacity for membrane permeabilization. This derivative is a powerful tool for probing our hypothesis that sterol binding is primary mechanism of action for the antifungal activity of AmB. Furthermore, the loss in sterol binding capacity for AmdeB and natamycin aglycone provide further evidence of the putatively dominant and general role of the mycoamine appendage in the antifungal activity of polyene macrolide natural products.

2-6 ANTIFUNGAL ACTIVITY

In collaboration with Dr. Daniel Palacios and Dr. Kaitlyn Gray, we examined the ability of our derivatives to kill *S. cerevisiae* cells in standardized broth microdilution assays (Figure 2.7A).

AmB, which binds ergosterol and forms ion channels, showed potent antifungal activity with a minimum inhibitory concentration (MIC) of 0.5 μM. AmdeB, the non-sterol binding aglycone, was completely inactive against *S. cerevisiae* even up to 500 μM.[1,2] Natamycin, which binds ergosterol but does not form ion channels, was just four-fold less potent than AmB (MIC = 2 μM). Like AmdeB, natamycin aglycone was also completely inactive up to 500 μM. Most importantly, C35deOAmB still maintained antifungal activity (MIC = 3 μM). Interestingly, both natamycin and C35deOAmB, which bind ergosterol but lack the capacity to permeabilize membranes, have remarkably similar MICs. We tested our probes against the clinically relevant yeast *C. albicans* and observed a very similar set of results.

A

	AmB	AmdeB	natamycin	natamycin aglycone	C35deOAmB
S. cerevisiae	0.5	>500	2	>500	3
C. albicans	0.25	>500	4	>500	4

toxic concentration (μM)
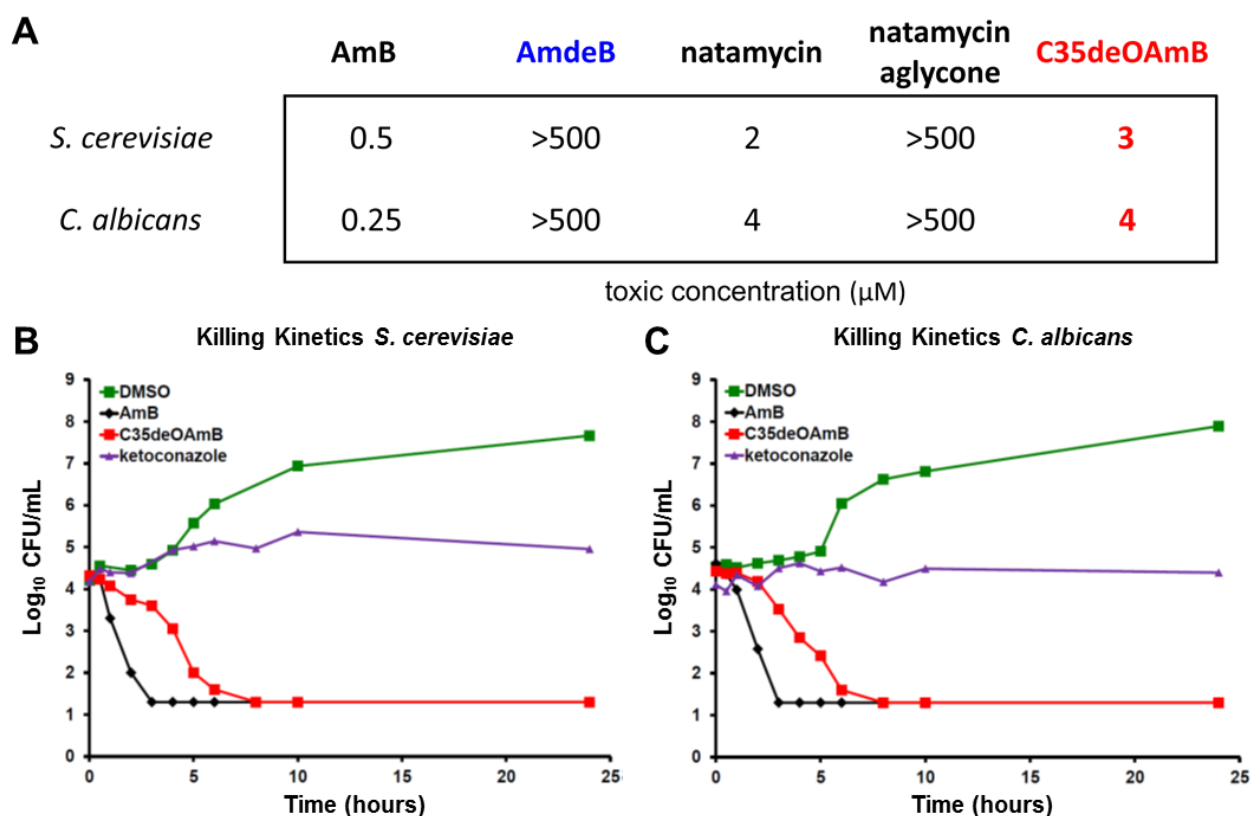
Figure 2.7: Yeast toxicity assays (A) MICs from microbroth dilution assays of all five probes. Killing kinetics studies with (B) *S. cerevisiae* and (C) *C. albicans* where AmB and C35deOAmB demonstrate potent fungicidal activity in contrast to the known fungistatic agent ketoconazole.

To further probe whether ergosterol binding was a fungicidal or fungistatic mode of action, Dr. Kaitlyn Gray performed yeast killing kinetics studies to differentiate between both modes in *S. cerevisiae* (Figure 2.7B).[32] AmB showed a dramatic decrease in colony forming units (CFUs) below the limit of detection, consistent with AmB being a known fungicidal agent. While ketoconazole, a known fungistatic agent, maintained the number of CFUs across the 24 hour study.

30

Most importantly, C35deOAmB causes a significant decrease in CFUs, providing evidence that ergosterol binding is a fungicidal mechanism of action. A similar set of results was also seen in *C. albicans* (Figure 2.7B).

Finally, the hypothesis that ergosterol binding is the primary mechanism of action would predict that there would be a significant number of AmB molecules relative to ergosterol molecules at the MIC. To test this hypothesis, in collaboration with Dr. Daniel Palacios, we quantified the number of ergosterol molecules in a yeast cell at the MIC via extraction and high performance liquid chromatography (HPLC) quantification (Figure 2.8).[33] Acidic and alkaline reflux disrupted the membrane integrity, which enabled extraction of the ergosterol from the lysed yeast cells. The amount of ergosterol extracted was compared to a standard curve via HPLC analysis. We found that at the MIC, there is over a magnitude greater amount of AmB molecules per a yeast cell compared to the number of ergosterol molecules per a yeast cell in both *S. cerevisiae* and *C. albicans*.
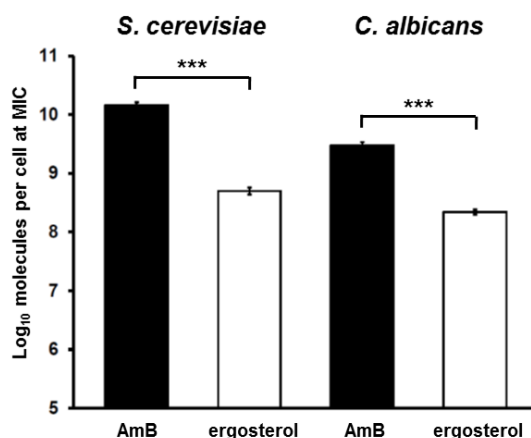
Figure 2.8: Quantification of the number of molecules of ergosterol per yeast cell compared to the number of AmB molecules per yeast cell at the MIC concentration.

Collectively, these results strongly support the hypothesis that mycosamine-mediated ergosterol binding is the primary mechanism of action of AmB and that its ion channel formation ability is a complementary mechanism that further increases the potency of this natural product.[20] Furthermore, the conservation of the mycosamine sugar in the large family of polyene macrolides combined with the requirement for this moiety to bind ergosterol highly suggests that mycosamine-mediated ergosterol binding is the primary antifungal mechanism of action across this entire family of natural products.

2-7 SUMMARY

Utilizing the ICC platform,[25] we have completed the synthesis of C35deOAmB and with this probe, determined the primary mechanism of action for mycosamine-containing polyene macrolides. C35deOAmB retains the ability to bind ergosterol, but is unable to permeabilize membranes similar to natamycin, another polyene macrolide. Despite the loss in capacity for membrane permeabilization, both natamycin and C35deOAmB demonstrate similar potent antifungal activity. Removal of the mycosamine sugar from AmB and natamycin completely abolishes sterol binding ability and antifungal activity for both polyene macrolides. These results strongly support the conclusion that mycosamine-mediated sterol binding is the primary mechanism of action of mycosamin-containing polyene macrolides. This finding has important implications in several areas.

First, the rapid development of antibiotic resistance has resulted in an emergent global public health crisis.[34-36] However, despite its extensive use for over half a century, AmB resistance has remained exceptionally rare.[37,38] Thus, clinically relevant antimicrobial mechanisms that evade resistance exist, and include AmB's mode(s) of action. The discovery that AmB acts primarily by binding a functionally vital lipid suggests that this may represent a mechanism of action with the potential to evade resistance in the clinical setting. Additionally, the possession of a dual mode of action, i.e., lipid binding and membrane permeabilization, likely contributes to AmB's resistance-refractory nature. This dual mechanism property is shared with the antimicrobial peptide nisin that also operates primarily by binding the critically vital Lipid II in bacterial membranes and secondarily promotes membrane permeabilization.[39]

Second, the discovery that ergosterol binding rather than ion channel formation is the primary mechanism of action of AmB suggests that the cytocidal effects of these two mechanisms may be separable. This has important implications for the development of small molecules that can replace the function of missing or deficient ion channel proteins in human disease. The discovery that membrane permeabilization is a relatively minor contributor to the cytocidal activity has led to the recent discovery that this achievable as AmB has been utilized to restore the physiology of a yeast strain missing a critical protein ion channel.[40]

Finally, extensive efforts to improve the therapeutic index of AmB has been guided by the classic mechanistic model in which ion channel formation is paramount to its biological activity.[3-8] These studies have focused on selectively forming ion channels in yeast cells versus human cells.

However, the discovery that ergosterol binding is the primary mechanism for its fungicidal activity against yeast suggests that cholesterol binding may be the primary mechanism of toxicity in humans. If that is case, improving the therapeutic index of AmB can focus on the much simpler problem of selectively binding ergosterol over cholesterol.

2-8 EXPERIMENTAL SECTION

Materials.

Commercially available materials were purchased from Sigma-Aldrich, Alfa Aesar, Strem, Avanti Polar Lipids, or Fisher Scientific and were used without further purification unless stated otherwise. Amphotericin B was a generous gift from Bristol-Myers Squibb Company. All solvents were dispensed from a solvent purification system that passes solvents through packed columns according to the method of Pangborn and coworkers[41] (THF, Et$_2$O, CH$_2$Cl$_2$, toluene, dioxane, hexanes : dry neutral alumina; DMSO, DMF, CH$_3$OH : activated molecular sieves). Water was obtained from a Millipore MilliQ water purification system.

Reactions.

All reactions were performed in oven- or flame-dried glassware under an atmosphere of argon unless otherwise indicated. Reactions were monitored by analytical thin layer chromatography performed using the indicated solvent on E. Merck silica gel 60 F$_{254}$ plates (0.25mm). Compounds were visualized using a UV (λ_{254}) lamp or stained by an acidic solution of KMnO$_4$.

Purification and Analysis.

Flash chromatography was performed as described by Still and coworkers[42] using the indicated solvent on E. Merck silica gel 60 230-400 mesh. ^{1}H NMR spectra were recorded at 23 °C on one of the following instruments: Varian Unity 400, Varian Unity 500, Varian Unity Inova 500NB. Chemical shifts (δ) are reported in parts per million (ppm) downfield from tetramethylsilane and referenced internally to the residual protium in the NMR solvent (CHCl$_3$, δ = 7.26) or to added tetramethylsilane. ^{13}C spectra were recorded at 23 °C with a Varian Unity 500. Chemical shifts (δ) are reported downfield of tetramethylsilane and are referenced to the carbon resonances in the NMR solvent (CDCl$_3$, δ = 77.16, center line) or to added tetramethylsilane. High

resolution mass spectra (HRMS) were obtained at the University of Illinois mass spectrometry facility. All synthesized compounds gave HRMS within 5 ppm of calculated values.
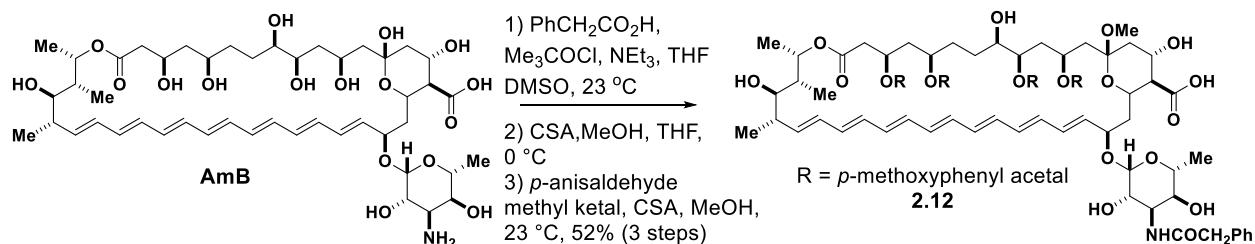
Acetal Protected 2.12

Trimethyl acetyl chloride (400 μL, 3.25 mmol, 2 eq) was added to a solution of phenyl acetic acid (662 mg, 4.86 mmol, 3 eq) in THF (30 mL). Triethylamine (900 μL, 6.46 mmol, 4 eq) was added to the reaction, and it was stirred for 6 hours at 23 °C. The reaction was placed in an ice bath, and DMSO (30 mL) was added over 2 minutes as the solution cooled. Once the reaction mixture reached 0 °C, AmB (1.50 g, 1.62 mmol, 1 eq) was added. The yellow-tan suspension was stirred for 90 minutes at 0 °C. The reaction was then poured into diethyl ether (1.8 L) with rapid stirring. After 15 minutes of stirring, the resulting yellow precipitate was vacuum filtered and washed 3 times with diethyl ether (200 mL). The yellow powder was placed under vacuum for 8 hours prior to the next reaction.

Three 1.5 gram batches of N-phenyl acyl amphotericin B were pooled together for the succeeding reactions. The yellow solid (5.00 g, 4.80 mmol, 1 eq) was dissolved in a mixture of methanol (90 mL, 0.05 M) and THF (90 mL) and the solution was cooled to 0 °C. (±) Camphorsulfonic acid (223 mg, 0.96 mmol, 0.2 eq) was added to the cooled solution and the reaction was stirred for one hour at 0 °C. The reaction was quenched at 0 °C with triethylamine (130 μL, 0.96 mmol, 0.2 eq) and the volume of the solvent was reduced *in vacuo* by approximately 50 percent. The solution was poured into 3.6 L of a 1:1 ether:hexane solution and the resulting precipitate was isolated via vacuum filtration. The yellow solid was taken forward to the next step without further purification.

The yellow solid (*ca* 5 g, 4.8 mmol, 1 eq) was dissolved in methanol (80 mL) and *p*-anisaldehyde methyl acetal (12 mL, 70 mmol, 146 eq) was added to the reaction. Subsequently,

(±) camphorsulfonic acid (449 mg, 1.93 mmol, 0.4 eq) was added and the reaction was stirred at 23 °C for one hour. The reaction was quenched by the addition of triethylamine (270 μL, 1.92 mmol, 0.4 eq) and the solvent was removed *in vacuo*. The crude was purified via flash chromatography (SiO2; 3% → 10% MeOH/DCM/0.15 AcOH) to yield **2.12** as an orange solid (3.20 g, 2.48 mmol, 52% over three steps) of approximately 70% purity which was carried forward without further purification.

R = *p*-methoxyphenyl acetal
2.12
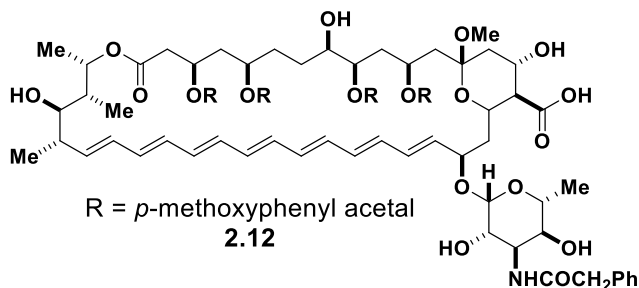
TLC (10% MeOH/DCM/0.1% AcOH)

R_f = 0.15 stained by anisaldeyde.

^{1}H NMR (500 MHz, acetone-d_6)

δ 7.42 (d, J = 8.5 Hz, 2H), 7.34 (d, J = 8.5 Hz, 4H), 7.27 (t, J = 7.5 Hz, 2H), 7.22 (app. t, J = 7.5 Hz, 1H), 6.86 (dd, J = 3.0, 9.0 Hz, 4H), 6.44-6.19 (m, 12H), 5.87 (dd, J = 5.5, 15.0 Hz, 1H), 5.56 (dd, J = 9.5, 13.5 Hz, 1H), 5.51 (s, 1H), 5.46 (s, 1H), 5.28-5.25 (m, 1H), 4.67 (app. t, J = 6.0 Hz, 1H), 4.61 (s, 1H), 4.24-4.09 (m, 3H), 3.96-3.84 (m, 4H), 3.77 (s, 6H), 3.65 (s, 2H), 3.44-3.42 (m, 1H), 3.38-3.29 (m, 3H), 3.04 (s, 3H), 2.57 (dd, J = 6.0, 16.5 Hz, 1H), 2.42-2.37 (m, 1H), 2.32-2.27 (m, 2H), 2.21 (app. t, J = 10.0 Hz, 1H), 2.16-2.10 (m, 1H), 1.89-1.81 (m, 3H), 1.76-1.63 (m, 4H), 1.56-1.43 (m, 4H), 1.36-1.27 (m, 3H), 1.21 (d, J = 5.5 Hz, 3H), 1.18 (d, J = 6.0 Hz, 3H), 1.10 (d, J = 6.5 Hz, 3H), 1.00 (d, J = 7.5 Hz, 3H).

^{13}C NMR (125 MHz, acetone-d_6)

δ 169.8, 160.6, 160.5, 136.9, 134.2, 133.8, 133.0, 132.9, 132.7, 132.6, 130.1, 129.1, 128.3, 128.2, 127.3, 113.9, 101.1, 100.8, 100.6, 97.9, 81.1, 76.4, 74.4, 73.2, 72.9, 70.7, 70.5, 67.2,

67.0, 57.2, 56.4, 55.5, 48.7, 43.6, 43.3, 41.5, 37.9, 34.0, 33.3, 18.9, 18.2, 17.6, 11.9.

HRMS (ESI)

calculated for $C_{72}H_{93}NO_{20}$ (M+Na)$^+$:   1314.6189

found: 1314.6213
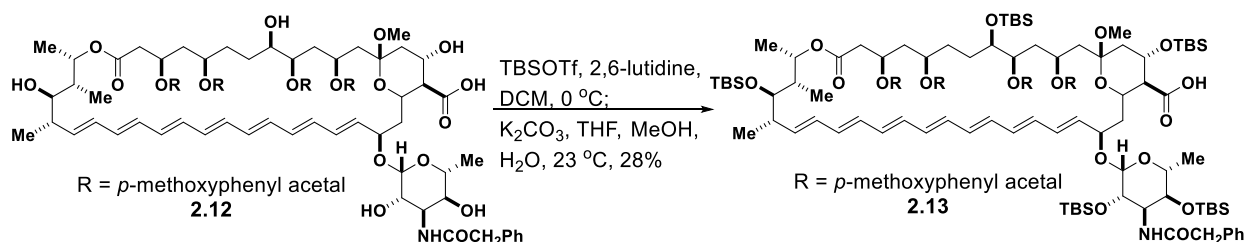
TBS Protected 4.59

Prior to the reaction, **2.12** was coevaporated with acetonitrile (3 x 25 mL) and left under vacuum for a minimum of eight hours. The resulting orange solid (2.98 g, 2.31 mmol, 1 eq) was dissolved in dichloromethane (70 mL) and 2,6-lutidine (3.5 mL, 30 mmol, 13 eq) was added to the solution. The reaction was subsequently cooled to 0 °C and *tert*-butyldimethylsilyl trifluromethane sulfonate (5 mL, 22 mmol, 9.5 eq) was added dropwise over approximately 15 minutes. The reaction was stirred for 1 hour at 0 °C and was then quenched by the addition of 50 mL saturated aqueous sodium bicarbonate. The biphasic mixture was transferred to a 2 L separatory funnel and was diluted with diethyl ether (1 L). The layers were separated and the organic phase was washed with saturated aqueous sodium bicarbonate (1 x 100 mL) and water (1 x 100 mL). The combined aqueous washings were back-extracted with diethyl ether (1 x 50 mL) and the combined organic extracts were washed with saturated aqueous copper sulfate (5 x 100 mL). The combined copper sulfate washings were back-extracted with diethyl ether (1 x 100 mL) and the combined organic extracts were washed with water (1 x 100 mL) and brine (1 x 100 mL), dried over sodium sulfate and concentrated *in vacuo*.

The resulting brown oil was taken up in THF:MeOH:H$_2$O (70 mL, 3:1:1 v/v/v) and potassium carbonate (3.2 g, 23 mmol, 10 eq) was added. Within approximately five minutes the reaction transitioned from turbid to clear. The reaction was stirred for 30 minutes at 23 °C and was then quenched by the addition of 50 mL potassium phosphate buffer (50 mL, pH 7.0). The mixture

was transferred to a 1 L separatory funnel and was extracted with diethyl ether (3 x 250 mL). The combined organic extracts were dried over sodium sulfate and concentrated *in vacuo*. The crude was purified via flash chromatography (SiO$_2$; 30% $\rightarrow$ 100% EtOAc) to yield the title compound **2.13** as a yellow solid (1.21 g, 0.65 mmol, 28%).

R = *p*-methoxyphenyl acetal
2.13
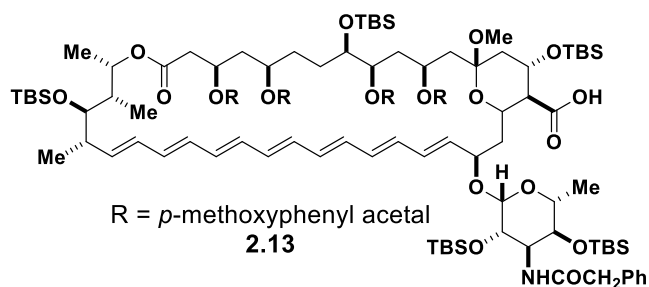
TLC (30% EtOAc/hexanes)

R_f = 0.2 stained by anisaldehyde.

^{1}H NMR (500 MHz, acetone-d_6)

δ 7.39 (d, *J* = 8.5 Hz, 2H), 7.37-7.27 (m, 4H), 7.24-7.22 (m, 1H), 6.98 (d, *J* = 7.5 Hz, 1H), 6.87-6.84 (m, 4H), 6.50 (d, *J* = 9 Hz, 1H), 6.44-6.30 (m, 8H), 6.28-6.18 (m, 2H), 6.06 (dd, *J* = 10, 15 Hz, 1H), 5.81 (dd, *J* = 6, 15 Hz, 1H), 5.66 (dd, *J* = 9.5, 15 Hz, 1H), 5.45 (s, 2H) 4.85 (bs, 1H), 4.66 (app t, 6 Hz, 1H), 4.58 (s, 1H), 4.25 (dt, 4.5, 10.5 Hz, 1H), 4.21-4.16 (m, 1H), 4.01-3.91(m, 2H), 3.92-3.87 (m, 3H), 3.79 (s, 3H), 3.71 (s, 3H), 3.71-3.69 (m, 1H), 3.60 (s, 3H), 3.58-3.55 (m, 1H), 3.42-3.37 (m, 2H), 3.05 (s, 3H), 2.52 (dd, *J* = 7.5, 17.5 Hz, 1H), 2.41 (s, 2H), 2.27 (d, *J* = 5 Hz 1H), 2.28 (t, 3.5 Hz, 1H), 2.25-2.23 (m, 1H), 2.11 (dd, *J* = 4, 12 Hz, 1H), 1.92-1.84 (m, 2H), 1.73-1.69 (m, 1H), 1.66-1.61 (m, 1H), 1.59-1.47 (m, 2H), 1.44-1.40 (m, 1H), 1.34-1.27 (m, 2H), 1.23 (d, *J* = 6.5 Hz, 3H), 1.18 (d, *J* = 6 Hz, 3H), 1.16-1.15 (m, 1H), 1.00 (d, *J* = 7 Hz, 3H), 0.95 (d, *J* = 7 Hz, 3H), 0.928, (s, 9H), 0.899 (s, 9H), 0.865 (s, 9H), 0.845 (s, 9H), 0.757 (s, 9H), 0.120 (s, 3H), 0.114 (s, 3H), 0.108 (s, 3H), 0.098 (s, 3H), 0.073 (s, 3H), 0.071 (s, 3H), 0.059 (s, 3H), 0.029 (s, 3H), -0.044, (s, 3H), -0.054 (s, 3H), -0.134 (s, 3H).

^{13}C NMR (125 MHz, acetone-d_6)

δ 173.5, 170.2, 169.4, 160.1, 160.0, 157.5, 135.6, 134.1, 133.8, 133.2, 132.9, 132.5, 132.1, 132.0, 131.1, 130.6, 129.8, 129.7, 128.6, 128.1, 127.9, 127.8, 127.7, 120.4, 120.3, 113.4, 113.3, 101.0, 100.8, 100.6, 100.4, 100.2, 97.6, 75.5, 74.4, 73.0, 72.8, 72.3, 68.2, 67.0, 56.7, 56.0, 55.0, 54.9, 54.8, 43.2, 40.7, 26.2, 26.18, 26.05, 25.99, 25.91, 25.79, 25.72, 25.60, 25.40, 23.80, 18.44, 18.30, 18.11, 17.87, -3.65, -3.75, -3.93, -4.27, -4.42, -4.54, -4.63, -4.80, -5.22.

HRMS (ESI)

calculated for $C_{102}H_{163}NO_{20}Si_5$ (M + Na)$^+$: 1885.0513
found : 1885.0470

R = *p*-methoxyphenyl acetal
2.13

DIAD
PPh$_3$, THF
45 °C, 84%

R = *p*-methoxyphenyl acetal
2.8
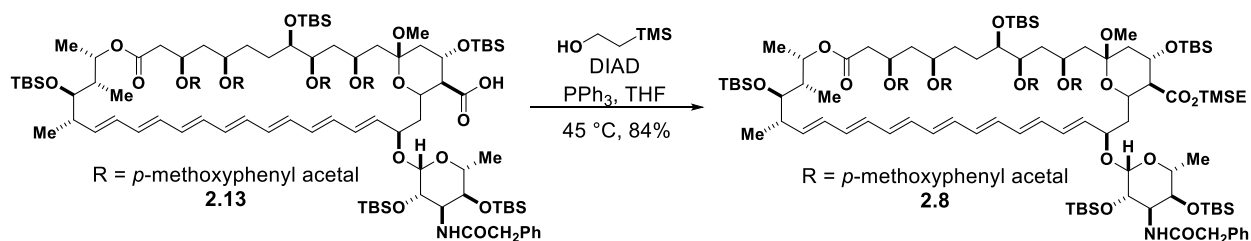
Trimethylsilyl ethyl ester 4.45

A 200 mL round bottom flask was charged with penta *tert*-butyldimethyl silyl **4.59** (1.2 g, 0.61 mmol, 1 eq) and THF (35 mL) was added. The solution was cooled to 0 °C and 2-(trimethylsilyl) ethanol (0.28 mL, 1.9 mmol, 3 eq) was added followed by triphenylphosphine (420 mg, 1.6 mmol, 2.5 eq). The reaction was stirred at 0 °C for approximately 10 minutes and then diisopropyl azodicarboxylate (0.28 mL, 1.4 mmol, 2.2 eq) was added dropwise. The reaction was then transferred to a 45 °C water bath and was stirred for 2 hours. After 2 hours the reaction was concentrated *in vacuo* and was subsequently dissolved in hexanes (100 mL). The hexanes solution was stirred for 10 minutes, the resulting precipitate was removed via vacuum filtration and the filtrate was concentrated *in vacuo*. The crude was purified via flash chromatography (SiO$_2$; 0% → 20% EtOAc/hexanes) to yield the trimethylsilyl ethyl ester **4.45** as yellow foamy solid (1.06 g, 0.539 mmol, 84%).

R = p-methoxyphenyl acetal
2.8
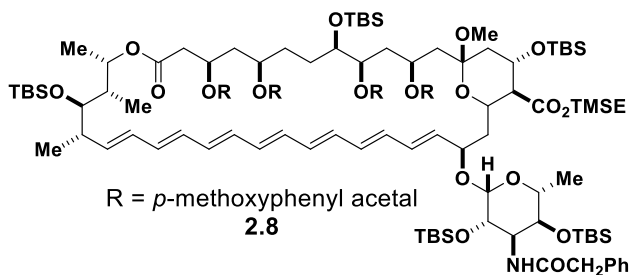
TLC (20% EtOAc/hexanes)

R_f = 0.32, stained by anisaldehyde.

^{1}H NMR (500 MHz, acetone d_6)

δ 7.38 (d, J = 8.5 Hz, 2H), 7.37-7.27 (m, 6H), 7.23-7.20 (m, 1H), 6.87-6.83 (m, 4H), 6.42-6.30 (m, 9H), 6.25-6.18 (m, 2H), 6.07 (dd, J = 10, 15.5 Hz, 1H), 5.80 (dd, J = 6.5, 14.5 Hz, 1H), 5.67 (dd J = 9.5, 15.5 Hz, 1H) 5.45 (s, 2H), 4.86 (bs, 1H), 4.61 (app t J = 7 Hz, 1H), 4.57 (s, 1H), 4.24-4.15 (m, 4H), 4.02 (dt, J = 2, 6 Hz, 1H), 3.93-3.92 (m, 2H), 3.89-3.85 (m, 3H), 3.78 (s, 3H), 3.77 (s, 3H), 3.75-3.71 (m, 2H), 3.57 (s, 3H), 3.41-3.37 (m, 3H), 3.06 (s, 3H), 2.52 (dd, J = 7.5, 17.5 Hz, 1H), 2.44-2.40 (m, 1H), 2.31 (app t, J = 9.5 Hz, 1H), 2.28-2.24 (m, 3H), 2.00-1.95 (m, 1H), 1.89-1.85 (m, 1H), 1.81 (dd, J = 6.5, 13.5 Hz, 1H), 1.72-1.69 (m, 1H), 1.65-1.60 (m, 2H), 1.54-1.50 (m, 1H), 1.45-1.43 (app d, J = 12.5 Hz, 1H), 1.23 (d, J = 6 Hz, 3H), 1.21-1.20 (m, 1H), 1.18 (d, J = 9.5 Hz, 3H), 1.01 (app t, J = 7 Hz, 1H), 1.06-1.04 (m, 1H), 1.01 (d, J = 6.5 Hz, 3H), 0.940 (d, J = 7 Hz, 3H), 0.928 (s, 9H), 0.916-0.912 (m, 1H), 0.900 (s, 9H), 0.888-0.885 (m, 1H), 0.864 (s, 9H), 0.842 (s, 9H), 0.749 (s, 9H), 0.118 (s, 3H), 0.107 (s, 3H), 0.099 (s, 3H), 0.069 (s, 3H), 0.055 (s, 9H), 0.038 (s, 3H), 0.020 (s, 3H), -0.002 (s, 3H), -0.046 (s, 3H), -0.084 (s, 3H), -0.169 (s, 3H).

^{13}C NMR (125 MHz, acetone-d_6)

δ 172.7, 169.5, 169.4, 160.1, 160.0, 136.2, 135.7, 134.1, 133.7, 133.2, 133.1, 132.8, 132.5, 132.3, 132.1, 132.0, 130.6, 129.7, 128.5, 128.0, 127.7, 126.9, 113.4, 101.0, 100.5, 100.2, 98.1, 80.6, 75.4, 75.3, 74.3, 74.2, 72.9, 72.5, 72.3, 68.4, 67.2, 62.8, 58.8, 56.5, 55.8, 55.0, 54.9, 54.8, 47.9, 43.5, 42.8, 40.8, 37.4, 36.2, 32.8, 32.2, 27.5, 27.4, 26.1, 26.0, 25.9, 25.6, 25.3, 21.9, 21.8, 21.7, 19.3, 18.5, 18.3, 18.1, 17.9, 17.8, 17.7, -1.51, -1.72, -2.01, -3.73, -3.77, -3.93, -4.28, -4.38, -4.49, -4.62, -4.74, -5.33.

HRMS (ESI)

        calculated for $C_{107}H_{175}NO_{20}Si_6$ (M + Na)$^+$:   1985.1221

        found: 1985.1249

Isothermal Titration Calorimetry

General Information.

      Experiments were performed using a NanoITC isothermal titration calorimeter (TA Instruments, Wilmington, DE). Solutions of the compounds to be tested were prepared by diluting a 15.0 mM stock solution of the compound in DMSO to 150 μM with K buffer (5.0 mM HEPES/KHEPES, 150 mM KCl, pH = 7.4). The final DMSO concentration in the solution was 1% v/v. POPC LUVs were prepared and phosphorus and ergosterol content was quantified as described below. The LUV solutions were diluted with buffer and DMSO to give a final phospholipid concentration of 8.0 mM in a 1% DMSO/K buffer solution. Immediately prior to use, all solutions were degassed under vacuum at 20 °C for 10 minutes. The reference cell of the instrument (volume = 0.190 mL) was filled with a solution of 1% v/v DMSO/K buffer.

LUV Preparation.

      Palmitoyl oleoyl phosphatidylcholine (POPC) was obtained as a 20 mg/mL solution in CHCl$_3$ from Avanti Polar Lipids (Alabaster, AL) and was stored at -20 °C under an atmosphere of dry argon and used within 1 month. A 4 mg/mL solution of ergosterol in CHCl$_3$ was prepared monthly and stored at 4 °C under an atmosphere of dry argon. Prior to preparing a lipid film, the solutions were warmed to ambient temperature to prevent condensation from contaminating the solutions. A 13 x 100 mm test tube was charged with 1.2 mL POPC and 350 μL of the ergosterol solution. For sterol-free liposomes, a 13 x 100 mm test tube was charged with 1.2 mL POPC. The solvent was removed with a gentle stream of nitrogen and the resulting lipid film was stored under high vacuum for a minimum of eight hours prior to use. The film was then hydrated with 1 mL of 5 mM K buffer and vortexed vigorously for approximately 3 minutes to form a suspension of multilamellar vesicles (MLVs). The resulting lipid suspension was pulled into a Hamilton (Reno, NV) 1 mL gastight syringe and the syringe was placed in an Avanti Polar Lipids Mini-Extruder. The lipid solution was then passed through a 0.20 μm Millipore (Billerica, MA) polycarbonate filter 21 times, the newly formed large unilamellar vesicle (LUV) suspension being collected in

the syringe that did not contain the original suspension of MLVs to prevent the carryover of MLVs into the LUV solution.

Determination of Phosphorus Content.

Determination of total phosphorus was adapted from the report of Chen and coworkers.[43] Three 10 µL samples of the LUV suspension were added to three separate 7 mL vials. Subsequently, the solvent was removed with a stream of N_2. To each dried LUV film, and a fourth vial containing no lipids that was used as a blank, was added 450 µL of 8.9 M H_2SO_4. The four samples were incubated open to ambient atmosphere in a 225 °C aluminum heating block for 25 min and then removed to 23 °C and cooled for 5 minutes. After cooling, 150 µL of 30% w/v aqueous hydrogen peroxide was added to each sample, and the vials were returned to the 225 °C heating block for 30 minutes. The samples were then removed to 23 °C and cooled for 5 minutes before the addition of 3.9 mL water. Then 500 µL of 2.5% w/v ammonium molybdate was added to each vial and the resulting mixtures were then vortexed briefly and vigorously five times. Subsequently, 500 µL of 10% w/v ascorbic acid was added to each vial and the resulting mixtures were then vortexed briefly and vigorously five times. The vials were enclosed with a PTFE lined cap and then placed in a 100 °C aluminum heating block for 7 minutes. The samples were removed to 23 °C and cooled for approximately 15 minutes prior to analysis by UV/Vis spectroscopy. Total phosphorus was determined by observing the absorbance at 820 nm and comparing this value to a standard curve obtained through this method and a standard phosphorus solution of known concentration.

Determination of Ergosterol Content.

Ergosterol content was determined spectrophotometrically. A 50 µL portion of the LUV suspension was added to 450 µL 2:18:9 hexane:isopropanol:water (v/v/v). Three independent samples were prepared and then vortexed vigorously for approximately one minute. The solutions were then analyzed by UV/Vis spectroscopy and the concentration of ergosterol in solution was determined by the extinction coefficient of 10400 L mol^{-1} cm^{-1} at the UV_{max} of 282 nm and was compared to the concentration of phosphorus to determine the percent sterol content. The extinction coefficient was determined independently in the above ternary solvent system. LUVs prepared by this method contained between 7 and 14% ergosterol.

Titration Experiment.

Titrations were performed by injecting the LUV suspension at ambient temperature into the sample cell (volume = 0.191 mL) which contained the 150 μM solution of the compound in question at 25 °C. The volume of the first injection was 0.23 μL. Consistent with standard procedure,[44] due to the large error commonly associated with the first injection of ITC experiments, the heat of this injection was not included in the analysis of the data. Next, nineteen 2.52 μL injections of the LUV suspension were performed. The spacing between each injection was 240 seconds to ensure that the instrument would return to a stable baseline before the next injection was made. The rate of stirring for each experiment was 300 rpm.

Data Analysis.

NanoAnalyze software (TA Instruments) was used for baseline determination and integration of the injection heats, and Microsoft Excel was used for subtraction of dilution heats and the calculation of overall heat evolved. To correct for dilution and mixing heats, the heat of the final injection from each run was subtracted from all the injection heats for that particular experiment.[45] By this method, the overall heat evolved during the experiment was calculated using the following formula:

$$\mu cal_{overall} = \sum_{i=1}^{n}(\Delta h_{injection}^{i} - \Delta h_{injection}^{n})$$

Where i = injection number, n = total number of injections, $\Delta h_{injection}^{i}$ = heat of the ith injection, and $\Delta h_{injection}^{n}$ = the heat of the final injection of the experiment. Values represent the mean ± SD of at least three experiments.

Potassium Efflux Assays
General Information.

Ion selective measurements were obtained using a Denver Instruments (Denver, CO) Model 225 pH meter equipped with a World Precision Instruments (Sarasota, FL) potassium selective electrode inside a Faraday cage. The electrode filled with 1000 ppm KCl standard solution and conditioned in a 1000 ppm KCl standard solution for 30 minutes prior to ion selective measurements. Measurements were made on 3 mL solutions that were magnetically stirred in 7

mL Wheaton vials incubated in a 30 °C aluminum block (*S. cerevisiae*) or at 23 °C (LUVs). The instrument was calibrated daily with KCl standard solutions to 10, 100, and 1000 ppm potassium. The potassium concentration was sampled every 30 seconds throughout the course of the efflux experiments.

Growth Conditions for *S. cerevisiae*.

      S. cerevisiae was maintained with yeast peptone dextrose (YPD) growth media consisting of 10 g/L yeast extract, 20 g/L peptone, 20 g/L dextrose, and 20 g/L agar for solid media. The media was sterilized by autoclaving at 250 °F for 30 min. Dextrose was subsequently added as a sterile 40% w/v solution in water (dextrose solutions were filter sterilized). Solid media was prepared by pouring sterile media containing agar (20 g/L) onto Corning (Corning, NY) 100 x 20 mm polystyrene plates. Liquid cultures were incubated at 30 °C on a rotary shaker and solid cultures were maintained at 30 °C in an incubator.

Potassium Efflux from *S. cerevisiae*.

      The protocol to determine potassium efflux from *S. cerevisiae* was adapted from a similar experiment utilizing *C. albicans*.[46] An overnight culture of *S. cerevisiae* in YPD was centrifuged at 300 g for 5 minutes at 23 °C. The supernatant was decanted and the cells were washed twice with sterile water. After the second wash step, the cells were suspended in 150 mM NaCl, 5 mM HEPES pH 7.4 (Na buffer) to an OD_{600} of 1.5 (~$1x10^9$ CFU/mL) as measured by a Shimadzu (Kyoto, Japan) PharmaSpec UV-1700 UV/Vis spectrophotometer. A 3 mL sample of the cell suspension was then incubated in a 30 °C aluminum block with stirring for approximately 10 minutes before data collection. The probe was then inserted and data was collected for 5 minutes before adding 30 μL of the compound in question as a 0.3 mM or 3.0 mM solution in DMSO. The cell suspension was stirred and data were collected for 30 minutes and then 30 μL of a 1% aqueous solution of digitonin was added to effect complete potassium release and data were collected for an additional 15 minutes. The experiment was performed independently three times for each small molecule.

Data Analysis.

      The data from each run was normalized to the percent of total potassium release, from 0 to

100%. Thus for each experiment a scaling factor S was calculated using the following relationship:

$$\left[\frac{[K^+]_{final}}{[K^+]_{initial}} - 1 \right] \cdot S = 100$$

Each concentration data point was then multiplied by S before plotting as a function of time.

LUV Preparation.

Palmitoyl oleoyl phosphatidylcholine (POPC) was obtained as a 25 mg/mL solution in $CHCl_3$ from Avanti Polar Lipids (Alabaster, AL) and was stored at -20 °C under an atmosphere of dry argon and used within 3 months. A 4 mg/mL solution of ergosterol in $CHCl_3$ was prepared monthly and stored at 4 °C under an atmosphere of dry argon. Prior to preparing a lipid film, the solutions were warmed to ambient temperature to prevent condensation from contaminating the solutions. A 13 x 100 mm test tube was charged with 640 μL POPC and 230 μL of the ergosterol solution. The solvent was removed with a gentle stream of nitrogen and the resulting lipid film was stored under high vacuum for a minimum of eight hours prior to use. The film was then hydrated with 1 mL of 150 mM KCl, 5 mM HEPES pH 7.4 (K buffer) and vortexed vigorously for approximately 3 minutes to form a suspension of multilamellar vesicles (MLVs). The resulting lipid suspension was pulled into a Hamilton (Reno, NV) 1 mL gastight syringe and the syringe was placed in an Avanti Polar Lipids Mini-Extruder. The lipid solution was then passed through a 0.20 μm Millipore (Billerica, MA) polycarbonate filter 21 times, the newly formed large unilamellar vesicle (LUV) suspension being collected in the syringe that did not contain the original suspension of MLVs to prevent the carryover of MLVs into the LUV solution. To obtain a sufficient quantity of LUVs, three independent 1 mL preparations were pooled together for the dialysis and subsequent potassium efflux experiments. The newly formed LUVs were dialyzed using Pierce (Rockford, IL) Slide-A-Lyzer MWCO 3,500 dialysis cassettes. The samples were dialyzed three times against 600 mL of Na buffer. The first two dialyses were two hours long, while the final dialysis was performed overnight.

Determination of Phosphorus Content.

Determination of total phosphorus was adapted from the report of Chen and coworkers.[9] The LUV solution was diluted tenfold with Na buffer and three 10 μL samples of the diluted LUV

suspension were added to three separate 7 mL vials. Subsequently, the solvent was removed with a stream of N_2. To each dried LUV film, and a fourth vial containing no lipids that was used as a blank, was added 450 μL of 8.9 M H_2SO_4. The four samples were incubated open to ambient atmosphere in a 225 °C aluminum heating block for 25 min and then removed to 23 °C and cooled for 5 minutes. After cooling, 150 μL of 30% w/v aqueous hydrogen peroxide was added to each sample, and the vials were returned to the 225 °C heating block for 30 minutes. The samples were then removed to 23 °C and cooled for 5 minutes before the addition of 3.9 mL water. Then 500 μL of 2.5% w/v ammonium molybdate was added to each vial and the resulting mixtures were then vortexed briefly and vigorously five times. Subsequently, 500 μL of 10% w/v ascorbic acid was added to each vial and the resulting mixtures were then vortexed briefly and vigorously five times. The vials were enclosed with a PTFE lined cap and then placed in a 100 °C aluminum heating block for 7 minutes. The samples were removed to 23 °C and cooled for approximately 15 minutes prior to analysis by UV/Vis spectroscopy. Total phosphorus was determined by observing the absorbance at 820 nm and comparing this value to a standard curve obtained through this method and a standard phosphorus solution of known concentration.

Determination of Ergosterol Content.

Ergosterol content was determined spectrophotometrically. The LUV solution was diluted tenfold with Na buffer, and 50 μL of the dilute LUV suspension was added to 450 μL 2:18:9 hexane:isopropanol:water (v/v/v). Three independent samples were prepared and then vortexed vigorously for approximately one minute. The solutions were then analyzed by UV/Vis spectroscopy and the concentration of ergosterol in solution was determined by the extinction coefficient of 10400 L mol^{-1} cm^{-1} at the UV_{max} of 282 nm and was compared to the concentration of phosphorus to determine the percent sterol content. The extinction coefficient was determined independently in the above ternary solvent system. LUVs prepared by this method contained between 7 and 14% ergosterol.

Efflux from LUVs.

The LUV solutions were adjusted to 1 mM in phosphorus using Na buffer. 3 mL of the 1 mM LUV suspension was added to a 7 mL vial and the solution was gently stirred. The potassium ISE probe was inserted and data were collected for one minute prior to the addition of the

compound. Then, 30 μL of a 0.1 mM, 1.0 mM, or 3.0 mM DMSO solution of the compound in question was added and data were collected for five minutes. Then to effect complete potassium release, 30 μL of a 10% v/v solution of triton X-100 was added and data were collected for an additional five minutes. The experiment was duplicated with similar results.

Data Analysis.

The data from each run were analyzed in the same manner as the efflux data from *S. cerevisiae.*

Antifungal Assays

Growth Conditions for *S. cerevisiae.*

S. cerevisiae was maintained with yeast peptone dextrose (YPD) growth media consisting of 10 g/L yeast extract, 20 g/L peptone, 20 g/L dextrose, and 20 g/L agar for solid media. The media was sterilized by autoclaving at 250 °F for 30 min. Dextrose was subsequently added as a sterile 40% w/v solution in water (dextrose solutions were filter sterilized). Solid media was prepared by pouring sterile media containing agar (20 g/L) onto Corning (Corning, NY) 100 x 20 mm polystyrene plates. Liquid cultures were incubated at 30 °C on a rotary shaker and solid cultures were maintained at 30 °C in an incubator.

Growth Conditions for *C. albicans*.

C. albicans was cultured in a similar manner to *S. cerevisiae* except both liquid and solid cultures were incubated at 37 °C.

Broth Microdilution Minimum Inhibitory Concentration (MIC) Assay.

The protocol for the broth microdilution assay was adapted from the Clinical and Laboratory Standards Institute document M27-A2.[47] 50 mL of YPD media was inoculated and incubated overnight at either 30 °C (*S. cerevisiae*) or 37 °C (*C. albicans*) in a shaker incubator. The cell suspension was then diluted with YPD to an OD_{600} of 0.10 (~5 x 10^5 cfu/mL) as measured by a Shimadzu (Kyoto, Japan) PharmaSpec UV-1700 UV/Vis spectrophotometer. The solution was diluted 10-fold with YPD, and 195 μL aliquots of the dilute cell suspension were added to sterile Falcon (Franklin Lakes, NJ) Microtest 96 well plates in triplicate. Compounds were

prepared either as 400 μM (AmB, MeAmB) or 2 mM (AmdeB, MeAmdeB) stock solutions in DMSO and serially diluted to the following concentrations with DMSO: 1600, 1200, 800, 400, 320, 240, 200, 160, 120, 80, 40, 20, 10 and 5 μM. 5 μL aliquots of each solution were added to the 96 well plate in triplicate, with each column representing a different concentration of the test compound. The concentration of DMSO in each well was 2.5% and a control well to confirm viability using only 2.5% DMSO was also performed in triplicate. This 40-fold dilution gave the following final concentrations: 50, 40, 30, 20, 10, 8, 6, 4, 1, 0.5, 0.25 and 0.125 μM. The plates were covered and incubated at 30 °C (*S. cerevisiae*) or 37 °C (*C. albicans*) for 24 hours prior to analysis. The MIC was determined to be the concentration of compound that resulted in no visible growth of the yeast. The experiments were performed in duplicate and the reported MIC represents an average of two experiments.

Ergosterol Content Determination

Determination of Ergosterol Standard Curve

Ergosterol was prepared as a 0.1 mg/mL stock solution in $CHCl_3$ and serially diluted to the following concentrations with $CHCl_3$: 0.1, 0.08, 0.06, 0.03, 0.01 and 0.005 mg/mL. 10 μL aliquots of each solution were analyzed by analytical RP-HPLC (Waters Sunfire C_{18}, ODB 5 micron, 4.6 x 150 mm, 2 mL/min flow rate, MeCN:ethanol (200 proof) 80:20 isocratic over 10 minutes) in triplicate. Ergosterol was detected at 280 nm. Ergosterol concentration was plotted against the integration of the ergosterol peak (t_r = 5.1 min) the data was fitted with a linear least squares fit using Excel giving a standard curve.

Determination of Stigmasterol Standard Curve

Stigmasterol was prepared as a 4 mg/mL stock solution in toluene and serially diluted to the following concentrations with $CHCl_3$: 4, 2, 1, 0.5, 0.25 and 0.125 mg/mL. 10 μL aliquots of each solution were analyzed by analytical RP-HPLC (Waters Sunfire C_{18}, ODB 5 micron, 4.6 x 150 mm, 2 mL/min flow rate, MeCN:ethanol (200 proof) 80:20 isocratic over 10 minutes) in triplicate. Stigmasterol was detected at 210 nm. Stigmasterol concentration was plotted against the integration of the ergosterol peak (t_r = 7.8 min) the data was fitted with a linear least squares fit using Excel giving a standard curve.

Ergosterol Determination

Determination of total ergosterol was adapted from the report of Arnezeder and coworkers.[33] The starting yeast cultures were prepared identical to the yeast used in the MIC assays. 50 mL of YPD media was inoculated and incubated overnight at either 30 °C (*S. cerevisiae*) or 37 °C (*C. albicans*) in a shaker incubator. 15 mL of the overnight culture was centrifuged (300 g, 23 °C) for 5 minutes. The supernatant was decanted and the cells were resuspended in 15 mL of Na buffer (150 mM NaCl, 5 mM HEPES, pH 7.4) and centrifuged (300 g, 23 °C) for 5 minutes. This process was repeated two additional times and after the third wash, the cells were suspended in Na buffer to an OD_{600} of 1.3 as measured by a Shimadzu (Kyoto, Japan) PharmaSpec UV-1700 UV/Vis spectrophotometer. 40 mL of the OD_{600} = 1.3 yeast suspension were centrifuged (600 g, 23 °C) for 10 minutes. The supernatant was decanted and the cells were resuspended in 50 mL sterile water and centrifuged (300 g, 23 °C) for 5 minutes. The supernatant was decanted and the resulting yeast pellet was suspended in 10 mL of 0.1 M aqueous HCl and transferred to 40 mL I-Chem vial. 0.9 mL of a 4 mg/mL standard solution of stigmasterol in toluene was added to the sample as an internal standard. The sample was incubated at 90 °C for 20 minutes and transferred to a 300 mL round bottom flask equipped with a stir bar. The I-Chem vial was washed with 50 mL of ethanol and 50 mL of 50% aqueous KOH and the washings were added to the 300 mL round bottom flask. The 300 mL round bottom flask was stirred at reflux for 30 minutes and then allowed to cool to room temperature. The solution was extracted three times with 30 mL of petroleum ether. The combined organic layers were dried over Na_2SO_4 and concentrated *in vacuo*. The resulting solid was dissolved in 3 mL of 3:1 isopropanol:acetone and filtered through a 0.22 μm low protein binding Durapore (PVDF) membrane. 10 μL aliquots of the filtered solution were analyzed by analytical RP-HPLC (Waters Sunfire C_{18}, ODB 5 micron, 4.6 x 150 mm, 2 mL/min flow rate, MeCN:ethanol (200 proof) 80:20 isocratic over 10 minutes) in triplicate. Ergosterol was detected at 280 nm and stigmasterol was detected at 210 nm. Ergosterol and stigmasterol concentrations were determined by comparing the integration of the ergosterol peak to the standard curves described above. The stigmasterol internal standard was used to adjust the ergosterol concentration for any loss of material during the extraction process. The experiment described above was repeated in triplicate for both *S. cerevisiae* and *C. albicans*.

Determination of Cell Concentration at OD_{600} = 1.3

10 μL of the OD$_{600}$ = 1.3 yeast suspension described above was diluted tenfold with Na buffer. 10 μL of the diluted suspension was injected into the INCYTO Neubauer Improved Disposable Hemocytometer. Yeast cells were counted with an AMG EVOS fl Microscope. The cell concentration determination was repeated in triplicate.

Determination of Cell Concentration in the MIC Assay

The overnight cultures *S. cerevisiae* and *C. albicans* in YPD that were used in the ergosterol determination above were diluted with YPD to an OD$_{600}$ of 0.10. This was done at the same time as the sterol determination experiment above to ensure that the sterol content directly related to the cell count. 10 μL of the suspension was injected into the INCYTO Neubauer Improved Disposable Hemocytometer. Yeast cells were counted with an AMG EVOS fl Microscope. In the MIC assay, an OD$_{600}$ = 0.10 yeast suspension was diluted 10-fold prior to running the assay so all cell counts were divided by 10 to get the cell concentration in the MIC assay. The cell concentration determination was repeated in triplicate.

2-9 REFERENCES

1. Palacios, D. S.; Anderson, T. M.; Burke, M. D. *J. Am. Chem. Soc.* **2007**, *129*, 13804-13805.
2. Palacios, D. S.; Dailey, I.; Siebert, D. M.; Wilcock, B. C.; Burke, M. D. *Proc. Natl. Acad. Sci. USA* **2011**, *108*, 6733-6738.
3. Volmer, A. A.; Szpilman, A. M.; Carreira, E. M. *Nat. Prod. Rep.* **2010**, *27*, 1329-1349.
4. Murata, M.; et al. *Pure Appl. Chem.* **2009**, *81*, 1123-1129.
5. Bolard, J. *Biochim. Biophys. Acta* **1986**, *864*, 257-304.
6. Baginski, M.; Resat, H.; Borowski, E. *Biochim. Biophys. Acta* **2002**, *1567*, 63-78.
7. de Kruijff, B.; Demel, R.A. *Biochim Biophys Acta* **1974**, *339*, 57-70.
8. Andreoli, T.E. *Ann. NY. Acad. Sci.* **1974**, *235*, 448-468.
9. Heese-Peck, A.; et al. *Mol. Biol. Cell* **2002**, *13*, 2664-2680.
10. Jin, H.; McCaffery, J. M.; Grote, E. *J. Cell. Biol.* **2008**, *180*, 813-826.
11. Klose, C.; et al. *J. Biol. Chem.* **2010**, *285*, 30224-30232.
12. Kato, M.; Wickner, W. *EMBO J.* **2001**, *20*, 4035-4040.
13. te Welscher, Y. M.; et al. *Antimicrob. Agents Chemother.* **2010**, *54*, 2618-2625,
14. te Welscher, Y. M.; et al. *J. Biol. Chem.* **2008**, *283*, 6393-6401.

15. te Welscher, Y. M.; van Leeuwen, M. R.; de Kruijff, B.; Dijksterhuis, J.; Breukink, E. *Proc. Natl. Acad. Sci. USA* **2012**, *109*, 11156-11159.

16. Zhang, Y. Q. *PLoS Pathog.* **2010**, *6*, e1000939.

17. Sanglard, D.; Odds, F. C. *Lancet Infect. Dis.* **2002**, *2*, 73-85.

18. Hsuchen, C. –C.; Feingold, D. S. *Nature* **1974**, *251*, 656-659.

19. Vincent, B. M.; Lancaster, A. K.; Scherz-Shouval, R.; Whitesell, L.; Lindquist, S. *PLoS Biol.* **2013**, *11*, e1001692.

20. Gray, K. C.; et al. *Proc. Natl. Acad. Sci. USA* **2012**, *109*, 2234-2239.

21. Hoogevest, P. V.; de Kruijff, B. *Biochim Biophys Acta* **1978**, *511*, 397-407.

22. Szpilman, A. M.; Manthorpe, J. M.; Carreira, E. M. *Angew. Chem. Int. Ed.* **2008**, *47*, 4339-4342.

23. Szpilman, A. M.; Cereghetti, D. M.; Manthorpe, J. M.; Wurtz, N. R.; Carreira, E. M. *Chem. Eur. J.* **2009**, *15*, 7117-7128.

24. Duplantier, A. J.; Masamune, S. *J. Am. Chem. Soc.* **1990**, *112*, 7079-7081.

25. Gillis, E. P.; Burke, M. D. *J. Am. Chem. Soc.* **2007**, *129*, 6716-6717.

26. Nicolaou, K. C.; Chakraborty, T. K.; Daines, R. A.; Simpkins, N. S. *J. Chem. Soc., Chem. Commun.* **1986**, 413-416.

27. Nicolaou, K. C.; Chakraborty, T. K.; Daines, R. A.; Simpkins, N. S. *J. Chem. Soc., Chem. Commun.* **1987**, 686-689.

28. Nicolaou, K. C.; et al. *J. Am. Chem. Soc.* **1988**, *110*, 4660-4672.

29. Rogers, B. N.; Selsted, M. E.; Rychnovsky, S. D. *Bioorg. Med. Chem. Lett.* **1997**, *7*, 3177-3182.

30. Tsuchikawa, H.; Matsushita, N.; Matsumori, N.; Murata, M.; Oishi, T. *Tetrahedron Lett.* **2006**, *47*, 6187-6191.

31. Lee, S. J.; Anderson, T. M.; Burke, M. D. *Angew. Chem. Int. Ed.* **2010**, *49*, 8860-8863.

32. Klepser, M. E.; Ernst, E. J.; Lewis, R. E.; Ernst, M. E.; Pfaller, M. A. *Antimicrob. Agents Chemother.* **1998**, *42*, 1207-1212.

33. Arnezeder, C. H.; Koliander, W.; Hampel, W. A. *Anal. Chim. Acta* **1989**, *225*, 129-136.

34. Taubes, G. *Science* **2008**, *321*, 356-361.

35. Monk, B. C.; Goffeau, A. *Science* **2008**, *321*, 367-369

36. Ellis, D. *J. Antimicrob. Chemother.* **2002**, *49*, 7-10.

37. Seco, E. M.; Miranzo, D.; Nieto, C.; Malpartida, F. *Appl. Microbiol. Biotechnol.* **2010**, *85*, 1797-1807.

38. Cannon, R. D.; et al. *Microbiol.* **2007**, *153*, 3211-3217.

39. Hasper, H. E.; et al. *Science* **2006**, *313*, 1636-1637.

40. Cioffi, A. G.; Hou, J.; Grillo, A. S.; Diaz, K. A.; Burke, M. D. *J. Am. Chem. Soc.* **2015**, *137*, 10096-10099.

41. Pangborn, A. B; Giardello, M. A; Grubbs, R. H.; Rosen, R. K.; Timmers, F.J. *Organometallics* **1996**, *15*, 1518-1520.

42. Still, W,C; Kahn, M.; Mitra, A. *J. Org. Chem.* **1978**, *43*, 2923-2925.

43. Chen, P.S.; Toribara, T.Y.; Warner, H. *Anal. Chem.* **1956**, *28*, 1756-1758.

44. Heerklotz, H.; Seelig, J. *Biochim. Biophys. Acta* **2000**, *1508*, 69-85.

45. This is a standard protocol for ITC experiments, for example see: te Welscher, Y. M.; ten Napel, H. H.; Balague, M. M.; Souza, C. M.; Riezman, H.; de Kruijff, B.; Breukink, E. *J. Biol. Chem.* **2008**, *283*, 6393-6401.

46. Hammond SM, Lambert PA, Kliger BN (1974) The mode of action of polyene antibiotics; induced potassium leakage in Candida albicans. *J Gen Microbiol* 81:325-330.

47. Clinical and Laboratory Standards Institute. Reference Method for Broth Dilution Antifungal Susceptibility Testing, M27-A2, Approved Standard 2nd Ed. Vol. 22, Number 15, 2002.

CHAPTER 3

DISCOVERY OF A LIGAND-SELECTIVE ALLOSTERIC MODEL IN THE DEVELOPMENT OF LESS TOXIC AND RESISTANCE-EVASIVE AMPHOTERICIN B DERIVATIVES

The discovery that sterol binding is the primary mechanism by which amphotericin B (AmB) kills cells enables the focus on selective binding for ergosterol over cholesterol in the pursuit of less toxic AmB derivatives. However, more selective pharmaceutical actions are generally more prone to the development of resistance. To understand whether greater sterol selectivity leads to diminished capacity to evade resistance required an atomistic understanding of the interaction between AmB and both ergosterol and cholesterol. The leading model predicted the C2' hydroxyl forms a key hydrogen bond to the 3β hydroxyl of both sterols. In contrast to this model, deletion or epimerization of the C2' hydroxyl resulted in selective binding for ergosterol over cholesterol and thus substantially diminished toxicity to human cells. A possible reason for this selectivity is that the alterations of the C2' hydroxyl are ligand-selective allosteric modifications. Guided by this ligand-selective allosteric modification model, a new class of AmB urea derivatives that can be efficiently and scalably accessed from the natural product were developed. The AmB ureas showed preferential binding to ergosterol over cholesterol and thus were significantly less toxic than AmB to human cells and in mice while maintaining potent antifungal activity *in vitro* and in a murine model of systemic candidiasis. The increase in ergosterol selectivity did not impact their ability evade resistance in any appreciable way. Therefore, these findings revealed that selective antimicrobial action and the capacity to evade resistance are not mutually exclusive and that the derivatives disclosed herein are potential candidates to be clinically viable substitutes for AmB.

C2'deOAmB was prepared by Dr. Brandon Wilcock and Dr. Brice Uno. C2'epiAmB was prepared by Dr. Brice Uno. Deoxycholate formulation of AmB and C2'epiAmB was prepared by Lingbowei Hu. AmB urea derivatives were prepared by Dr. Stephen Davis. MIC experiment with pathogenic fungal strains and *in vivo* murine efficacy and toxicity studies were performed by Karen Marchillo and Dr. David Andes. All resistance and fitness studies were performed by Dr. Benjamin Vincent, Dr. Luke Whitesell, and Prof. Susan Lindquist. Portions of this chapter were adapted from Wilcock, B. C.; Endo, M. M.; Uno, B. E.; Burke, M. D. *J. Am. Chem. Soc.* **2013**, *135*, 8488-

8491 and Davis S. A.; Vincent B. M.; Endo, M. M.; Whitesell, L.; Marchillo, K.; Andes, D. R.; Lindquist, S.; Burke, M. D. *Nat. Chem. Biol.* **2015**, *11*, 481-487.

3-1 BACKGROUND

As described in Chapter 2, we determined that AmB primarily kills yeast cells via the binding[1] and extraction[2] of ergosterol. This would suggest that the binding of structurally similar mammalian sterol cholesterol would likely account for the toxicity to human cells. Like ergosterol for yeast, cholesterol plays a number of essential roles in human physiology, especially for the proper functioning of the kidneys. Cholesterol is suggested to be the binding partner for over 250 human proteins,[3] including a number channels[4,5] and regulators[6] that are important for proper renal ion homeostasis. Furthermore, it is vital for renal cytoresistance,[7,8] protection from oxidative damage,[9,10] formation of cell-cell junctions[11,12] and caveolae,[13] and several signaling pathways.[14-16] Furthermore, another cholesterol-binding small molecule, β-methylcyclodextrin, is also known to cause kidney damage in animal models.[17,18] Collectively, these studies suggest that the binding and extraction of cholesterol may be sufficient to kill human cells and cause nephrotoxicity. These findings enables the focus toward increased therapeutic derivatives of AmB to be on maximizing the selectivity for ergosterol over cholesterol. However, it has remained unclear if decreases in toxicity would come at the cost of AmB's ability to evade resistance for over half a century[19-21] as less selective pharmaceutical actions are generally associated with decreased vulnerability to pathogen resistance.[22,23]

The continuing increase in antimicrobial resistance has become a growing global health crisis. One of the major mechanisms by which resistance develops is mutations to the drug binding site.[24] This mechanism is highly prevalent as most antimicrobials bind a microbe-specific but easily mutable protein. This allows for the selective toxicity but gives rise to the evolution of resistance due to the easily mutable nature of the target. An example of this phenomenon are the azole antifungals that selectively bind the ergosterol biosynthesis protein lanosterol 14α-demethylase.[25] However, mutations to the binding site of this protein yield azole-resistant strains.[26] Conversely, a protein target has never been identified for AmB and instead it binds a multifaceted and vital lipid.[1,2] Potentially, AmB's promiscuous sterol binding is what necessitates the substantial changes required for the development of resistance to AmB *in vitro*, which in turn dramatically reduces the pathogenicity. Based on this analysis, the increases in ergosterol selectivity would result in the loss of in the resistance-evasive capacity of AmB.

3-2 DESIGN OF PROBES TO UNDERSTAND THE ATOMISTIC INTERACTIONS IN THE BINDING BETWEEN AmB AND STEROLS

In order to rationally design less toxic AmB derivatives that still evade resistance, we needed greater atomistic details in the binding between AmB and both ergosterol and cholesterol. As discussed in Chapter 2, the deletion of the mycosamine sugar from AmB results in the complete loss of sterol binding capacity and thus biological activity.[27,28] However, it still remained unclear what role each of the heteroatoms of the mycosamine appendage have in this binding event. Towards the goal of understanding the atomistic interactions involved in binding between AmB and sterols, we pursued functional group deletions on the mycosamine sugar.
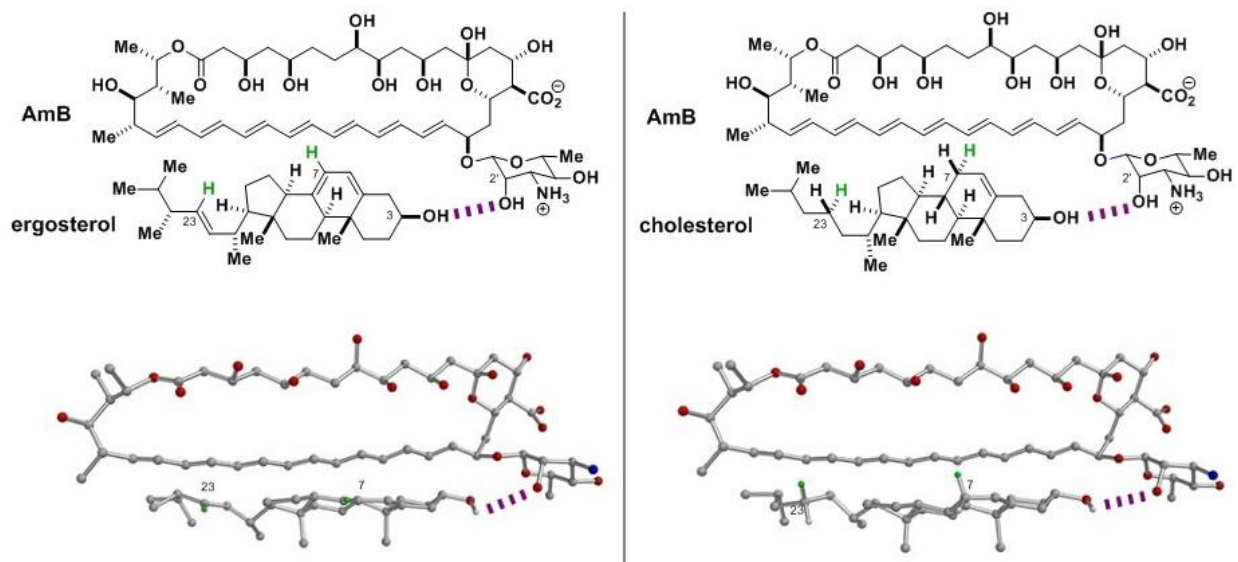
Figure 3.1: Mechanistic models of the interaction between AmB and both ergosterol and cholesterol. The axial C2' hydroxyl is predicted to form a hydrogen bond with 3β hydroxyl of both sterols.

The leading structural models of the AmB-sterol interaction predicted that the conspicuous axial C2' hydroxyl of AmB forms a critical hydrogen bond with the 3β hydroxyl of both ergosterol and cholesterol (Figure 3.1).[29-32] However, experimental studies to probe this putative interaction have yielded conflicting results. Membrane permeabilization studies with conformationally constrained AmB derivatives concluded that this hydrogen bond is critical in the binding for both sterols. In contrast, recent computational studies suggested that this putative hydrogen bond is only involved in the binding with ergosterol and not cholesterol.[33] Furthermore, a derivative of AmB where the C2' hydroxyl is epimerized and the C41 carboxylate was methyl esterified still maintained its antifungal and membrane permeabilization activity.[34] However, an additional

54

modification where the epimerized C2' hydroxyl is methyl etherified caused substantial decreases in both activities. While significant, these studies had limitations in understanding the role of the C2' hydroxyl in sterol binding due to the complication of additional steric bulk of the methyl ether and that sterol binding was not directly examined. To understand this putative interaction, we pursued synthesizing a derivative of AmB where the C2' hydroxyl was deleted and directly determine its impact on the binding to ergosterol and cholesterol. Towards this goal, my colleagues Dr. Brandon Wilcock and Dr. Brice Uno synthesized the derivative lacking the C2' hydroxyl, C2'deOAmB.[35,36]
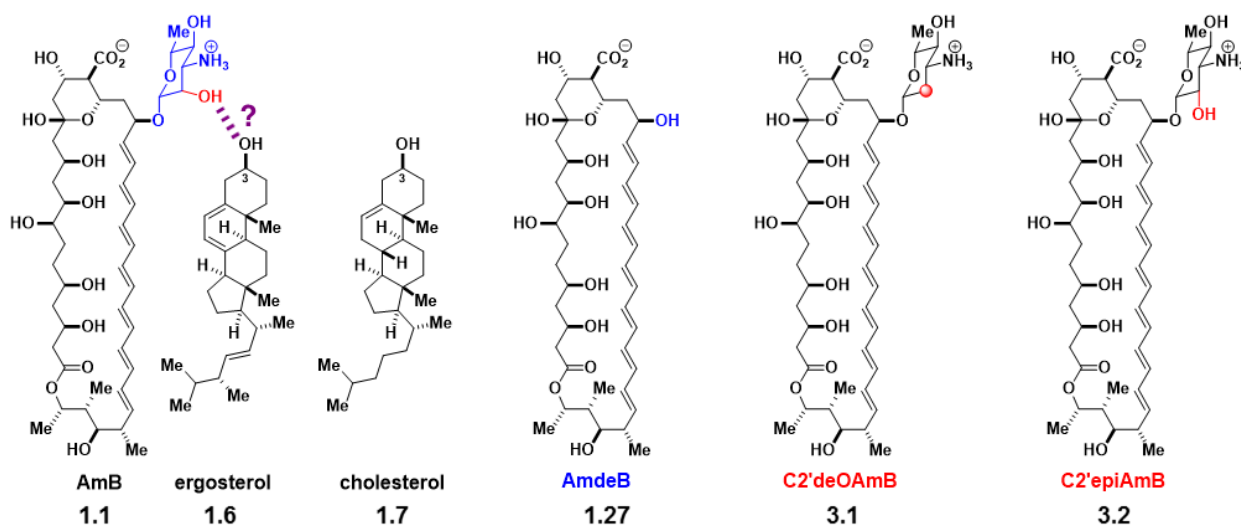
Figure 3.2: Chemical structures of the natural products AmB and its derivatives to probe the atomistic interaction between AmB and both ergosterol and cholesterol.

3-3 DISCOVERY OF STEROL-SELECTIVE BINDING AND DIMINISHED TOXICITY OF C2'deOAmB

The leading structural model displaying a critical interaction between the C2' hydroxyl and sterols would predict that C2'deOAmB would no longer be able to bind ergosterol or cholesterol similarly to AmdeB. Sensitive detection of cholesterol binding remained via traditional methods, so I developed an optimized ITC-based assay. Towards this pursuit, the concentration of the analyte (AmB or its derivative) and the titrant (sterol-containing LUVs) would need to be increased. However, AmB's minimal solubility in aqueous buffer severely limited further increases in its concentration. I removed the 150 mM KCl from the K buffer utilized in the ITC studies in Chapter

2, which had a profound effect on AmB's solubility as we could increase its concentration from 150 μM up to 600 μM.

With the increased concentration of AmB, I tested AmB's capacity to bind ergosterol and cholesterol with these optimized conditions. AmB demonstrated a small net exotherm when titrated with sterol-free POPC LUVs. I repeated this with 10% ergosterol-containing POPC LUVs and consistent with previous reports, I observed a statistically significant increase in net exotherm indicating the direct interaction of AmB with ergosterol (Figure 3.3).[35] This experiment was repeated with 10% cholesterol-containing POPC LUVs and similar to the ergosterol-containing LUVs, a statistically significant albeit smaller net increase was observed demonstrating that we had an assay to detect cholesterol binding with AmB (Figure 3.3).[35] I further validated this assay by testing AmdeB through the same series of experiments and observed no increase in net exotherm for ergosterol and cholesterol determining that AmdeB doesn't bind either sterol (Figure 3.3).[35]

Figure 3.3: Isothermal titration calorimetry with C2'deOAmB titrated with 10% ergosterol-containing, 10% cholesterol-containing, or sterol-free LUVs. * $P \leq 0.05$, ** $P \leq 0.01$, *** $P \leq 0.001$, and NS = not significant.

Having validated the optimized ITC assay, I was in position to test the hypothesis that the C2' hydroxyl was crucial in binding both sterols with the critical probe C2'deOAmB. When titrating C2'deOAmB with ergosterol-containing LUVs, we received the surprising result of a strong increase in net exotherm compared to that of the sterol-deficient LUVs (Figure 3.3).[35] Thus, in stark contrast to the leading model, C2' hydroxyl was not required to bind ergosterol. Surprisingly, we alternatively were unable to detect cholesterol binding in this experiment with

cholesterol-containing LUVs (Figure 3.3).[35] Based on this, the C2' hydroxyl plays a major role in the binding of cholesterol, but not ergosterol.

Based on our mechanistic understanding of AmB described in Chapter 2, we predicted that C2'deOAmB would still be toxic to yeast cells, but no longer toxic to human cells. I tested C2'deOAmB in microbroth dilution assay and determined its MIC to be 1 µM against both *S. cerevisiae* and *C. albicans* similar to AmB's MIC for both yeast (Figure 3.4).[35] After confirming its retained antifungal activity, I tested its toxicity against both human red blood cells and primary renal proximal tubule epithelial cells (RPTECs). Up to the limits of solubility in both assays, I observed no toxicity to either human cell type similarly to AmdeB (Figure 3.4).[35] Based on these findings, C2'deOAmB could be a candidate for further development as a potential clinical replacement for AmB.

		AmB	AmdeB	C2'deOAmB
ergosterol-containing yeast cells	*S. cerevisiae*	0.5	>500	1
	C. albicans	0.25	>500	1
cholesterol-containing human cells	red blood cells	8.5	>500	>500
	renal epithelial cells	2.4	>80	>80

toxic concentration (µM)

DMSO (vehicle) AmB (2 uM) AmdeB (80 uM) C2'deOAmB (80 uM)

Figure 3.4: *In vitro* toxicity assays with C2'deOAmB showing MICs from microbroth dilution assays, minimum hemolytic concentrations (MHCs) where 90% hemolysis against red blood cells, and minimum toxicity concentrations (MTCs) where 90% loss of viability in primary renal proximal tubule epithelial cells (RPTECs). Representative images of primary RPTECs administered with small molecule at given concentration.

3-4 DEVELOPMENT OF AN ALLOSTERIC MODIFICATION MODEL FOR STEROL-SELECTIVE BINDING

It remained unclear as to why sterol selective binding was observed upon deletion of the C2' hydroxyl. One potential reason is that AmB binds ergosterol and cholesterol in two distinct modes. While this possibility has not been ruled out, it is highly unlikely as both sterols are

structurally very similar. We instead favored a second model based on the phenomenon of ligand-selective allosteric effects observed in proteins.[37-41] In this model, AmB is capable of binding both ergosterol and cholesterol. However, deleting the C2' hydroxyl group results in a shift to a (set of) conformation that selectively binds ergosterol over cholesterol. Based on this model, we would hypothesize that, similarly to its deoxygenation, the epimerization of the C2' hydroxyl group would result in a similar selectivity in sterol binding.

Towards testing this model, Dr. Brice Uno synthesized C2'epiAmB in which the C2' hydroxyl was epimerized from its native axial position to the equatorial position on the mycosamine sugar (Figure 3.2).[18] With this probe in hand, I tested its capacity to bind membrane-embedded ergosterol and cholesterol via the optimized ITC assay I had developed. Similar to C2'deOAmB, when titrating C2'epiAmB with ergosterol-containing LUVs, I observed a strong difference in net exotherm while titration with cholesterol-containing LUVs resulted in no difference (Figure 3.5). As we had hypothesized, like C2'deOAmB, C2'epiAmB demonstrated a similar differential in binding affinity for ergosterol over cholesterol.
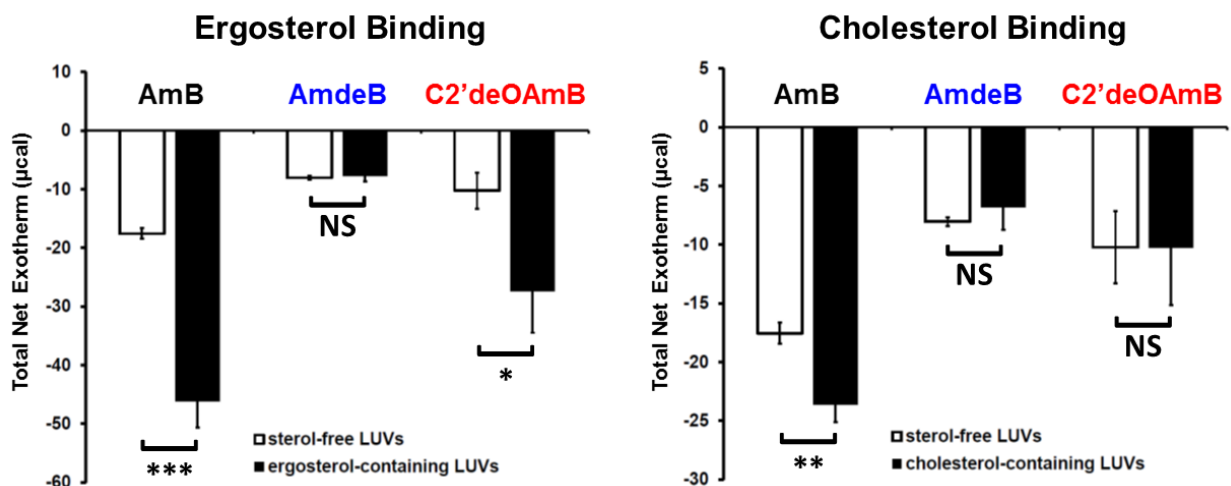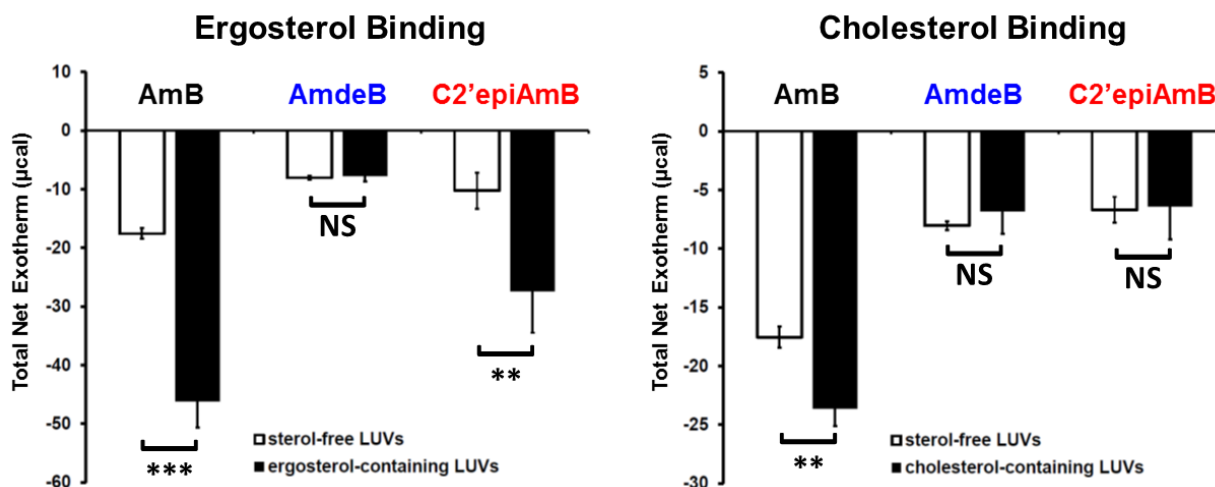

Figure 3.5: Isothermal titration calorimetry with C2'epiAmB titrated with 10% ergosterol-containing, 10% cholesterol-containing, or sterol-free LUVs. ** $P \leq 0.01$, *** $P \leq 0.001$, and NS = not significant.
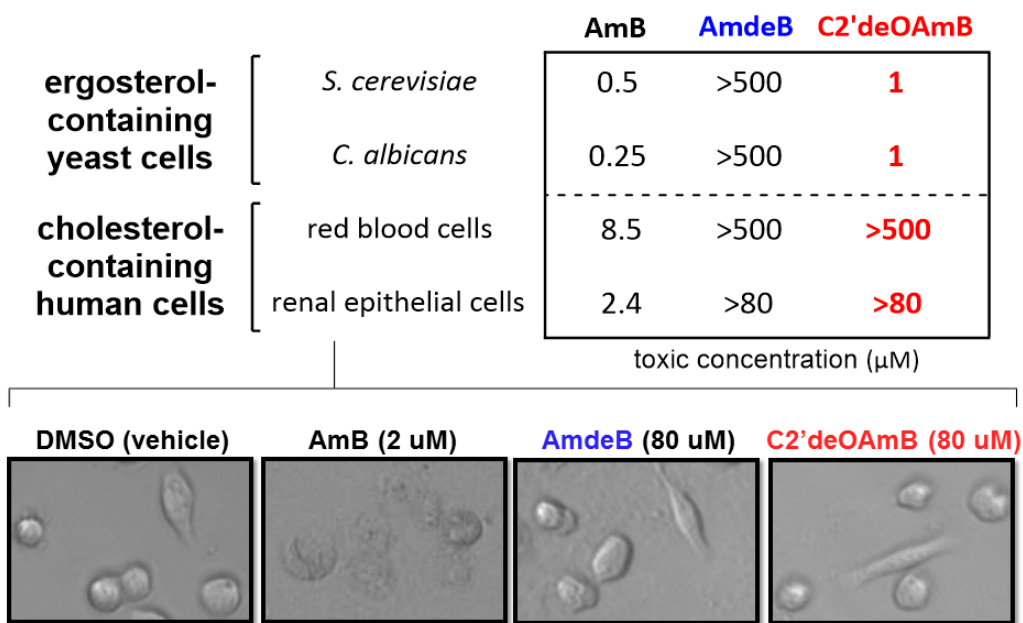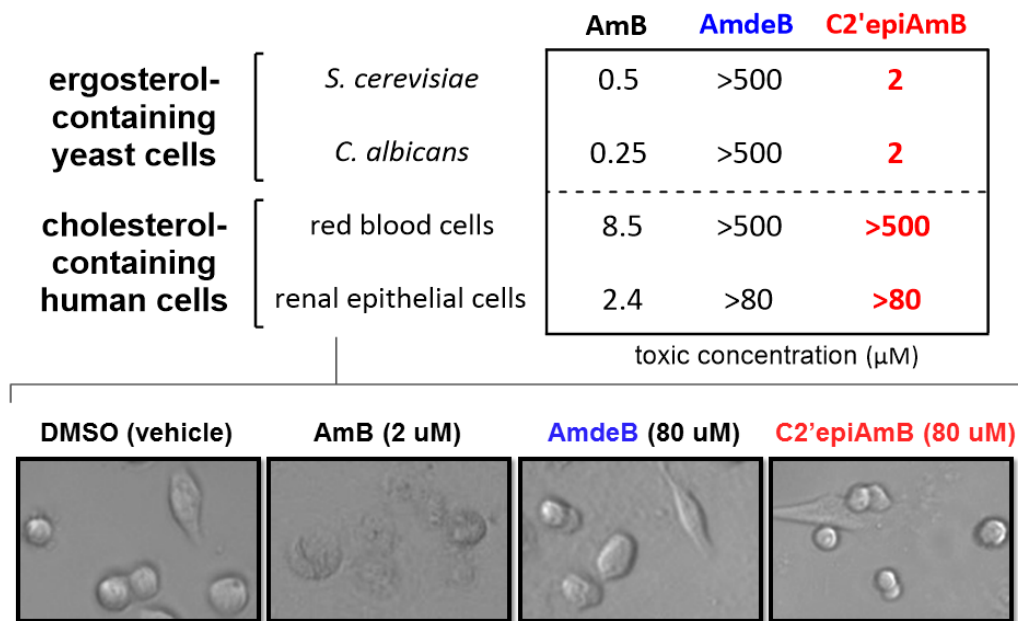
Figure 3.6: *In vitro* toxicity assays with C2'epiAmB showing MICs from microbroth dilution assays, minimum hemolytic concentrations (MHCs) where 90% hemolysis against red blood cells, and minimum toxicity concentrations (MTCs) where 90% loss of viability in primary renal proximal tubule epithelial cells (RPTECs). Representative images of primary RPTECs administered with small molecule at given concentration.

To test whether C2'epiAmB's selective binding translated to an increase in therapeutic index, I tested its toxicity to both fungal and mammalian cells. Against both *S. cerevisiae* and *C. albicans*, I observed potent antifungal activity with an MIC of 2 μM for both yeast strains (Figure 3.6). Furthermore, like C2'deOAmB, C2'epiAmB showed no toxicity with both red blood cells (>500 μM) and primary RPTECs (>80 μM) (Figure 3.6). From these results, C2'epiAmB represents another potential less toxic candidate for the clinical replacement of AmB.

Towards this goal, we pursued the evaluation of C2'epiAmB in invasive candidiasis murine models. Administration of AmB *in vivo* is commonly executed as an intraperitoneal (IP) or intravenous (IV) injection with deoxycholate due to poor solubility of AmB in aqueous media. Based on the deoxycholate formulation of AmB, my colleague Lingbowei Hu developed a similar formulation with C2'epiAmB that enabled us to test C2'epiAmB's *in vivo* efficacy and toxicity. Having developed the deoxycholate formulation, we collaborated with Dr. David Andes at the University of Wisconsin in Madison who had developed the most widely employed mouse model of invasive candidiasis.[42-44] In this model, neutropenic mice were inoculated with *C. albicans* and then treatment was administered via a single IP injection two hours post-infection at four doses (1 mg of compound per kg body weight (mg/kg), 4 mg/kg, 8 mg/kg, and 16 mg/kg). Efficacy was

evaluated by quantification of kidney fungal burden at 6, 12, and 24 hours post-inoculation. Treatment with AmB-deoxycholate at 1 mg/kg yielded a substantial reduction in fungal burden (Figure 3.7). However, consistent with the *in vitro* data, we observed a decrease in *in vivo* antifungal activity with C2'epiAmB-deoxycholate requiring higher administration to reduce the fungal burden to similar levels as AmB (Figure 3.7).
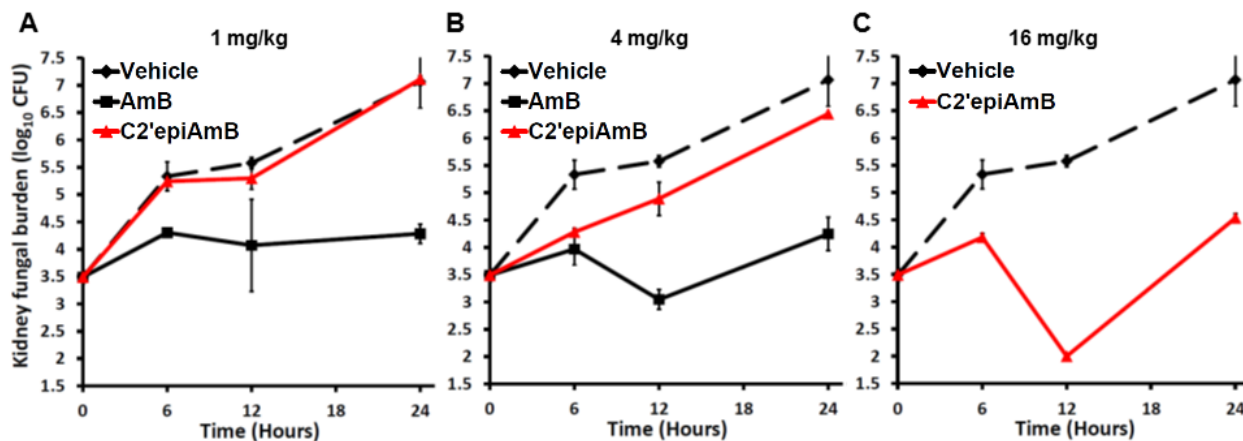
Figure 3.7: Efficacy of AmB and C2'epiAmB in mice. Quantification of the fungal burden in the kidneys of neutropenic mice infected with *C. albicans* after 6 hours, 12 hours, and 24 hours post-intraperitoneal injection of AmB or C2'epiAmB at dosages of (A) 1 mg per kg body weight, (B) 4 mg per kg body weight, and (C) 16 mg per kg body weight.

Despite the reduced efficacy compared to AmB, we determined the acute toxicity in mice by administering treatment via a single IV injection to healthy, uninfected mice and monitored for lethality over 24 hours. Lethality was first observed for the AmB-deoxycholate-treated mice at 4 mg/kg administration while complete lethality was observed at the 8 mg/kg dose. In stark contrast, all mice treated with even 128 mg/kg of C2'epiAmB-deoxycholate survived with no observable toxicity (Figure 3.8). This was highly encouraging as C2'epiAmB showed only a slight attenuation of efficacy while demonstrating a substantial decrease in toxicity *in vivo*.
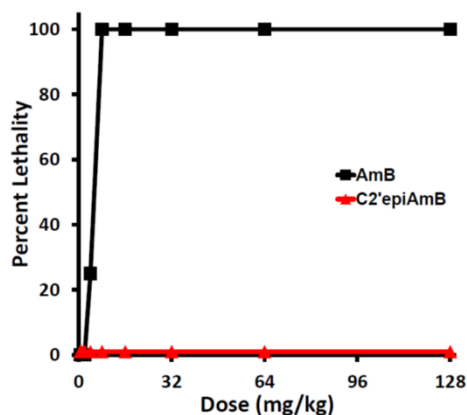
Figure 3.8: Toxicity of AmB and C2'epiAmB in mice. Dose response toxicity determined by lethality after 24 hour post-intravenous injection of AmB or C2'epiAmB (four mice per dosage).

Collectively, these results provide additional support for the ligand-selective allosteric model. With this model in mind, we noted that the crystal structure of *N*-iodoacetyl AmB shows a prominent water-bridged hydrogen bond between the C2' hydroxyl and C13 hemiketal (Figure 3.9).[45,46] We reasoned that this crystal structure may represent the ground-state conformation of AmB and the deletion or epimerization of the C2' hydroxyl disrupts this critical stabilizing element leading to selective binding of ergosterol over cholesterol.

While we are still excited in pursuing both C2'deOAmB and C2'epiAmB for further development, limited synthetic access to both derivatives has hindered further study. Specifically, it has remained unclear whether the improved therapeutic index of both derivatives would come at the cost of AmB's resistance-evasive capacity. Furthermore, a viable clinical replacement of AmB would need to be accessible on the multiple metric tons to supply the annual global demand. Without a practical route toward C2'deOAmB or C2'epiAmB, we sought a different derivative that could demonstrate a similar improvement in therapeutic index, but could be potentially accessible on scale to meet global demand.
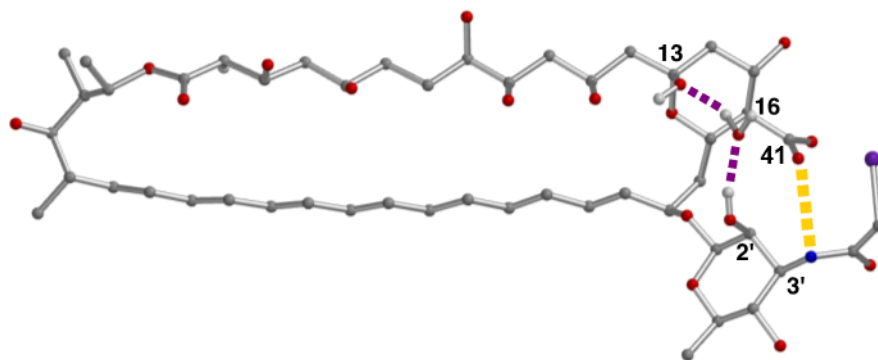
Figure 3.9: Crystal structure of *N*-iodoacetylAmB showing the water-bridged hydrogen bond between the C2' hydroxyl and C13 hemiketal. This model suggests a potential intramolecular salt bridge between the C41 carboxylate and C3' ammonium.

3-5 STEROL-SELECTIVE BINDING AND DIMINISHED TOXICITY OF AmB UREAS

Further analysis of the crystal structure of *N*-iodoacetylAmB would seem to suggest,[29,30] in addition to the water-bridged hydrogen bond between the C2' hydroxyl and C13 hemiketal, a potential intramolecular salt bridge between the C41 carboxylate and C3' ammonium ions (Figure 3.9). We postulated that disruption of this polar interaction could result in sterol-selective binding similar to that which was observed with C2'deOAmB and C2'epiAmB.[19] Due to its unique chemical reactivity, the C41 carboxylate has been modified is several different methods including

but not limited to esterification,[47,48] amidation,[49] and reduction,[11,12] which has yielded AmB derivatives that have produced modest improvements in therapeutic index. However, all of these derivatives maintained the C16-C41 carbon-carbon bond. Dr. Stephen Davis serendipitously discovered that diphenyl phosphoryl azide (DPPA) promotes the stereospecific Curtius rearrangement to cleave the C16-C41 carbon-carbon bond to form a stable oxazolidonone intermediate.[50] This oxazolidonone can be mildly opened with methyl amine, ethylene diamine, and β-alanine allyl ester to produce the AmB methyl urea (AmBMU), AmB amino urea (AmBAU), and AmB carboxylatoethyl urea (AmBCU), respectively.

| AmB | AmdeB | AmBAU | AmBMU | AmBCU |
| 1.1 | 1.27 | 3.3 | 3.4 | 3.5 |
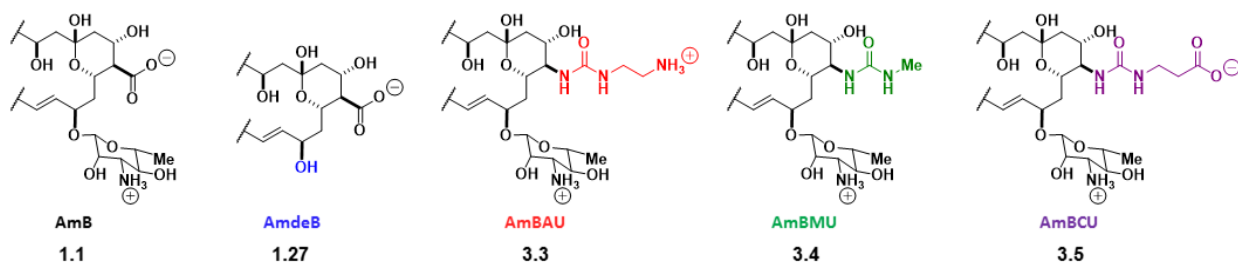
Figure 3.10: Crystal structure of *N*-iodoacetylAmB showing the water-bridged hydrogen bond between the C2' hydroxyl and C13 hemiketal. This model suggests a potential intramolecular salt bridge between the C41 carboxylate and C3' ammonium.

With this new series of AmB derivatives, I tested their capacities to bind sterols via ITC. Like C2'deOAmB and C2'epiAmB, all three AmB urea derivatives retained the capacity to bind ergosterol, but within the limits of detection of this experiment, showed no binding to cholesterol.[34] As described in Chapter 2, we previously found that the binding[1] and extracting[2] of sterol is how AmB kills yeast cells, so I analyzed the ability of all three derivatives to extract ergosterol from *S. cerevisiae* membranes using an ultracentrifugation-based membrane isolation assay to quantify the amount of ergosterol remaining in the membrane.[2] Like AmB, the AmB ureas greatly reduced the quantity of ergosterol in these yeast cells,[34] demonstrating that they retained the capacities to bind and extract ergosterol, but could no longer bind cholesterol.
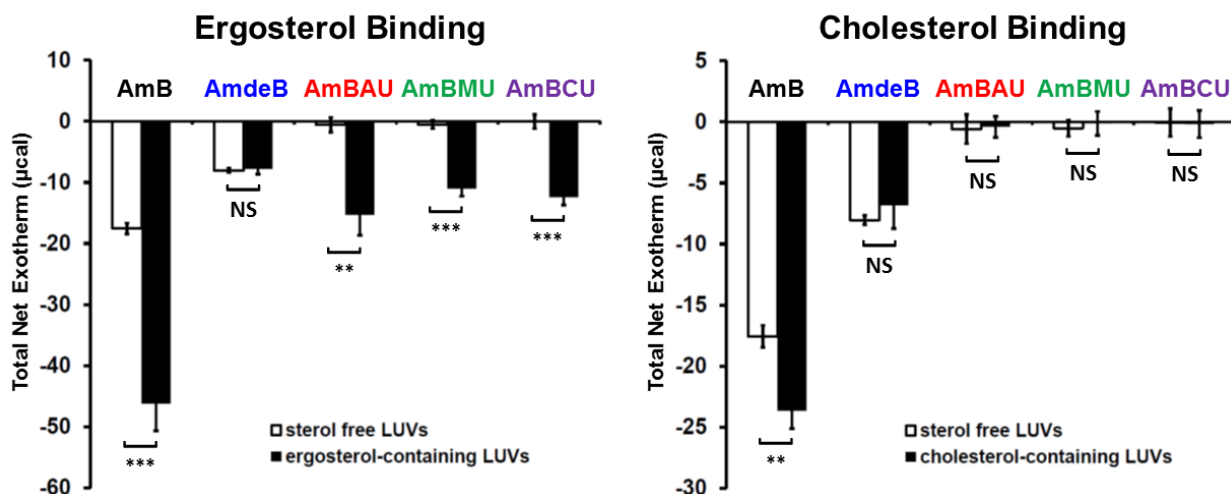
Figure 3.11: Isothermal titration calorimetry with AmBAU, AmBMU, and AmBCU titrated with 10% ergosterol-containing, 10% cholesterol-containing, or sterol-free LUVs. ** $P \leq 0.01$, *** $P \leq 0.001$, and NS = not significant.
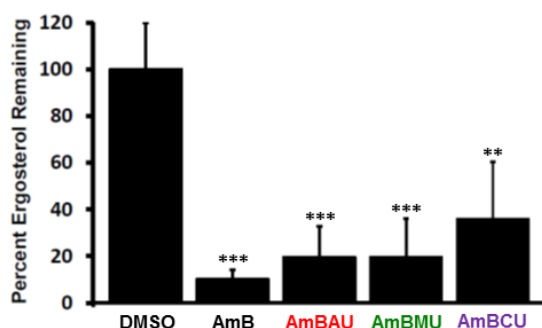
Figure 3.12: Ergosterol extraction from *S. cerevisiae* membranes after two hours of treatment with AmB, AmBAU, AmBMU, or AmBCU. Values normalized to DMSO control. ** $P \leq 0.01$, *** $P \leq 0.001$, and NS = not significant.

The observed selectivity for ergosterol over cholesterol translated into a substantial increase in therapeutic index *in vitro*. The AmB ureas were tested against *S. cerevisiae* and human red blood cells alongside a series of previously reported AmB derivatives that contained modifications at the C41 carboxylate and/or C3' ammonium. These derivatives included reduction of the C41 carboxylate (MeAmB),[11,12] esterification to a methyl ester (AmBME),[31,32] amidation to a methyl amide (AmBMA),[33] and a double modified derivative that was reported to have the greatest increase in therapeutic index (AmBTABA).[51] All of the previously reported derivatives produced modest improvements in therapeutic index. Conversely, the AmB urea derivatives retained potent antifungal activity, but were remarkably less toxic to human red blood cells with the toxicities of AmBMU and AmBAU exceeding 500 µM (Figure 3.13).[34]

amphotericin	MIC (μM) S. cerevisiae	MHC$_{90}$ (μM) red blood cells	amphotericin	MIC (μM) S. cerevisiae	MHC$_{90}$ (μM) red blood cells
AmB 1.1	0.5	8.55 ± 2.20	AmBTABA 3.7	0.25	48.5 ± 8.7
AmE 1.14	0.25	30.67 ± 5.38	AmBAU 3.3	0.25	>500
MeAmB 1.26	0.5	22.03 ± 6.26	AmBMU 3.4	0.5	>500
AmBMA 3.6	0.25	15.32 ± 3.39	AmBCU 3.5	3	323.8 ± 30.2
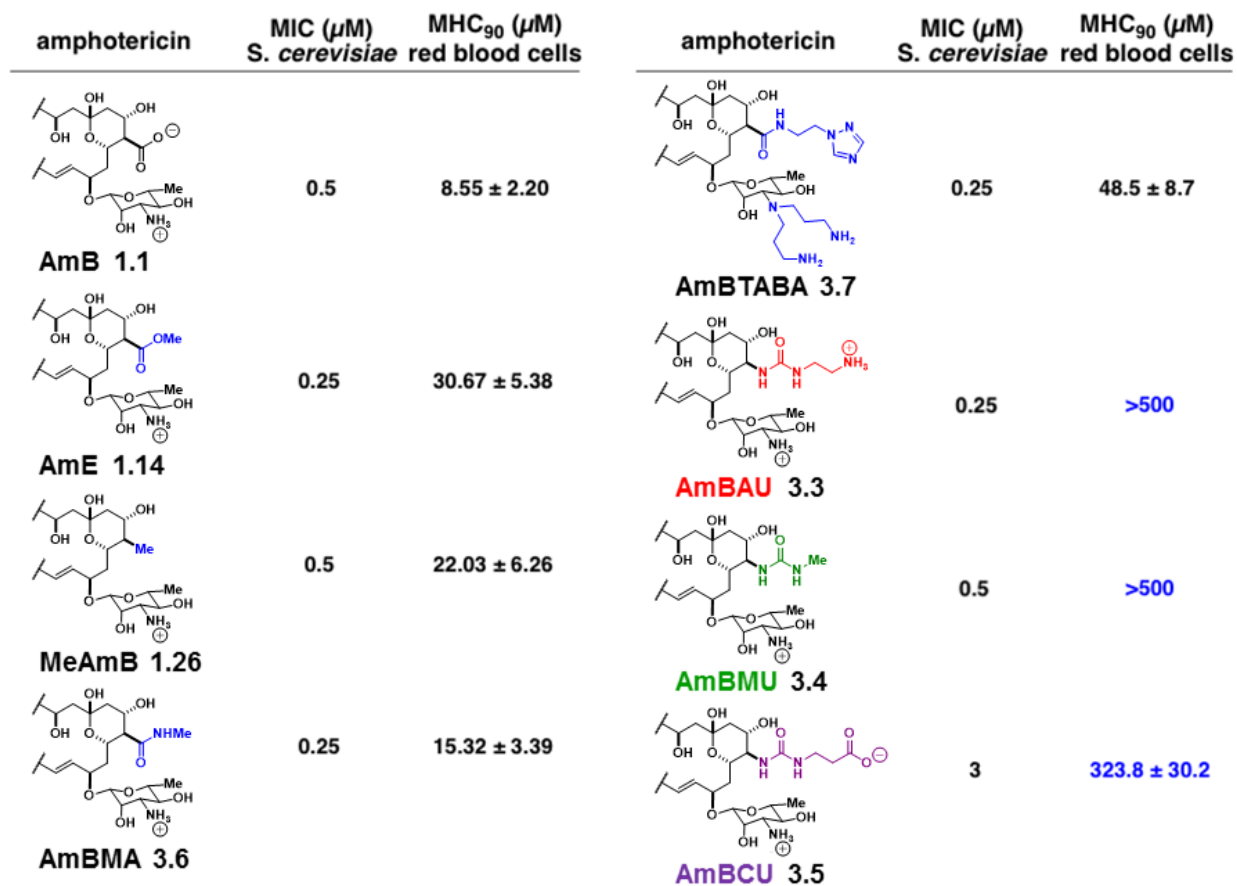
Figure 3.13: *In vitro* toxicity to *S. cerevisiae* and human red blood cells for AmB, the AmB ureas, and other previously reported AmB derivatives with modifications to the C41 carboxylate.

	MIC (µg/mL)											MTC (µM)	
	Candida albicans K1	Candida glabrata 760	Candida tropicalis 5810	Candida parapsilosis 22019	Cryptococcus neoformans H99	Cryptococcus neoformans 89-610	Cryptococcus neoformans T1	Aspergillus fumigatus 41	Aspergillus fumigatus 293	Aspergillus fumigatus 11628	Aspergillus fumigatus 14532	hTERT1 RPTEC	Primary RPTEC
AmB	0.25	0.06	0.06	0.06	0.06	0.125	0.125	1	1	0.5	0.5	6.4 ± 1.3	2.4 ± 0.3
AmBAU	0.5	0.25	1	0.25	1	1	1	4	2	1	2	37.6 ± 4.8	11.3 ± 0.4
AmBMU	0.5	0.25	1	0.25	1	1	1	2	2	0.5	1	>80	44.4 ± 2.1
AmBCU	0.5	1	2	1	1	1	1	4	4	2	2	>80	>80

Figure 3.14: *In vitro* toxicity to a panel of pathogenic fungal strains and human renal proximal tubule epithelial cells (RPTECs) for AmB and the AmB ureas.

Intrigued by substantial increase in therapeutic index for the AmB urea derivatives, we performed further *in vitro* studies with these derivatives. Dr. David Andes tested the ureas against a panel of pathogenic *Candida*, *Cryptococcus*, and *Aspergillus* strains including *Cryptococcus neoformans* 89-610 and T1 that are fluconazole resistant[52] and *Aspergillus fumigatus* 11628 and 14532, which are voriconazole resistant.[53] AmBCU was generally less potent than AmBMU and AmBAU, which retained near equipotent activity as AmB (Figure 3.14).[34] I performed further *in*

vitro toxicity studies with the AmB derivatives against primary human RPTECs[54] and human telomerase reverse transcriptase 1 (hTERT1) RPTECs.[55] The AmB ureas were substantially less toxic to both renal cells (Figure 3.14).[34]
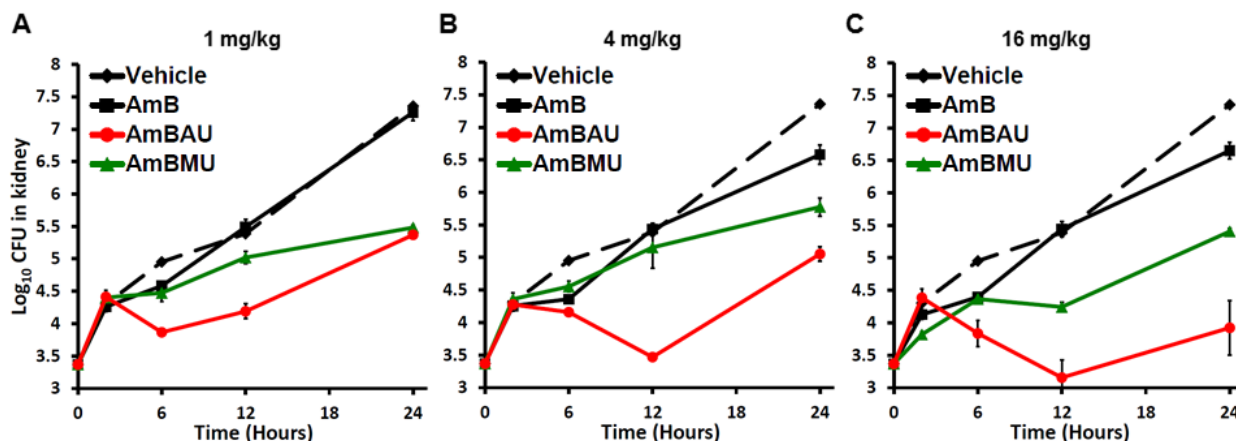
Figure 3.15: Efficacy of AmB, AmBAU, and AmBMU. Quantification of the fungal burden in the kidneys of neutropenic mice infected with *C. albicans* after 2 hours, 6 hours, 12 hours, and 24 hours post-intraperitoneal injection of AmB or C2'epiAmB at dosages of (A) 1 mg per kg body weight, (B) 4 mg per kg body weight, and (C) 16 mg per kg body weight.

Based on their favored *in vitro* activity, we continued to evaluate AmBMU and AmBAU for their efficacy and toxicity *in vivo*. Dr. David Andes tested both derivatives for their efficacy in his mouse model of candidiasis.[26-28] Interestingly, both derivatives were substantially more effective than AmB at reducing the fungal burden in the kidneys at all three doses. We speculate that this unexpected increase in efficacy may be due to the greater than 20 fold increase in water solubility compared to AmB.[34] Both compounds were then tested for their acute mouse toxicity via single intravenous injection. All the mice died from treatment with AmB at a dose of 4 mg/kg within seconds of administration. Conversely, AmBAU became greater than 50% lethal at a dose of 64 mg/kg.[34] Furthermore, AmBMU showed no lethality even up to 64 mg/kg.[34] These derivatives lend further support for our ligand-selective allosteric model and represent a fascinating platform for AmB derivatives that can be easily accessed on large scale and demonstrate a substantial increase in therapeutic index.
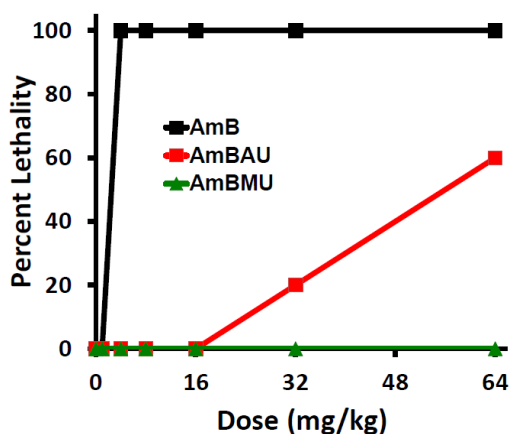
Figure 3.16: Toxicity of AmB, AmBAU, and AmBMU in mice. Dose response toxicity determined by lethality after 24 hour post-intravenous injection of AmB, AmBAU, and AmBMU (five mice per dosage).

3-6 AmB UREAS MAINTAIN RESISTANCE-EVASIVE ABILITY

At this point, the question still remained whether improvement in the therapeutic index came at the cost of the ability to evade resistance. Due to its unique mechanism of action,[1] AmB is not susceptible to the major mechanisms of antimicrobial resistance as its lipid target is not easily mutable as protein or RNA targets and it is not a substrate for secretion via efflux pumps or drug detoxifying enzymes.[56] Furthermore, ergosterol plays a major role in a vast array of processes in yeast physiology.[57-61] Additionally, mutations to genes involved in ergosterol biosynthesis can alter the sterol structure and/or content of the membrane enabling AmB resistance *in vitro*.[62] However, these mutations have a considerable fitness cost *in vivo*, which substantially reduces fungal virulence[63] and would explain why clinically relevant resistance to AmB is incredibly rare.[64]

To test whether the improved sterol selectivity of AmBAU and AmBMU had impacted their ability to evade resistance, we collaborated with Dr. Benjamin Vincent, Dr. Luke Whitesell, and Prof. Susan Lindquist at the Massachusetts Institute of Technology. We compared the MICs of AmB, AmBAU, and AmBMU against a panel of lab-generated *C. albicans* strains that contained mutations to seven different nonessential ergosterol biosynthesis genes. Interestingly, AmBAU and AmBMU had *in vitro* profiles very similar to that of AmB where only the *erg2*, *erg6*, and *erg3erg11* mutants had any substantial resistance (Figure 3.17A).[34] All three mutations are known to result in avirulence in yeast[47] likely due to the inability for many ergosterol-dependent proteins to utilize this mutated sterol. As a result, all known mutations to nonessential ergosterol biosynthesis genes do not seem to a threat to the efficacy of both urea derivatives.

66
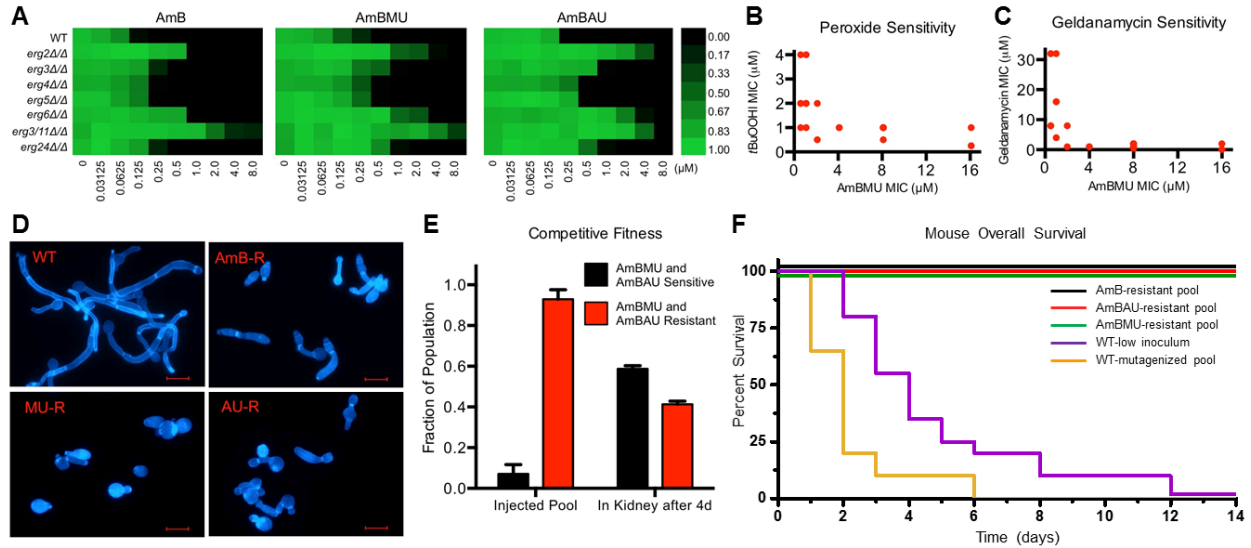
Figure 3.17: (A) MICs for AmB, AmBAU, and AmBMU against lab-generated strains with mutations in seven nonessential ergosterol biosynthesis genes. MICs for (B) *tert*-butyl peroxide and (C) geldanamycin for various AmBAU- and AmBMU-resistant strains. (D) Representative images of filamentation in response to fetal bovine serum at 37°C, stained with Calcofluor white, scale bar 10 µm. (E) *In vivo* competitive fitness study (F) Overall mice survival following inoculation with AmB-resistant pool, AmBAU-resistant pool, AmBMU-resistant pool, a pool of parental wild-type, and a pool of five passaged and mutagenized wild-type mutants. Figure was adapted from reference 34.

To understand if there are additional mutations that could result in resistance to AmB, AmBAU, or AmBMU, resistance mutants were generated via gradual resistance-selection in liquid culture and five to eight mutants were created for each small molecule. Importantly, all resistant mutants were cross-resistant across all three molecules, which would suggest there were no new mechanisms of resistance from the two AmB urea derivatives.[34] Genome sequencing of the mutants revealed that contained mutations in the *ERG2* or *ERG6* locus and subsequently underwent loss of heterozygosity. AmB-resistant mutants had previously been shown to substantial defects in fitness and are highly sensitive to oxidative stress that are consistently encountered during the infection process.[47] Similar to AmB-resistant mutants, all of the mutants resistant to AmBAU or AmBMU were found to be extremely sensitive to the oxidative stressors *tert*-butyl hydrogen peroxide (Figure 3.17B) and the Hsp90 inhibitor geldanamycin (Figure 3.17C). Moreover, wild-type yeast readily filament *in vitro*, which is thought to play an important role in virulence in *Candida* (Figure 3.17D).[65,66] AmB-resistant mutations result in the crippling of the ability to filament and thus lead to avirulence in yeast.[47] Similarly, we found that in response to stimulation with fetal bovine serum, AmBAU- and AmBMU-resistant mutants were also unable to filament (Figure 3.17D).[34]

Encouraged by these *in vitro* fitness studies, we tested whether resistance to AmBAU or AmBMU would likewise reduce fitness *in vivo*. Mice were infected with a pool of yeast strains

comprised of one strain of the wild-type (AmBAU- and AmBMU-sensitive) and 15 strains that were AmBAU- or AmBMU-resistant (with each strain comprising of $1/16^{th}$ of the total population). The infection was allowed to progress untreated for four days. Following infection, fungal colonies were isolated from the kidneys and tested for their sensitivity to AmBAU and AmBMU. Based on those results, the fraction of AmBAU- and AmBMU-resistant were determined from the total population isolated from the kidneys. Over the course of just four days, the percentage of AmBAU- or AmBMU-resistant strains dropped substantially and were overtaken by the AmBAU- and AmBMU-sensitive wild-type strain (Figure 3.17E).[34]

As a final analysis of *in vivo* fitness, we tested whether AmBAU- or AmBMU-resistant mutants had retained the ability to cause lethal infection. Mice were infected with pools of AmB-, AmBAU-, or AmBMU-resistant mutants and were compared to the survival of the mice infected by wild-type strains. A low inoculum of the wild-type strain resulted in complete lethality for all mice over the two week analysis window (Figure 3.17F). Similarly, infection of wild-type strains that had undergone random mutagenesis over five *in vitro* passages like the resistant mutants also killed all mice (Figure 3.17F). In stark contrast, all mice inoculated with AmB-, AmBAU-, or AmBMU-resistant strains survived the infection over the two week period. (Figure 3.17F).[34] Collectively, these results demonstrate that AmBAU and AmBMU are not any more vulnerable to the development of resistance than AmB, which has managed to evade resistance for over half a century. Therefore, these findings reveal that selective antimicrobial action and the capacity to evade resistance are not mutually exclusive and have the potential to be clinically viable substitutes for AmB.

3-7 THESIS SUMMARY

This thesis describes the mechanistic understanding of the ion channel-forming, antimycotic natural product, AmB. To probe the roles of ergosterol binding and membrane permeabilization in the antifungal activity of AmB, a derivative lacking the C35 hydroxyl group, C35deOAmB, was synthesized using an iterative cross-coupling (ICC)-based strategy. This critical probe retained the capacity to bind ergosterol, could no longer cause membrane permeabilization, and was able to maintain potent but slightly reduced antifungal activity. Its antifungal activity was comparable to natamycin, another member of the polyene macrolide family that similarly binds ergosterol and notably does not form ion channels. Deletion of the mycosamine

appendage from AmB and natamycin eliminates the ability to bind ergosterol and thus abrogates the antifungal activity of both natural products. Collectively, these results demonstrate that the primary mechanism by which AmB and likely all mycosamine-containing polyene macrolides kill yeast is via mycosamine-mediated ergosterol binding and that the capacity to permeabilize membranes only further increases their potency.

This finding has substantial implications in the mechanistic understanding of how AmB kills human cells and causes nephrotoxicity. It suggests that the operative mechanism for killing human cells is the binding of the major mammalian sterol: cholesterol. To further probe the atomistic interactions involved in the binding between AmB and both sterols, a derivative of AmB lacking the C2' hydroxyl was synthesized. This hydroxyl was predicted to be key in the binding with both ergosterol and cholesterol. Conversely, C2'deOAmB maintained the capacity to bind ergosterol but not cholesterol and thus maintained potent antifungal activity but was substantially less toxic to human cells. To explain this sterol selectivity, a ligand-selective allosteric modification model was developed. Consistent with this model, epimerization of the C2' hydroxyl resulted in C2'epiAmB which shared a similar activity profile with C2'deOAmB. Guided by this model, a new class of AmB derivatives were synthesized: the AmB ureas. Like both C2'-modified derivatives, the AmB ureas had increased selectivity for ergosterol over cholesterol and were significantly less toxic than AmB. Due to the accessibility of this new class of AmB derivatives, they were further evaluated for efficacy and toxicity in a mouse model of disseminated candidiasis and found to be more efficacious and less toxic than AmB *in vivo*. Furthermore, the AmB ureas still maintained the ability to evade resistance.

Collectively, the studies described in this thesis significantly advances the mechanistic understanding of this critically important natural product. These findings enable the pursuit of increased therapeutic derivatives of AmB to focus on maximizing the binding selectivity for ergosterol over cholesterol. Furthermore, these results lay the foundation towards utilizing the ion channel forming capacity of AmB as a molecular surrogate for missing protein ion channels that underlie a number of human diseases.

3-8 EXPERIMENTAL SECTION

Materials.

Commercially available materials were purchased from Sigma-Aldrich, AKSci, Alfa Aesar, Strem, Avanti Polar Lipids, Lipoid, Silicycle, or Fisher Scientific and were used without further purification unless stated otherwise. Amphotericin B was a generous gift from Bristol-Myers Squibb Company. All solvents were dispensed from a solvent purification system that passes solvents through packed columns according to the method of Pangborn and coworkers[67] (THF, Et_2O, CH_2Cl_2, toluene, dioxane, hexanes : dry neutral alumina; DMSO, DMF, CH_3OH : activated molecular sieves). Water was obtained from a Millipore MilliQ water purification system.

Isothermal Titration Calorimetry

General Information.

Experiments were performed using a NanoITC isothermal titration calorimeter (TA Instruments, Wilmington, DE). Solutions of the compounds to be tested were prepared by diluting a 60.0 mM stock solution of the compound in DMSO to 600 μM with K buffer (5.0 mM HEPES/KHEPES, pH = 7.4). The final DMSO concentration in the solution was 1% v/v. POPC LUVs were prepared and phosphorus and ergosterol content was quantified as described below. The LUV solutions were diluted with buffer and DMSO to give a final phospholipid concentration of 12.0 mM in a 1% DMSO/K buffer solution. Immediately prior to use, all solutions were incubated at 37°C for 30 minutes and degassed under vacuum at 37°C for 10 minutes. The reference cell of the instrument (volume = 0.190 mL) was filled with a solution of 1% v/v DMSO/K buffer.

LUV Preparation.

Palmitoyl oleoyl phosphatidylcholine (POPC) was obtained as a 20 mg/mL solution in $CHCl_3$ from Avanti Polar Lipids (Alabaster, AL) and was stored at -20°C under an atmosphere of dry argon and used within 1 month. A 4 mg/mL solution of ergosterol in $CHCl_3$ was prepared monthly and stored at 4°C under an atmosphere of dry argon. A 4 mg/mL solution of cholesterol in $CHCl_3$ was prepared monthly and stored at 4°C under an atmosphere of dry argon. Prior to preparing a lipid film, the solutions were warmed to ambient temperature to prevent condensation from contaminating the solutions. A 13 x 100 mm test tube was charged with 800 μL POPC and

230 µL of the ergosterol solution. For cholesterol-containing liposomes, a 13 x 100 mm test tube was charged with 800 µL POPC and 224 µL of the cholesterol solution. For sterol-free liposomes, a 13 x 100 mm test tube was charged with 800 µL POPC. The solvent was removed with a gentle stream of nitrogen and the resulting lipid film was stored under high vacuum for a minimum of eight hours prior to use. The film was then hydrated with 1 mL of K buffer and vortexed vigorously for approximately 3 minutes to form a suspension of multilamellar vesicles (MLVs). The resulting lipid suspension was pulled into a Hamilton (Reno, NV) 1 mL gastight syringe and the syringe was placed in an Avanti Polar Lipids Mini-Extruder. The lipid solution was then passed through a 0.20 µm Millipore (Billerica, MA) polycarbonate filter 21 times, the newly formed large unilamellar vesicle (LUV) suspension being collected in the syringe that did not contain the original suspension of MLVs to prevent the carryover of MLVs into the LUV solution.

Determination of Phosphorus Content.

Determination of total phosphorus was adapted from the report of Chen and coworkers.[68] The LUV solution was diluted tenfold with K buffer and three 10 µL samples of the diluted LUV suspension were added to three separate 7 mL vials. Subsequently, the solvent was removed with a stream of N_2. To each dried LUV film, and a fourth vial containing no lipids that was used as a blank, was added 450 µL of 8.9 M H_2SO_4. The four samples were incubated open to ambient atmosphere in a 225°C aluminum heating block for 25 min and then removed to 23°C and cooled for 5 minutes. After cooling, 150 µL of 30% w/v aqueous hydrogen peroxide was added to each sample, and the vials were returned to the 225°C heating block for 30 minutes. The samples were then removed to 23°C and cooled for 5 minutes before the addition of 3.9 mL water. Then 500 µL of 2.5% w/v ammonium molybdate was added to each vial and the resulting mixtures were then vortexed briefly and vigorously five times. Subsequently, 500 µL of 10% w/v ascorbic acid was added to each vial and the resulting mixtures were then vortexed briefly and vigorously five times. The vials were enclosed with a PTFE lined cap and then placed in a 100°C aluminum heating block for 7 minutes. The samples were removed to 23°C and cooled for approximately 15 minutes prior to analysis by UV/Vis spectroscopy. Total phosphorus was determined by observing the absorbance at 820 nm and comparing this value to a standard curve obtained through this method and a standard phosphorus solution of known concentration.

Determination of Ergosterol Content.

Ergosterol content was determined spectrophotometrically. A 50 μL portion of the LUV suspension was added to 450 μL 2:18:9 hexane:isopropanol:water (v/v/v). Three independent samples were prepared and then vortexed vigorously for approximately one minute. The solutions were then analyzed by UV/Vis spectroscopy and the concentration of ergosterol in solution was determined by the extinction coefficient of 10400 L mol^{-1} cm^{-1} at the UV$_{max}$ of 282 nm and was compared to the concentration of phosphorus to determine the percent sterol content. The extinction coefficient was determined independently in the above ternary solvent system. LUVs prepared by this method contained between 7 and 14% ergosterol.

Titration Experiment.

Titrations were performed by injecting the LUV suspension at ambient temperature into the sample cell (volume = 0.191 mL) which contained the 600 μM solution of the compound in question at 25°C. The volume of the first injection was 0.23 μL. Consistent with standard procedure,[69] due to the large error commonly associated with the first injection of ITC experiments, the heat of this injection was not included in the analysis of the data. Next, six 7.49 μL injections of the LUV suspension were performed. The spacing between each injection was 720 seconds to ensure that the instrument would return to a stable baseline before the next injection was made. The rate of stirring for each experiment was 300 rpm.

Data Analysis.

NanoAnalyze software (TA Instruments) was used for baseline determination and integration of the injection heats, and Microsoft Excel was used for subtraction of dilution heats and the calculation of overall heat evolved. To correct for dilution and mixing heats, the heat of the final injection from each run was subtracted from all the injection heats for that particular experiment.[70] By this method, the overall heat evolved during the experiment was calculated using the following formula:

$$\mu\mathrm{cal}_{overall} = \sum_{i=1}^{n} (\Delta h_{injection}^{i} - \Delta h_{injection}^{n})$$

Where i = injection number, n = total number of injections, $\Delta h_{injection}^{i}$ = heat of the ith injection, $\Delta h_{injection}^{n}$ = the heat of the final injection of the experiment.

Antifungal Assays

Growth Conditions for *S. cerevisiae*.

    S. cerevisiae was maintained with yeast peptone dextrose (YPD) growth media consisting of 10 g/L yeast extract, 20 g/L peptone, 20 g/L dextrose, and 20 g/L agar for solid media. The media was sterilized by autoclaving at 250°F for 30 min. Dextrose was subsequently added as a sterile 40% w/v solution in water (dextrose solutions were filter sterilized). Solid media was prepared by pouring sterile media containing agar (20 g/L) onto Corning (Corning, NY) 100 x 20 mm polystyrene plates. Liquid cultures were incubated at 30°C on a rotary shaker and solid cultures were maintained at 30°C in an incubator.

Growth Conditions for *C. albicans*.

    C. albicans was cultured in a similar manner to *S. cerevisiae* except both liquid and solid cultures were incubated at 37°C.

Growth Conditions and MIC Assay for *C. albicans, C. tropicalis, C. parapsilosis, and C. glabarata*.

    The organisms were maintained, grown, subcultured, and quantified on Sabouraud dextrose agar (SDA; Difco Laboratories, Detroit, MI). 24 hours prior to the study, the organisms were subcultured at 35°C. MIC determinations were performed in duplicate on at least two occasions using the Clinical and Laboratory Standards Institute M27-A3 microbroth methodology.[71]

Growth Conditions and MIC Assay for *C. neoformans*.

    C. neoformans MIC was determined as previously reported after 48 hours.[36]

Growth Conditions and MIC Assay for *C. fumigatus*.

    The organisms were maintained, grown, subcultured, and quantified on potato dextrose agar (PDA; Difco Laboratories, Detroit, MI). MIC determinations were performed in duplicate on at least two occasions using the Clinical and Laboratory Standards Institute M28-A2 microbroth methodology[72] at 48 hours.

Broth Microdilution Minimum Inhibitory Concentration (MIC) Assay.

The protocol for the broth microdilution assay was adapted from the Clinical and Laboratory Standards Institute document M27-A2.[73] 50 mL of YPD media was inoculated and incubated overnight at either 30°C (*S. cerevisiae*) or 37°C (*C. albicans*) in a shaker incubator. The cell suspension was then diluted with YPD to an OD_{600} of 0.10 (~5 x 10^5 cfu/mL) as measured by a Shimadzu (Kyoto, Japan) PharmaSpec UV-1700 UV/Vis spectrophotometer. The solution was diluted 10-fold with YPD, and 195 μL aliquots of the dilute cell suspension were added to sterile Falcon (Franklin Lakes, NJ) Microtest 96 well plates in triplicate. Compounds were prepared either as 400 μM (AmB, MeAmB) or 2 mM (AmdeB, MeAmdeB) stock solutions in DMSO and serially diluted to the following concentrations with DMSO: 1600, 1200, 800, 400, 320, 240, 200, 160, 120, 80, 40, 20, 10 and 5 μM. 5 μL aliquots of each solution were added to the 96 well plate in triplicate, with each column representing a different concentration of the test compound. The concentration of DMSO in each well was 2.5% and a control well to confirm viability using only 2.5% DMSO was also performed in triplicate. This 40-fold dilution gave the following final concentrations: 50, 40, 30, 20, 10, 8, 6, 4, 1, 0.5, 0.25 and 0.125 μM. The plates were covered and incubated at 30°C (*S. cerevisiae*) or 37°C (*C. albicans*) for 24 hours prior to analysis. The MIC was determined to be the concentration of compound that resulted in no visible growth of the yeast. The experiments were performed in duplicate and the reported MIC represents an average of two experiments.

Hemolysis Assays

Erythrocyte Preparation.

The protocol for the hemolysis assay was adapted from the report of Paquet and coworkers.[35] Whole human blood (sodium heparin) was purchased from Bioreclamation LLC (Westbury, NY) and stored at 4°C and used within two days of receipt. To a 2.0 mL eppendorf tube, 1 mL of whole human blood was added and centrifuged at 10,000 g for 2 minutes. The supernatant was removed and the erythrocyte pellet was washed with 1 mL of sterile saline and centrifuged at 10,000 g for 2 minutes. The saline wash was repeated for a total of three washes. The erythrocyte pellet was suspended in 1 mL of RBC buffer (10 mM NaH_2PO_4, 150 mM NaCl, 1 mM $MgCl_2$, pH 7.4) to form the erythrocyte stock suspension.

Minimum Hemolysis Concentration (MHC) Assay.

Compounds were prepared as 1.03 mM (AmB) or 12.8 mM (C2'deOAmB and AmdeB) stock solutions in DMSO and serially diluted to the following concentrations with DMSO: 7689, 5126, 2563, 2050, 1538, 1025, 769, 513, 384, 256, 205, 154, 103, 77, 51, 26 μM. To a 0.2 mL PCR tube, 24 μL of RBC buffer and 1 μL of compound stock solution were added, which gave final concentrations of 500, 300, 200, 100, 80, 60, 40, 30, 20, 15, 10, 8, 6, 4, 3, 2, 1 μM. Positive and negative controls were prepared by adding 1 μL of DMSO to MilliQ water or RBC buffer, respectively to 0.2 mL PCR tube. To each PCR tube, 0.63 μL of the erythrocyte stock suspension was added and mixed by inversion. The samples were incubated at 37°C for 2 hours. The samples were mixed by inversion and centrifuged at 10,000 g for 2 minutes. 15 μL of the supernatant from each sample was added to a 384-well place. Absorbances were read at 540 nm using a Biotek H1 Synergy Hybrid Reader (Wanooski, VT). Experiments were performed in triplicate and the reported MHC represents an average of three experiments.

Data Analysis.

Percent hemolysis was determined according to the following equation:

$$\% \ hemolysis = \frac{Abs._{sample} - Abs._{neg.}}{Abs._{pos.} - Abs._{neg.}} \times 100\%$$

Concentration vs. percent hemolysis was plotted and fitted to 4-parameter logistic (4PL)[74] dose response fit using OriginPro 8.6. The MHC was defined as the concentration to cause 90% hemolysis.

WST-8 Cell Proliferation Assays

Primary Renal Proximal Tubule Epithelial Cells Preparation.

Primary human renal proximal tubule epithelial cells (RPTECs) were purchased from ATCC (Manassas, VA) and immediately cultured upon receipt. Complete growth media was prepared using renal epithelial cell basal medium (ATCC, PCS-400-030), renal epithelial cell growth kit (ATCC, PCS-400-040), and penicillin-streptomycin (10 units/mL and 10 μg/mL).

Complete media was stored at 4°C in the dark and used within 28 days. Primary RPTECs were grown in CO_2 incubator at 37°C with an atmosphere of 95% air/5% CO_2.

WST-8 Reagent Preparation.

WST-8 cell proliferation assay kit (10010199) was purchased from Cayman Chemical Company (Ann Arbor, MI) and stored at -20 °C and used within 6 months of receipt. WST-8 reagent and electron mediator solution were thawed and mixed to prepare the WST-8 reagent solution. The solution was stored at -20 °C and used within one week.

WST-8 Assay.

A suspension of primary or TERT1 RPTECs in complete growth media was brought to a concentration of 1 x 10^5 cells/mL. A 96-well plate was seeded with 99 μL of the cell suspension and incubated at 37°C with an atmosphere of 95% air/5% CO_2 for 3 hours. Positive and negative controls were prepared by seeding with 100 μL of the cell suspension or 100 μL of the complete media. Compounds were prepared as 5 mM (AmB) and 8 mM (AmdeB, C2'deOAmB, C2'epiAmB, AmBAU, AmBMU, and AmBCU) stock solutions in DMSO and serially diluted to the following concentrations with DMSO: 8000, 6000, 4000, 3000, 2000, 1500, 1000, 800, 600, 400, 300, 200, 100, 50, 25, 10, 5, 2.5, 1, 0.5, 0.25, and 0.1 μM. 1 μL aliquots of each solution were added to the 96-well plate in triplicate, with each column representing a different concentration of the test compound. The 96-well plate was incubated at 37°C with an atmosphere of 95% air/5% CO_2 for 24 hours. After incubation, the media was aspirated and 100 μL of serum-free media was added and 10 μL of the WST-8 reagent solution was added to each well. The 96-well plate was mixed in a shaking incubator at 200 rpm for 1 minute and incubated at 37°C with an atmosphere of 95% air/5% CO_2 for 2 hours. Following incubation, the 96-well plate was mixed in a shaking incubator at 200 rpm for 1 minute and absorbances were read at 450 nm using a Biotek H1 Synergy Hybrid Reader (Wanooski, VT). Experiments were performed in triplicate and the reported cytotoxicity represents an average of three experiments.

Data Analysis.

Percent hemolysis was determined according to the following equation:

$$\% \ cell \ viability = \frac{Abs._{sample} - Abs._{neg.}}{Abs._{pos.} - Abs._{neg.}} \times 100\%$$

Concentration vs. percent hemolysis was plotted and fitted to 4-parameter logistic (4PL)[56] dose response fit using OriginPro 8.6. The MTC was defined as the concentration to cause 90% loss of cell viability.

Microscopy.

Cells were imaged using an AMG (Bothell, WA) EVOS fl Microscope after treatment with DMSO (vehicle) or the compounds at the indicated concentrations for 24 hours. Images were taken using transmitted light at 10x objective.

***In Vivo* Sterol Extraction Studies and Membrane Isolation.**

This assay was performed similar to that previously described.[2] Specifically, 75 mL overnight cultures of *Saccharomyces cerevisiae* were grown to stationary phase (OD ~1.7) in YPD media at 30°C, shaking. 49.5 mL of this culture was transferred to a 50 mL Falcon centrifuge tubes.

Cells were treated with 500 μL of DMSO, 500 μM AmB, 500 μM AmBAU, 500 μM AmBMU, or 500 μM AmBCU (final compound concentration of 5 μM). Falcon tubes were incubated in the shaking incubator at 30°C for 2 hours. Tubes were inverted at the 1 hour timepoint to resuspend.

Yeast membranes were isolated using a modified version of Haas' spheroplasting and isosmotic cell lysis protocol and differential ultracentrifugation. After treatment time, tubes were centrifuged for 5 minutes at 3000 g at 23°C. The supernatant was decanted and 5 mL of wash buffer (milliQ H_2O (89%), 1M aq. DTT (1%), and 1M aq. Tris buffer pH 9.4 (10%)) was added. Tubes were vortexed to resuspend and incubated in a 30°C water bath for 10 minutes. Tubes were then centrifuged for 5 minutes at 3000 g at 23°C and the supernatant decanted.

1 mL of spheroplasting buffer (1M aq. potassium phosphate buffer pH 7.5 (5%), 4M aq. sorbitol (15%), and YPD media (80%)) and 100 μL of a 5 mg/mL aq. solution of lyticase from *Arthrobacter luteus* (L2524 Sigma-Aldrich) was added to each tube, vortexed to resuspend. Tubes were incubated in a 30°C shaking incubator for 30 minutes. After incubation, tubes were centrifuged for 10 minutes at 1080 g at 4°C and the supernatant decanted.

1 mL of PBS buffer and 20 μL of a 0.4 mg/ml dextran in 8% Ficoll solution was added to each tube, mixed very gently to resuspend. This suspension was placed in an ice bath for 4 minutes and then transferred to a 30°C water bath for 3 minutes.

The suspensions were transferred to 2 mL Eppendorf tubes, vortexed to ensure complete lysis, and centrifuged at 15,000 g at 4°C to remove un-lysed cells and cell debris. The resulting supernatants were transferred to thick-wall polycarbonate ultracentrifuge tubes (3.5 mL, 13 x 51 mm, 349622 Beckman Coulter). PBS buffer was added to the tubes to bring the volume up to ~3 mL. The tubes were centrifuged for 1 hour at 100,000 g at 4°C in a Beckman Coulter TLA-100.3 fixed-angle rotor in a tabletop ultracentrifuge. The supernatant was poured off. The remaining membrane pellet was resuspended in 1 mL PBS buffer. 750 μL of the suspension was transferred to a 7 mL vial and stored at -80°C until further analysis.

Gas chromatography quantification of sterols.

The suspension was allowed to warm to room temperature and 20 μL of internal standard (4 mg/mL cholesterol in chloroform) was added. They were dissolved in 3 mL 2.5% ethanolic KOH, which was vortexed gently, capped, and heated in a heat block on a hot plate at 90°C for 1 hour. The vials were allowed to cool to room temperature. 1 mL of brine was added to the contents of each vial. Extraction was performed three times, each with 2 mL of hexane. Organic layers were combined, dried over MgSO4, filtered through Celite® 545, and transferred to another 7 mL vial. The contents of the vial were concentrated *in vacuo*. The lipid films were dried on high vac with P2O5 for 30 minutes to remove residual water.

To the resulting lipid films, 100 μL pyridine and 100 μL N,O-Bis(trimethylsilyl)trifluoroacetamide with 1% trimethylchlorosilane (T6381-10AMP Sigma-Aldrich) was added and vortexed gently. This solution was heated at 60°C for 1 hour to produce TMS ethers. The vials were placed in an ice bath and the solvent was evaporated off by nitrogen stream. Vials were kept at low temperature to prevent evaporation of the sterol ethers along with the solvent. The resulting films were resuspended in 100 μL of decane, filtered using a Supelco ISO-Disc PTFE Filter (4 mm x 0.2 μm) and transferred to a GC vial insert for analysis.

Gas chromatography analysis was carried out on an Agilent 7890A gas chromatograph equipped with FID and Agilent GC 7693 Autosampler. Samples were separated on a 30 m, 0.320 mm ID, 0.25 um film HP-5 capillary column (19091J-413 Agilent). Hydrogen was employed as a

carrier gas with a flow rate of 4 mL/min. Nitrogen make-up gas, hydrogen gas, and compressed air were used for the FID. A split/splitless injector was used in a 20:1 split. The injector volume was 2 μL. The column temperature was initially held at 250°C for 0.5 min, then ramped to 265°C at a rate of 10°C /min with a final hold time of 12.5 min. The injector and detector temperature were maintained at 270°C and 290°C, respectively.

Ethics Statement

All animal procedures were approved by the Institutional Animal Care and Use Committee at the University of Wisconsin according to the guidelines of the Animal Welfare Act, The Institute of Laboratory Animal Resources Guide for the Care and Use of Laboratory Animals, and Public Health Service Policy.

***In Vivo* Murine Efficacy Study**

All studies were approved by the Animal Research Committee of the William S. Middleton Memorial VA Hospital (Madison, WI). Efficacy was assessed by CFU count in the kidneys of neutropenic mice with a disseminated fungal infection as described previously by Andes et al.[26-28] A clinical isolate of *Candida albicans* (K-1) was grown and quantified on SDA. For 24 hours prior to infection, the organism was subcultured at 35°C on SDA slants. A 10^6 CFU/mL inoculum (CFU, colony forming units) was prepared by placing six fungal colonies into 5 mL of sterile, depyrogenated normal (0.9%) saline warmed to 35°C. Six-week-old ICR/Swiss specific-pathogen-free female mice were obtained from Harlan Sprague Dawley (Madison, WI). The mice were weighed (23−27 g) and given intraperitoneal injections of cyclophosphamide to render neutropenia (defined as <100 polymorphonuclear leukocytes/mm^3). Each mouse was dosed with 150 mg/kg of cyclophosphamide 4 days prior to infection and 100 mg/kg 1 day before infection. Disseminated candidiasis was induced via tail vein injection of 100 μL of inoculum. AmB, AmBAU, or AmBMU were reconstituted with 1.0 mL of 5% dextrose. Each animal in the treatment group was given a single 200 μL intraperitoneal (ip) injection of reconstituted AmB, AmBAU, or AmBMU 2 hours post-infection. Doses were calculated in terms of mg of compound/kg of body weight. At each time point (6, 12, and 24 hours post-infection), three animals per experimental condition were sacrificed by CO_2 asphyxiation. The kidneys from each animal were removed and homogenized. The homogenate was diluted serially 10-fold with 9% saline and plated on SDA. The plates were

incubated for 24 hours at 35°C and inspected for CFU viable counts. The lower limit of detection for this technique is 100 CFU/mL. All results are expressed as the mean $\log_{10}$ CFU per kidney for three animals.

In Vivo Murine Toxicity Study

All studies were approved by the Animal Research Committee of the William S. Middleton Memorial VA Hospital (Madison, WI). Uninfected Swiss ICR mice were used for assessment of infusion toxicity. Groups of five mice were treated with single intravenous doses of AmB, AmBAU, AmBMU (reconstituted with 1.0 mL of 5% dextrose), or sterile pyrogen-free 0.85% NaCl administered via the lateral tail vein over 30 seconds. Dose levels studies included 0.5, 1, 2, 4, 8, 16, 32, and 64 mg/kg. Following administration mice were observed continuously for one hour and then every 6 hours up to 24 hours for signs of distress or death.

Resistance Studies
Minimum Inhibitory Concentration and Growth Assays

Susceptibility of wild-type and resistant strains to AmB, AmBAU, AmBMU, tert-butyl peroxide (Sigma-Aldrich), geldanamycin and radicicol (A.G. Scientific) was determined in flat bottom, 96-well microtiter plates (Costar) using a broth microdilution protocol adapted from CLSI M27-A3. Overnight cultures (14-20 hr) were grown at 30°C in YPD, and approximately $5x10^3$ cells were seeded per well. For AmB, AmBAU, and AmBMU, MIC assays were performed at 37°C in RPMI buffered with MOPS (0.165M) with 10% fetal bovine serum (Sigma-Aldrich) added; for tert-butyl peroxide, geldanamycin, and radicicol, MIC's were determined in YPD at 30°C. MIC's were determined after 24 h incubation as the concentration of compound resulting in no visible growth in wells. For quantitative display of growth at drug dilutions, OD_{600} was measured in a spectrophotometer (Tecan) and displayed as heat maps using Java TreeView 1.1.3 (http://jtreeview.sourceforge.net).

Media and Growth Conditions

C. albicans was generally grown and maintained as described previously[15]. Stocks were stored in 15% glycerol at -80°C; strains were generally grown in YPD media at 30°C. Drugs were added directly to media from DMSO stocks.

In Vitro Gradual Selection of AmB, AmBAU, or AmBMU Resistance

Selection of resistance to AmB, AmBAU, and AmBMU was performed as follows. 1 mL overnight (14-20 hr) cultures of SC5314 (WT) were washed in PBS, then treated with 3% ethyl methanesulfonate (EMS) for 45 min. Cells were then washed 4x in YPD and resuspended in YPD and allowed to recover for 3 h. Cells were then inoculated to an OD_{600} of approximately 0.025-0.05 in 100 mL YPD containing 0.25 µM AmB or AmB-AU, or 0.375 µM AmB-MU. After 24-72 hours, a 1 mL aliquot was removed from any culture that had grown to saturation and subjected to another round of mutagenesis in the same manner as described above. After recovery, cells were then inoculated into a new YPD flask containing 2x higher concentration of the same drug. Cultures that grew were subjected to one more round of EMS mutagenesis before inoculating into a 2-fold higher drug concentration (total of 3 rounds of EMS mutagenesis) and then passaged at 2-fold higher increments of drug concentration until reaching 2 µM AmB or AmB-AU, or 3 µM AmB-MU. Cultures were passaged once more at 2 µM AmB or AmBAU or 3 µM AmBMU, then plated onto YPD media and frozen in glycerol stocks before further evaluation.

Filamentation Assay

Hyphal induction was performed by growing *C. albicans* overnight at 30°C in YPD, washing in PBS, and diluting 1:100 into RPMI+10% fetal bovine serum (Sigma-Aldrich) at 37°C in a culture tube on a rotating wheel. After 3 h, cultures were washed in PBS and resuspended in 250 µg/mL Calcofluor white in a microcentrifuge tube, and shaken at 30°C for 10 min. Cells were then washed twice in PBS, concentrated 10-fold, briefly sonicated in a water bath, and mounted on slides for visualization under a DAPI filter set at 60X magnification.

Murine Model of Systemic Infection

All animal protocols were performed in accordance with the Guide for the Care and Use of Laboratory Animals of the National Institutes of Health. Animals were maintained according to the guidelines of the MIT Committee on Animal Care (CAC). These studies were approved by the MIT CAC (protocol #0312-024-15). We used 7-12-week-old female Balb/c mice ordered from Taconic farms for all mouse virulence studies. All strains were prepared for inoculation by diluting overnight cultures (14-20 h) 1:100 into YPD and growing into log phase for 4-5 hours, then

washing 3x in PBS before. Strains were injected into the lateral tail vein in a volume of 100 μl. For mouse survival experiments, strains were grouped as follows: The wild-type Mutagenized pool consisted of 5 SC5314 colonies subjected in parallel to mutagenesis and passaging (as described above) without drug exposure, injected as of 1.6×10^5 cfu per strain (8×10^5 cfu total inoculum per mouse); the Wild-type low inoculum was the SC5314 parental strain injected at 1.6×10^5 cfu. AmB-Resistant, AmBAU-Resistant, and AmBMU-resistant pools were comprised of strains isolated from each selection in the presence of the indicated drug, using strains that exhibited >4-fold MIC increase for the drug used. Individual resistant strains were present in the pools at 1.6×10^5 cfu per mouse (8×10^5 total inoculum per mouse when pooled). Each strain or pool of strains was tested in at least two independent experiments, and data were pooled. Mice were weighed daily and monitored for signs of morbidity and sacrificed when body weight decreased by 20%, or when signs of extreme distress were apparent. For the competitive infection with quantification of kidney burden, a pool comprised of 16 strains at equal fraction of the population, one SC5314 wild-type and 5 strains each from selections for resistance to AmB, AmBAU, and AmBMU was used, with 3×10^4 cells of each strain inoculated per mouse (4.8×10^5 total inoculum). Three mice were used per experiment, in a total of two experiments. 4 days after infection, mice were sacrificed and kidneys were removed aseptically, homogenized, and plated onto YPD plates. Pools of the inoculum immediately before injection were also plated. 184 colonies were randomly selected from the pre-infection and 184 from the post-infection plates and tested for growth in 96-well plates in the presence of 1 μM AmBAU or 1.5 μM AmBMU, and the fraction of wells from the pre and post-infection pools exhibiting growth in either drug was determined.

Whole Genome Sequencing, Alignment, Mapping, and Variant Calling

Whole genome sequencing and analysis was performed as previously described[47].

3-9 REFERENCES

1. Gray, K. C.; et al. *Proc. Natl. Acad. Sci. USA* **2012**, *109*, 2234-2239.
2. Anderson, T. M.; et al. *Nat. Chem. Biol.* **2014**, *10*, 400-406.
3. Hulce, J. J.; Cognetta, A. B.; Niphakis, M. J.; Tully, S. E.; Cravatt, B. F. *Nat. Methods* **2013**, *10*, 259-264.
4. Procino, G.; et al. *Am. J. Physiol. Renal Physiol.* **2010**, *298*, F266-F278.
5. Balut, C.; et al. *Am. J. Cell Physiol.* **2006**, *290*, C87-C94.

6. Huber, T. B.; et al. *Proc. Natl. Acad. Sci. USA* **2006**, *103*, 17079-17086.

7. Zager, R. A.; Burkhart, K. M.; Johnson, A. C. M.; Sacks, B. M. *Kidney Int.* **1999**, *56*, 1788-1797.

8. Zager, R. A.; Johnson, A. *Kidney Int.* **2001**, *60*, 2299-2310.

9. Hinzpeter, A.; et al. *J. Biol. Chem.* **2007**, *282*, 2423-2432.

10. Megli, F. M.; Conte, E.; Ishikawa, T. *Biochim. Biophys. Acta* **2011**, *1808*, 2267-2274.

11. Márquez, M. G.; Favale, N. O.; Nieto, F. L.; Pescio, L. G.; Sterin-Speziale, N. *Biochim. Biophys. Acta* **2012**, *1818*, 491-501.

12. Stakewich, M. C.; Francis, S. A.; Vu, Q. U.; Schneeberger, E. E.; Lynch, R. D. *Lipids* **1996**, *31*, 817-828.

13. Hailstones, D.; Sleer, L. S.; Parton R. G.; Stanley, K. K. *J. Lipid Res.* **1998**, *39*, 369-379.

14. Sheng, R.; et al. *Nat. Comm.* **2014**, *5*, 4393.

15. Roitbak, T.; Surviladze, Z.; Tikkanen, R.; Wandinger-Ness, A. *Biochem. J.* **2005**, *392*, 29-38.

16. Liu, Y.; Flores, D.; Carrisoza-Gaytá, R.; Rohatgi, R. *Am. J. Physiol. Renal Physiol.* **2015**, *308*, F1229-F1237.

17. Frank, D. W.; Gray, J. E.; Weaver, R. N. *Am. J. Pathol.* **1976**, *83*, 367-382.

18. Tabata, S.; et al. *J. Toxicol. Pathol.* **1991**, *4*, 67-73.

19. Taubes, G. *Science* **2008**, *321*, 356-361.

20. Monk, B. C.; Goffeau, A. *Science* **2008**, *321*, 367-369.

21. Ellis, D. *J. Antimicrob. Chemother.* **2002**, *49*, 7-10.

22. Li, J.; et al. *Lancet Infect. Dis.* **2006**, *6*, 589-601.

23. Cortes, J. E.; et al. *New Engl. J. Med.* **2013**, *369*, 1783-1796.

24. White, T. C.; Marr, K. A.; Bowden, R. A. *Clin. Microb. Rev.* **1998**, *11*, 382-402.

25. Bodey, G. P. *Clin. Infect. Dis.* **1992**, *14*, 161-169.

26. Sanglard, D.; Ischer, F.; Koymans, L.; Bille, J. *Antimicrob. Agents Chemother.* **1998**, *42*, 241-253.

27. Palacios, D. S.; Anderson, T. M.; Burke, M. D. *J. Am. Chem. Soc.* **2007**, *129*, 13804-13805.

28. Palacios, D. S.; Dailey, I.; Siebert, D. M.; Wilcock, B. C.; Burke, M. D. *Proc. Natl. Acad. Sci. USA* **2011**, *108*, 6733-6738.

29. Baran, M.; Mazerski, J. *Biophys. Chem.* **2002**, *95*, 125-133.

30. Matsumori, N.; Sawada, Y.; Murata, M. *J. Am. Chem. Soc.* **2005**, *127*, 10667-10675.

31. Neumann, A.; Czub, J.; Baginski, M. *J. Phys. Chem. B* **2009**, *113*, 15875-15885.

32. Czub, J.; Neumann, A.; Borowski, D.; Baginski, M. *Biophys. Chem.* **2009**, *141*, 105-116.

33. Neumann, A.; Baginski, M.; Czub, J. *J. Am. Chem. Soc.* **2010**, *132*, 18266-18272.

34. Croatt, M. P.; Carreira, E. M. *Org. Lett.* **2011**, *13*, 1390-1393.

35. Wilcock, B. C.; Endo, M. M.; Uno, B. E.; Burke, M. D. *J. Am. Chem. Soc.* **2013**, *135*, 8488-8491.

36. Wilcock, B. C.; et al. *Nat. Chem.* **2012**, *4*, 996-1003.

37. Duggan, K. C.; et al. *Nat. Chem. Biol.* **2011**, *7*, 803-809.

38. Neant-Fery, M.; et al. *Proc. Natl. Acad. Sci. USA* **2008**, *105*, 9582-9587.

39. Knight, Z. A.; Shokat, K. M. *Chem. Biol.* **2005**, *12*, 621-637.

40. Koike, K.; et al. *J. Biol. Chem.* **2002**, *277*, 49495-49503.

41. Changeux, J. P.; Edelstein, S. J. *Neuron* **1998**, *21*, 959-980.

42. Andes, D.; Stamsted, T.; Conklin, R. *Antimicrob. Agents Chemother.* **2001**, *45*, 922-926.

43. Andes, D.; van Ogtrop, M. *Antimicrob. Agents Chemother.* **2000**, *44*, 938-942.

44. Andes, D.; van Ogtrop, M. *Antimicrob. Agents Chemother.* **1999**, *43*, 2116-2120.

45. Jarzembska, K. N.; et al. *Cryst. Growth Des.* **2012**, *12*, 2336-2345.

46. Ganis, P.; Avitabile, G.; Mechlinski, W.; Schaffner, C. P. *J. Am. Chem. Soc.* **1971**, *93*, 4560-4564.

47. Bonner, D. P.; Mechlinski, W.; Schaffner, C. P. *J. Antibiot.* **1972**, *25*, 261-262.

48. Keim, G. R.; et al. *Antimicrob. Agents Chemother.* **1976**, *10*, 687-690.

49. Tevyashova, A. N.; et al. *Antimicrob. Agents Chemother.* **2013**, *57*, 3815-3822.

50. Davis, S. A.; et al. *Nat. Chem. Biol.* **2015**, *11*, 481-487.

51. Paquet, V.; Volmer, A.A.; Carreira, E.M. *Chem. Eur. J.* **2008**, *14*, 2465-2481.

52. Cruz, M. C.; et al. *Antimicrob. Agents Chemother.* **2000**, *44*, 143-149.

53. Lepak, A. J.; Marchillo, K.; VanHecker, J.; Andes, D. R. *Antimicrob. Agents Chemother.* **2013**, *57*, 579-585.

54. Zager, R. A. *Am. J. Kidney Dis.* **2000**, *36*, 238-249.

55. Ellis, J. K.; et al. *Mol. Biosyst.* **2011**, *7*, 247-257.

56. Pfaller, M. A. *Am. J. Med.* **2012**, *125*, S3-S13.

57. Zhang, Y.- Q.; et al. *PLoS Pathog.* **2010**, *6*, e1000939.

58. Heese-Peck, A.; et al. *Mol. Biol. Cell* **2002**, *13*, 2664-2680.

59. Kato, M.; Wickner, W. *EMBO J.* **2001**, *20*, 4035-4040.

60. Klose, C.; et al. *J. Biol. Chem.* **2010**, *285*, 30224-30232.

61. Jin, H.; McCaffery, J. M.; Grote, K. *J. Cell Biol.* **2008**, *180*, 813-826.

62. Sanglard, D.; Ischer, F.; Parkinson, T.; Falconer, D.; Bille, J. *Antimicrob. Agents Chemother.* **2003**, *47*, 2404-2412.

63. Vincent, B. M.; Lancaster, A. K.; Scherz-Shouval, R.; Whitesell, L.; Lindquist, S. *PLoS Biol.* **2013**, *11*, e1001692.

64. Pfaller, M. A; et al. *J. Clin. Microbiol.* **2012**, *50*, 2040-2046.

65. Lo, H.- J.; et al. *Cell* **1997**, *90*, 939-949.

66. Mitchell, A. P. *Curr. Opin. Microbiol.* **1998**, *1*, 687-692.

67. Pangborn, A. B; Giardello, M. A; Grubbs, R. H.; Rosen, R. K.; Timmers, F.J. *Organometallics* **1996**, *15*, 1518-1520.

68. Chen, P.S.; Toribara, T.Y.; Warner, H. *Anal. Chem.* **1956**, *28*, 1756.

69. Heerklotz, H.; Seelig, J. *Biochim. Biophys. Acta* **2000**, *1508*, 69.

70. This is a standard protocol for ITC experiments, for example see: te Welscher, Y.M.; ten Nagel, H.H.; Masiá Balagué, M.; Souza, C.M.; Riezman, H.; deKruijff, B.; Breukink, E. *J. Biol. Chem.* **2008**, *283*, 6393.

71. Clinical and Laboratory Standards Institute. Reference Method for Broth Dilution Antifungal Susceptibility Testing, M27-A3, Approved Standard 3rd Ed. Vol. 28, April, 2008.

72. Clinical and Laboratory Standards Institute. Reference Method for Broth Dilution Antifungal Susceptibility Testing, M38-A2, Approved Standard 3rd Ed. Vol. 28, April, 2008.

73. Clinical and Laboratory Standards Institute. Reference Method for Broth Dilution Antifungal Susceptibility Testing, M27-A2, Approved Standard 2nd Ed. Vol. 22, November, 2002.

74. Sebaugh, J.L.; *Pharmaceut. Statist.* **2011**, *10*, 128-134.